1-1-2009

Optimal Control Of Voltage And Power In Mvdc Multi-Zonal Shipboard Power System

Padmavathy Kankanala

OPTIMAL CONTROL OF VOLTAGE AND POWER IN MVDC MULTI-ZONAL SHIPBOARD POWER SYSTEM

By

Padmavathy Kankanala

A Thesis
Submitted to the Faculty of
Mississippi State University
in Partial Fulfillment of the Requirements
for the Degree of Master of Science
in Electrical Engineering
in the Department of Electrical and Computer Engineering

Mississippi State, Mississippi

December 2009

OPTIMAL CONTROL OF VOLTAGE AND POWER IN MVDC MULTI-ZONAL SHIPBOARD POWER SYSTEM

By

Padmavathy Kankanala

Approved:

Noel N. Schulz Professor of Electrical and Computer Engineering (Major Advisor)	Anurag K. Srivastava Assistant Research Professor of Electrical and Computer Engineering (Co-Advisor)
Suresh C. Srivastava Adjunct Professor of Electrical and Computer Engineering (Committee Member)	James E. Fowler Professor and Director of Graduate Studies, Electrical and Computer Engineering
Sarah A. Rajala Dean of Bagley College of Engineering	

Name: Padmavathy Kankanala

Date of Degree: December 11, 2009

Institution: Mississippi State University

Major Field: Electrical Engineering

Major Professor: Dr Noel N. Schulz

Title of Study: OPTIMAL CONTROL OF VOLTAGE AND POWER IN MVDC MULTI-ZONAL SHIPBOARD POWER SYSTEM

Pages in Study: 98

Candidate for Master of Science

Recent advancements in Voltage Source Converters (VSCs) of high-voltage and high-power rating had a significant impact on the development of Multi-Terminal HVDC (MTDC) power transmission systems. The U.S. Navy has proposed Multi-Zonal Medium Voltage DC (MVDC) Shipboard Power System (SPS) architecture for the next generation of their surface combatant. A Multi-Zonal MVDC SPS consists of several VSCs exchanging power through a DC network. Following a system fault or damage, the current flow pattern in the DC distribution grid will change and the DC voltages across the VSCs will assume new values. DC voltage reference or power reference settings of VSCs have to be determined, in advance, which can maintain the DC voltage within desired margins (usually 5% around the nominal value) in steady state, under the pre-fault as well as the post-fault conditions. In this work, the reference settings have been pre-determined by: (1) Development of a sensitivity based algorithm for voltage control of VSCs of the DC system and (2) Development of an optimal algorithm for voltage and

power control of the VSCs. The algorithms have been tested on a simplified representation of the MVDC SPS architecture.

DEDICATION

I would like to dedicate this research to my family members.

ACKNOWLEDGMENTS

I would like to gratefully thank my advisor, Dr. Noel N. Schulz, for her support, guidance, and constant encouragement throughout the research work. I would like to thank my Committee Member, Dr. Suresh C. Srivastava, for his guidance and support throughout this research. Without their constant guidance it would not have been possible to complete this thesis. I would also like to thank Dr. Anurag K. Srivastava, for his willingness to serve on my graduate committee and for his support and valuable suggestions.

I gratefully acknowledge the financial support of the US Office of Naval Research (ONR) during my graduate program.

I would also like to thank my parents and friends for their support and love throughout the entire time.

TABLE OF CONTENTS

Page

DEDICATION ii

ACKNOWLEDGMENTS iii

LIST OF TABLES vii

LIST OF FIGURES ix

LIST OF SYMBOLS xi

LIST OF ACRONYMS xii

CHAPTER

I. INTRODUCTION 1

1.1 Introduction 1
1.2 Objective of the Research 2
1.3 Overview of thesis 3
1.4 Thesis organization 5

II. BACKROUND 7

2.1 Introduction 7
2.2 Architectures Proposed by the U.S. Navy 7
2.2.1 MVAC Architecture 9
2.2.2 HFAC Architecture 10
2.2.3 MVDC Architecture 11
2.3 Voltage Source Converter (VSC) 12
2.3.1 Introduction 12
2.3.2 Pulse Width Modulation 14
2.3.3 VSC Voltage Control 15
2.3.4 Injected DC Side Current 16

2.4 Two Terminal VSC-MVDC 18
2.4.1 Main Circuits 18
2.4.2 Control of VSC-MVDC 21
2.4.3 Coordination of Real Power Through VSC-MVDC 22
2.5 Advantages of VSC....24
2.6 Multi-Terminal MVDC (MTDC) 25
2.6.1 Characteristics of MTDC....25
2.7 Summary....26

III. PROBLEM DESCRIPTION AND TEST CASE 27

3.1 Introduction 27
3.2 Problem Statement....28
3.3 Test Case 28
3.3.1 Simplified MVDC Multi Zonal Shipboard System 28
3.4 Methodology & Proposed Algorithms 31
3.4.1 Conventional Method 31
3.4.2 Genetic Algorithms....32
3.4.3 Biogeography Based Optimization....32
3.5 Summary....33

IV. A SENSITIVITY BASED METHOD FOR OPTIMAL VOLTAGE REGULATION 34

4.1 Introduction....34
4.2 Methodology 36
4.2.1 System Under Study 36
4.2.2 Network Equations....37
4.2.3 Power Flow Problem by Newton-Raphson Method....39
4.2.4 Voltage Sensitivities Indices....40
4.2.5 Estimating the Desired Voltage Reference....43
4.3 Test Results 48
4.4 Summary 51

V. A CONVENTIONAL OPTIMIZATION BASED METHOD FOR OPTI MAL POWER AND VOLTAGE CONTROL 52

5.1 Introduction....52
5.2 Proposed Optimization Based Problem Formulation 53
5.3 Optimal Solution using Lagrange Multiplier Method 60
5.4 Major Solution Steps....62
5.5 Results on MVDC System....63
5.6 Summary....66

VI. A GENETIC ALGORITHM BASED OPTIMAL CONTROL OF POWER AND VOLTAGE 67

6.1 Introduction 68
6.2 Terminology 69
6.3 Solution Steps with Genetic Algorithm 72
6.4 Genetic Algorithm Applied to Optimal Voltage and Power Control 74
6.4.1 Tunable Parameters 74
6.4.2 The Optimization Problem Formulation 74
6.4.3 Results on MVDC System 76
6.5 Summary 78

VII. OPTIMAL VOLTAGE AND POWER CONTROL USING A BIOGEOGRAPHY BASED OPTIMIZATION 79

7.1 Introduction 79
7.2 Biogeography Based Optimization Concepts 81
7.3 Biogeography Based Optimization Technique 83
7.3.1 Migration 83
7.3.2 Mutation 84
7.4 Major Solution Steps of BBO 86
7.5 Application of the BBO Algorithm to Optimal Power and Voltage Control Problem 89
7.5.1 Tunable Parameters 89
7.5.2 The Optimization Problem Formulation 89
7.5.3 Results with BBO on the MVDC System 91
7.6 Comparison of BBO Results with Conventional Lagrange and GA Methods 93
7.7 Summary 93

VIII. CONCLUSION AND FUTURE WORK 95

8.1 Conclusions 95
8.2 Future Work 98

REFERENCES 99

LIST OF TABLES

TABLE Page

3.1 Converter Power Reference Settings 29

3.2 DC Line Resistance of MVDC Network 30

4.1 Allowable $\mathbf{V}_{ref}$ for different conditions and common accepted bound for the reference settings of VSC5 49

4.2 DC bus voltages with $\mathbf{V}_{dcref}$=0.9527 p.u. 50

4.3 DC bus voltages with $\mathbf{V}_{dcref}$=1.0485 p.u. 50

5.1 Allowed $\mathbf{V}_{ref}$ for different cases 64

5.2 DC Voltage subject to VSC power setting adjustment with Existing formulation[5] 64

5.3 DC Voltage subject to VSC power setting adjustment with New Alternative-1 formulation 65

5.4 DC Voltage subject to VSC power setting adjustment with New Alternative-2 formulation.....66

6.1 Differences between GAs and Traditional Algorithms 69

6.2 DC Voltage subject to GA based VSC power setting adjustment with Existing formulation[5] 77

6.3 DC Voltage subject to GA based VSC power setting adjustment with New Alternative-1 formulation 77

6.4 DC Voltage subject to GA based VSC power setting adjustment with New Alternative-2 formulation 78

7.1 DC Voltage subject to BBO based VSC power setting adjustment with Existing formulation [5] 92

7.2 DC Voltage subject to BBO based VSC power setting adjustment with New Alternative-1 formulation 92

7.3 DC Voltage subject to BBO based VSC power setting adjustment with New Alternative-2 formulation 93

7.4 Comparison of final objective function values with different algorithms 94

LIST OF FIGURES

FIGURE Page

2.1 Notional NGIPS MVAC System [2] 9

2.2 Notional NGIPS MVDC System [2] 12

2.3 Voltage Source Converter (VSC) [7] 13

2.4 (a) Typical switch function, $S_a(t)$ and

(b) Input Signal, $m_a(t)$ [9] 15

2.5 Equivalent circuit of VSC 17

2.6 Two Terminal VSC-MVDC [7] 18

2.7 Equivalent circuit of two-terminal VSC-MVDC 22

3.1 Simplified MVDC Shipboard Power System 29

4.1 Typical (N+1) terminal VSC based MVDC system [6] 36

4.2 a The solution range for $\boldsymbol{V}_{dc}^{k}$ [5] 45

4.2 b Allowed $\Delta \mathbf{V}_{\text{dcref}}$ due to $\boldsymbol{V}_{dci}^{k}$ limits [5] 46

4.3 The common range of $\Delta \mathbf{V}_{\text{dcref}}$ subject to voltage limits on all $\boldsymbol{V}_{dci}^{k}$ [5] 47

5.1 A Sample Three-Terminal VSC-MVDC system [7] 54

6.1 Genetic Algorithm Terminologies 71

6.2 Flowchart showing the Genetic Algorithm [26] 73

7.1 Island Migration Rate vs. Species [23] 82

7.2 A candidate solution [23] 84

7.3 Flowchart of the BBO 88

LIST OF SYMBOLS

V_{sa}, V_{sb}, V_{sc}	3-phase AC voltages of Voltage Source Converter (VSC)
m_a, m_b, mc	3-phase modulating signals of VSC
i_a,i_b, i_c	3-phase currents
v_a,v_b,v_c	Terminal voltages of the AC system, to which the VSC is connected
V_{dci}	DC voltage of the i^{th} converter (VSCi)
I_{dci}	DC current injected by the i^{th} converter (VSCi)
P_i	Real power of the i^{th} converter (VSCi)
P_{ref}	Real power reference of the VSC
V_{dcref}	DC voltage reference of DC Voltage Regulator
L_f	Inductance of series filter
R_f	Resistance of series filter
R_{dc}	DC line resistance
C	DC capacitance
V_{min}	Minimum voltage limit
V_{max}	Maximum voltage limit

LIST OF ACRONYMS

AC, ac	Alternating Current
DC, dc	Direct Current
VSC	Voltage Source Converter
NGIPS	Next Generation Integrated Power System
MVDC	Medium Voltage Direct Current
MVAC	Medium Voltage Alternating Current
HFAC	High Frequency Alternating Current
IFTP	Integrated Fight Through Power
MTDC	Multi-Terminal VSC-MVDC
QOS	Quality of Service
VR	DC Voltage Regulator
PD	Power Dispatcher
IGBT	Insulated Gate Bipolar Transistor
GTO	Gate Turn-Off Thyristor
PWM	Pulse Width Modulation
SPWM	Sinusoidal Pulse Width Modulation
GA	Genetic Algorithm
ANN	Artificial Neural Networks
PSO	Particle Swarm Optimization
BBO	Biogeography Based Optimization
ES	Evolutionary Strategies
SIV	Suitability Index Variables
HSI	Habitat Suitability Index

CHAPTER I

INTRODUCTION

1.1 Introduction

The U.S. naval electric shipboard power systems have currently employed the radial AC distribution system architecture [1]. In order to maximize survivability, enhance operational flexibility, minimize size and weight, and decrease the overall cost, the U.S. Navy has proposed two alternative distribution architectures for their future shipboard [2] power systems:

1. MVDC (Medium Voltage DC) distribution
2. HFAC (High Frequency AC) distribution

With recent developments in high-voltage, high-power, fully controlled Voltage Source Converters (VSCs) and their ability, in MVDC transmission system applications, to control real and reactive powers independently, the VSC based Multi-Zonal MVDC Shipboard Power System (SPS) architecture shows more promise and has drawn the attention of researchers working on naval shipboard systems. The VSC based MVDC SPSs are tightly-coupled, power-limited systems and their performance needs to be evaluated for security, reliability, and survivability.

A Multi-Zonal MVDC SPS will employ several VSCs exchanging power through a DC network. The current flow pattern in the DC grid and the DC voltages across the

VSCs will change under a system fault, accidental loss of a VSC, or system reconfiguration. The DC over-voltage may lead to failure in the solid-state switches and DC under-voltage may cause waveform distortion. Hence, DC grid voltage should be maintained within a narrow range (usually 5% around its nominal value) under the pre-fault as well as post fault conditions. This requires determination of optimal settings of DC voltage reference and power reference of the VSCs.

This thesis will focus on determining the reference settings such that the voltage at the DC terminal is maintained within a narrow range. In this thesis, a conventional optimization method and two of the heuristic algorithms (genetic algorithm and biogeography based optimization) have been used for solving the optimization problem.

1.2 Objective of the Research

With the U.S. Navy proposing the new architecture for the shipboard power, system utilizing the recent developments in the power electronic devices employing VSC, calls for more research to maintain the reliability and survivability of the system. When faults occur, as a result of battle damage or equipment failure it results in change in the DC voltage across the VSCs. This may lead to failure in the solid state switches. Hence, DC voltage should be maintained within a narrow range under steady state and also under transients. This requires pre-determination of optimal settings of DC voltage reference and power reference of the VSCs. Because of this need, it is desirable to find an accurate numerical method that solves the optimization problem quickly and determines the reference settings.

1.3 Overview of Thesis

The operation of point-to-point VSC-HVDC requires VSCs to operate in DC Voltage Regulator and Power Dispatcher modes [6,7]. An MTDC system generally consists of several VSCs, connected in shunt to a DC network, in Power Dispatcher mode except one in DC Voltage Regulator mode. A typical Multi-Terminal MVDC, based on VSC system, is shown in Figure 4.1[6]. The feedback control of the Power Dispatcher is configured so that it regulates the AC real power through it. The sign polarity of the power reference designates the direction of AC real power flow (positive for a rectifier and negative for an inverter). The feedback control of the DC Voltage Regulator is configured so that it regulates the DC voltage across its DC bus. Since the DC voltage across the DC bus depends on the charging of the DC capacitors, the DC Voltage Regulator controls the AC real power through it to null the error between the measured DC voltage and the DC voltage reference. The DC Voltage Regulator acts as a power slack because, while keeping the DC voltage charged to its reference setting, it maintains the power balance in the DC network. The DC Voltage Regulator takes on the complementary role (inverter or rectifier) as a power slack to maintain power balance in the DC system.

The steady state DC bus voltage $\mathbf{V}_i$ of a VSC_i (i=1,2,…N+1) depends on the resistance of the DC transmission lines and the $\mathbf{V}_{ref}$. For a given power setting $\boldsymbol{P}_i^{sp}$ (i=1,2…N), and V_{ref} for voltage regulator VSC, say at bus N+1, the voltages at the VSC_i (i=1,2,…N) buses can be solved by the Newton-Raphson method, similar to an AC power flow program [8]. The DC bus voltage $\mathbf{V}_i$ of VSC_i must satisfy the voltage limits, $\mathbf{V}_{min} \leq \mathbf{V}_i \leq \mathbf{V}_{max}$ (i=1,2,…N). $\mathbf{V}_{max}$ is set by the maximum safe voltage allowed across the

solid-state switches, such as Insulated-Gate Bipolar Transistors (IGBT) [9]. The lower limit, $\mathbf{V}_{min}$, prevents the SPWM (Sinusoidal Pulse Width Modulation) control of the converter from becoming over-modulated [9], whereupon low frequency harmonics appear on the AC side.

The worst case scenario consists of an accidental loss of a VSC. In the event of the loss of any converter, the power flow in the DC grid is redirected and, therefore, the bus voltages assume new values. As the surviving converters can be destroyed by over-voltage within a fraction of a second, there is no time for the controls to reset $\mathbf{V}_{ref}$, or P_i^{sp}, i=1,2,….N. For this reason, $\mathbf{V}_{ref}$, or P_i^{sp} (i=1,2,….N) should be optimally selected, in advance, which can meet the voltage constraints before and after the loss of any converter. If VSC working as slack bus is out of service or destroyed, then VSC at some other bus will be working as reference bus. In this work, the slack bus is always assumed to be within the system.

The reference settings have been pre-determined in two stages: (1) Optimal reference setting of voltage regulator based on a sensitivity based algorithm to ensure DC bus voltages at all the VSCs within acceptable margin under the pre-fault and post-fault conditions, and (2) Development of an optimization based algorithm to determine both optimal voltage reference and power reference settings of VSCs, in case the stage-1 setting is unable to maintain the DC voltages within acceptable range. Each stage of the solution requires simulation of N cases of post-fault DC power flow problems to be solved simultaneously with the pre-fault DC power flow problem. As mentioned earlier, in order to reduce the complexity, this work has assumed that the lost VSC will not include the DC Voltage Regulator.

1.4 Thesis Organization

The content of the thesis is summarized as follows. Chapter II gives the background information of the architectures proposed by the U.S. Navy, and a general overview of the Voltage Source Converters (VSCs). It introduces the main circuits present in the two-terminal VSC, gives its advantages, and then discusses the characteristics of the MTDC system.

Chapter III explains the problem statement, the test case used in this work, the methodology and the proposed algorithms.

Chapter IV discusses a sensitivity based method for optimal voltage regulation. It explains the mathematical formulation of the Newton-Raphson method and the Voltage Sensitivity indices method. It also presents the test case results on a simplified model of the MVDC multi-zonal shipboard power system.

Chapter V deals with the conventional optimization based method for optimal control of power and voltage. It explains the mathematical problem formulation and the optimal solution steps using Lagrange multiplier method. It presents the test case results on an MVDC shipboard system.

Chapter VI and Chapter VII deal with the application of proposed heuristic algorithms for solving the optimization problems. Chapter VI explains in detail about the Genetic Algorithm (GA) and the genetic operators (selection, crossover, mutation) involved in the algorithm. The applicability of the GA algorithm to a simplified MVDC system is presented. Chapter VII explains in detail about the Biogeography Based Optimization (BBO), its operators (immigration and emigration), and the mathematical

problem formulation. The application of proposed algorithm to a simplified MVDC system is presented. The BBO algorithm results are compared with the conventional method and genetic algorithms results, in terms of the final objective function values, for the analysis and validation of proposed algorithms.

Chapter VIII presents the main conclusions of the present thesis work and few suggestions on the scope for improvement and some future research work based on the proposed techniques.

CHAPTER II

BACKGROUND

2.1 Introduction

The primary objective of the present research work is to design a higher hierarchical control for a Multi-Terminal Medium Voltage Direct Current (MTDC) system so that in the event of the loss of any one Voltage Source Converter (VSC), the DC voltage is maintain within a margin of about 5%. The MTDC system considered is a MVDC ring system based on VSC.

The objective of this chapter is to present background related to power system architectures proposed by the US Navy and provide an overview of the control schemes. As the mathematical model and the equivalent circuit of the VSC, controlled by Pulse Width Modulation (PWM), are well known [9], section 2.3 of this chapter will only present a quick review. A two terminal MVDC link based on VSC stations is described. This chapter briefly introduces the main circuits of VSC-MVDC and the coordination of the pair of VSCs.

2.2 Architectures Proposed by the U.S. Navy

Advances in materials, controls, packaging and thermal management have played a significant role in improving efficiency, power density, availability of power, and other

desirable metrics in electric power systems. The US Navy, leveraging these advances, and in cooperation with industry, is developing the necessary architectures and modular building blocks, consisting of power generation, power conversion, energy storage, power distribution, and power load modules [2]. Each of these building blocks add their own contribution to the system of the architecture. Their design also allows for technical insertion as technology matures and requirements change. The architecture or Next Generation Integrated Power System (NGIPS), as referred by the U.S. Navy has to be established, derisked, and developed in order to install the common set of modules which then leads to the delivery and employment of an affordable, highly efficient, power dense and reliable electric warship [2].

With the electric propulsion, large electric load, weapon and support systems demand for more electrical power, the United States Navy has been looking into employing new electric ship designs. The exploring of employing new designs of a shipboard electric power system, the most important aim is the survivability and continuity (reliability) of the electrical power supply [2]. Survivability relates to the ability of the power system, to support the ship's ability to continue fulfilling its missions, even under threat of its damage. Power continuity (reliability) relates to ability of the power system to reliably provide power to the ship system under the normal operations. To meet the power requirements of the many classes of ship comprising the United States Navy, four different power architectures were presented [2].

1. Medium Voltage AC Power (Emphasizes Affordability)
2. High Frequency AC power (Near Term – Emphasizes Power Density)
3. Medium Voltage DC Power (Goal – Emphasizes Power Density)

4. Zonal Electrical Distribution(ZEDs)

2.2.1 *MVAC Architecture*

Figure 2.1 shows the notional Next Generation Integrated Power System (NGIPS) MVAC system architecture proposed by the U.S. Navy. A MVAC power architecture can be used where there is a requirement for high power density.

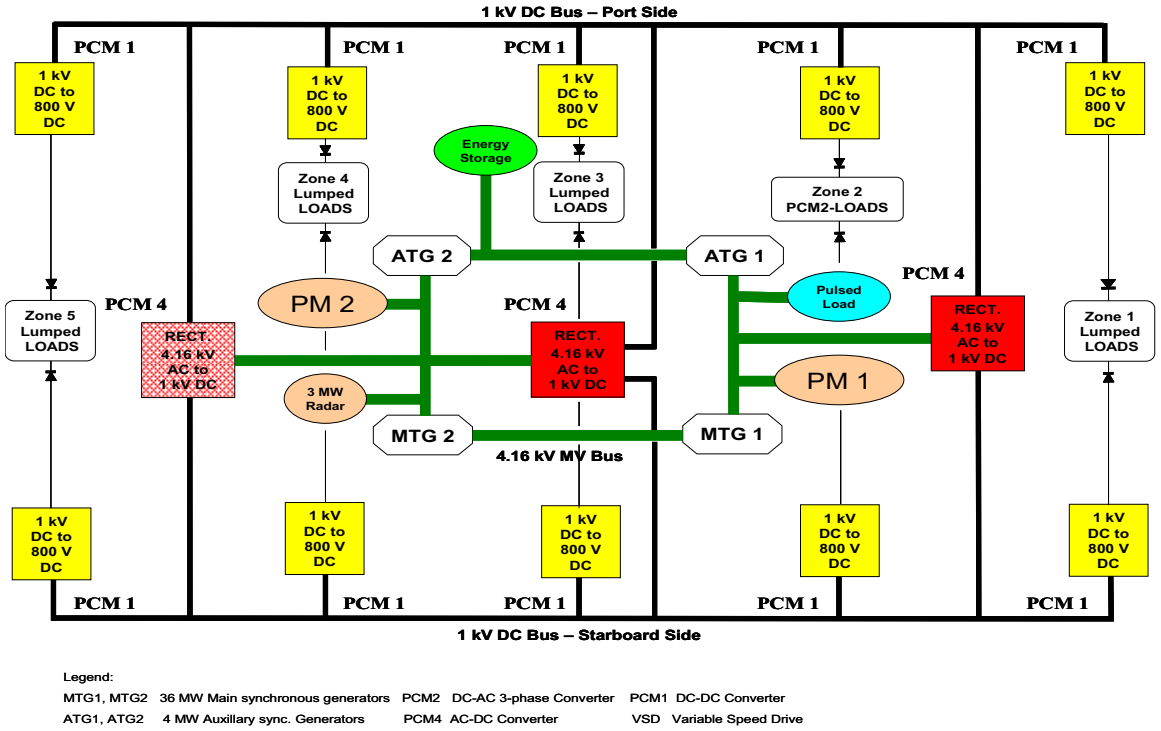

Figure 2.1 Notional NGIPS MVAC System [2]

The MVAC system, proposed by the Navy, utilizes two main generators, two auxiliary generators, each of 36 MW and 4 MW, respectively. The generators are connected to an AC ring bus operating at 4.16 kV, 60 Hz. The propulsion motors are

connected to the ring bus and supplied by the generators directly. The DC starboard side and port side operate at 1 kV connected to the ring bus through the Power Conversion Modules (PCMs). With the growing electrical load requirements, the need for reducing the weight of the electrical equipment and maintaining the system reliability, two alternative distribution schemes (MVDC and HFAC) have been proposed by the U.S Navy. Because of the recent development in power electronic devices, the MVDC architecture is getting more attention.

2.2.2 *HFAC Architecture*

HFAC power generation architecture has been proposed as one of the future architectures for the ship service distribution systems. In this, power is generated at a frequency greater than 60 Hz. and less than 400 Hz. The distribution voltage will be either 4.16 kV or 13.8 kV using a high impedance ground [2]. Some of the benefits offered are 1) it reduces the weight of transformer core (windings not included), 2) it minimizes or eliminates harmonic filters, 3) it minimizes or eliminates switching losses, 4) it has higher reliability, 5) it results in low dv/dt stress on insulation and 6) it minimizes acoustic noise. The main challenges faced by employing HFAC system are 1) requirement of higher switching speed by the power devices, 2) Electro Magnetic Interference (EMI) effect will worsen, 3) higher ground fault current, 4) power factor is lower as compared to the MVAC system, 5) requirement of large cabling, and 6) less infrastructure availability.

2.2.3 *MVDC Architecture*

Figure 2.2 shows the notional NGIPS MVDC system architecture. In MVDC architecture, the main power distribution can utilize DC supply at standard voltages ranging between ± 3000V DC to ± 10,000V DC using high-impedance ground.

The architecture for a MVDC power system is identical to the HFAC system. The primary difference is that instead of distributing HFAC power throughout the ship, the system distributes MVDC power [2].

A notional shipboard MVDC power system architecture, as proposed in [3], is shown in Figure 2.2. This MVDC architecture utilizes a medium voltage DC ring bus, operating at 5 kV, fed from the two main and the two auxiliary generators (MTG1, MTG2, ATG1, and ATG2) through transformers and rectifiers. The DC power is distributed along the length of the ship in five zones. The loads, converters, Power Conversion Modules (PCMs), and Power Distribution Modules (PDMs) are distributed in these zones.

Loads, requiring 800V DC, are supplied with the help of PCM1, which converts 5000V DC power to 800V DC. PCM4s are typically connected to the generators for AC to DC conversion. Other zonal loads, which require AC (such as propulsion motor load), are fed with the help of PCM2, which converts DC to AC. It also has converter-driven energy storage devices, such as a bank of capacitors or fuel cells; a pulsed load device, such as the charging circuit for a free electron laser gun; and high power sensors, such as a radar array. This study has considered a simplified model of the Multi-Zonal MVDC shipboard power system architecture. For the simulation purpose, all the loads are considered as lumped loads on the DC busbar.

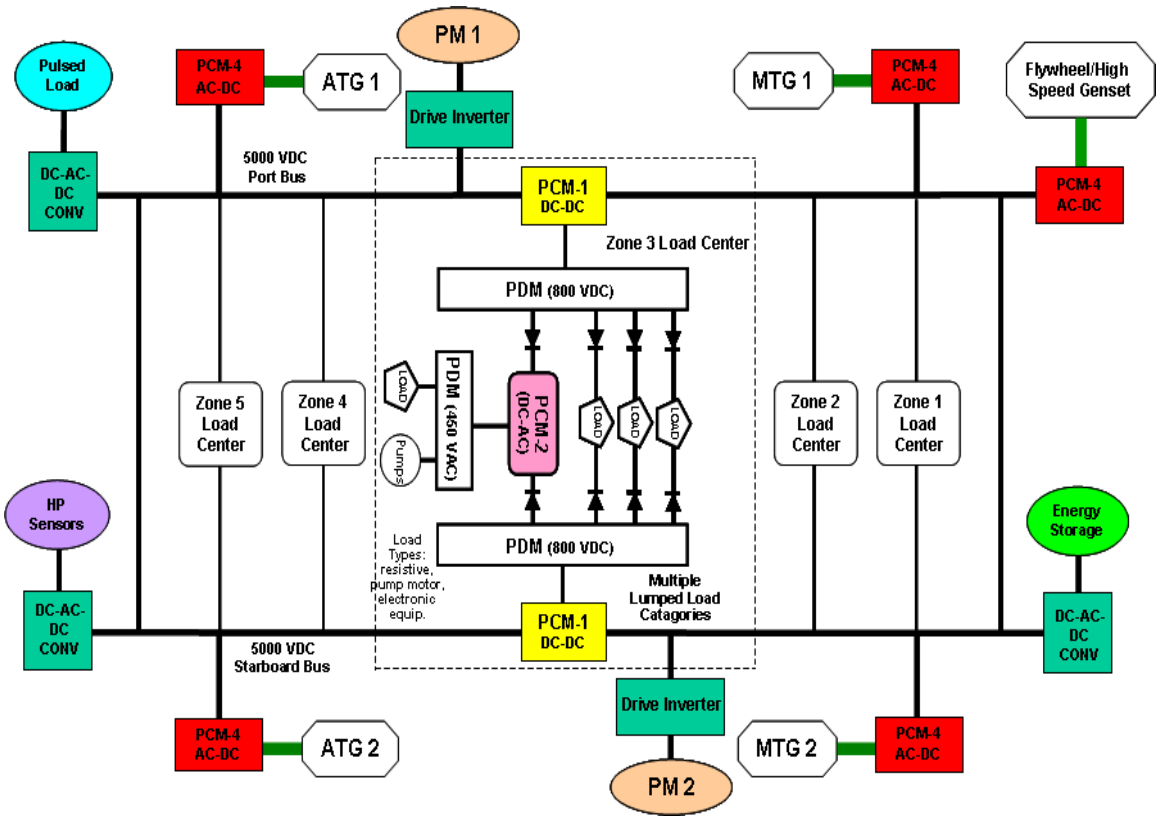

Figure 2.2 Notional NGIPS MVDC System [2]

2.3 Voltage Source Converter

2.3.1 Introduction

Figure 2.3 shows the circuit diagram of a 6-pulse VSC, which is the building block of the VSC-MVDC. Assuming that there exists a DC voltage, V_{dc}, across the DC bus, the three phase AC voltages $V_{sa}(t)$, $V_{sb}(t)$, $V_{sc}(t)$ are produced by the ON-OFF switching of the IGBTs (GTOs) in each leg of the bridge converter.

To derive the relation between AC and DC voltages, it is assumed that the IGBT switches of the VSC in Figure 2.3 have ideal ON/OFF characteristics and their actions are described by three switching functions, $S_a(t)$, $S_b(t)$, and $S_c(t)$, which are defined as follows:

$$S_{\emptyset}(t) = \begin{cases} 1 & switch\ U_{\emptyset}\ is\ ON\ and\ switch\ L_{\emptyset}\ is\ OFF \\ 0 & switch\ U_{\emptyset}\ is\ OFF\ and\ switch\ L_{\emptyset}\ is\ ON \end{cases}$$

where, the subscript ∅ refers to each of the 3 phases, i.e., ∅=a,b,c.

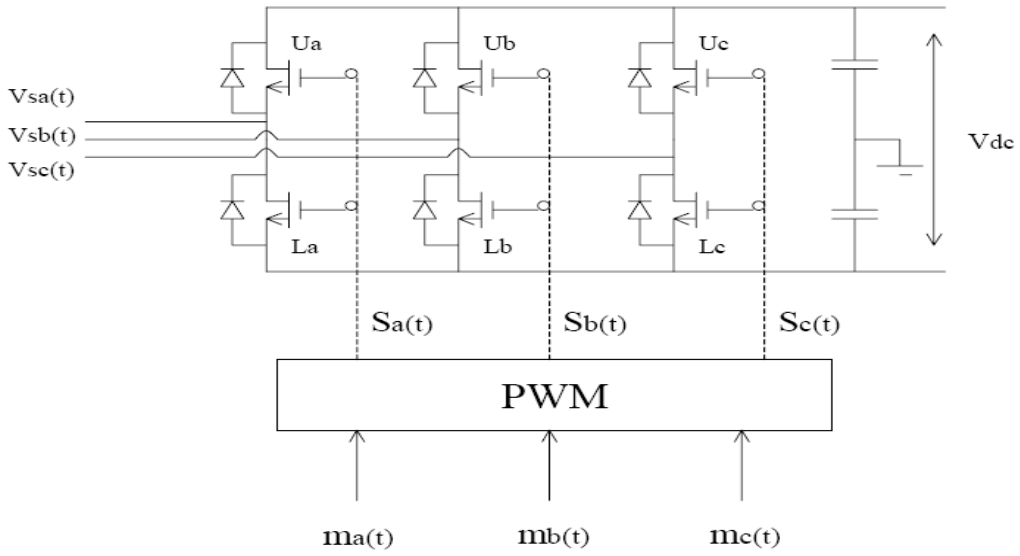

Figure 2.3 Voltage Source Converters (VSC) [7]

The 3-phase AC voltages on the AC side with respect to the grounded midpoint of the DC capacitors are given by

$$V_{sa}(t) = 0.5\, S_a(t) V_{dc}$$

$$V_{sb}(t) = 0.5\, S_b(t) V_{dc} \qquad (2.1)$$

$$V_{sc}(t) = 0.5\, S_c(t) V_{dc}$$

2.3.2 Pulse Width Modulation

There are many Pulse Width Modulation (PWM) techniques for generating the switch function signal $S_a(t)$ of Figure 2.4(a) from the modulating input signal $m_a(t)$ in Figure 2.4(b). Irrespective of the method, it is important that when the high frequency harmonics are filtered from the switch function signal $S_a(t)$, the residual signal is the modulating signal $m_a(t)$ of the a-phase. The switch function $S_a(t)$ is sent to the triggering circuits of the IGBTs of the a-phase, such that $V_{sa}(t)=0.5S_a(t)V_{dc}$, according to Equation (2.1). The waveform of $V_{sa}(t)$ is a replica of Figure 2.4(b).

A usable PWM technique is one in which all the significant switching harmonics reside in the high frequency end of the spectrum where these can be filtered economically.

After filtering

$$S_a(t)=K_1 m_a(t) \qquad (2.2)$$

where, K_1 is proportionality constant.

The a-phase filtered voltage w.r.t ground is given as:

$$V_{sa}(t)=Gm_a(t) \qquad (2.3)$$

where, the linear gain is $G=0.5K_1V_{dc}$

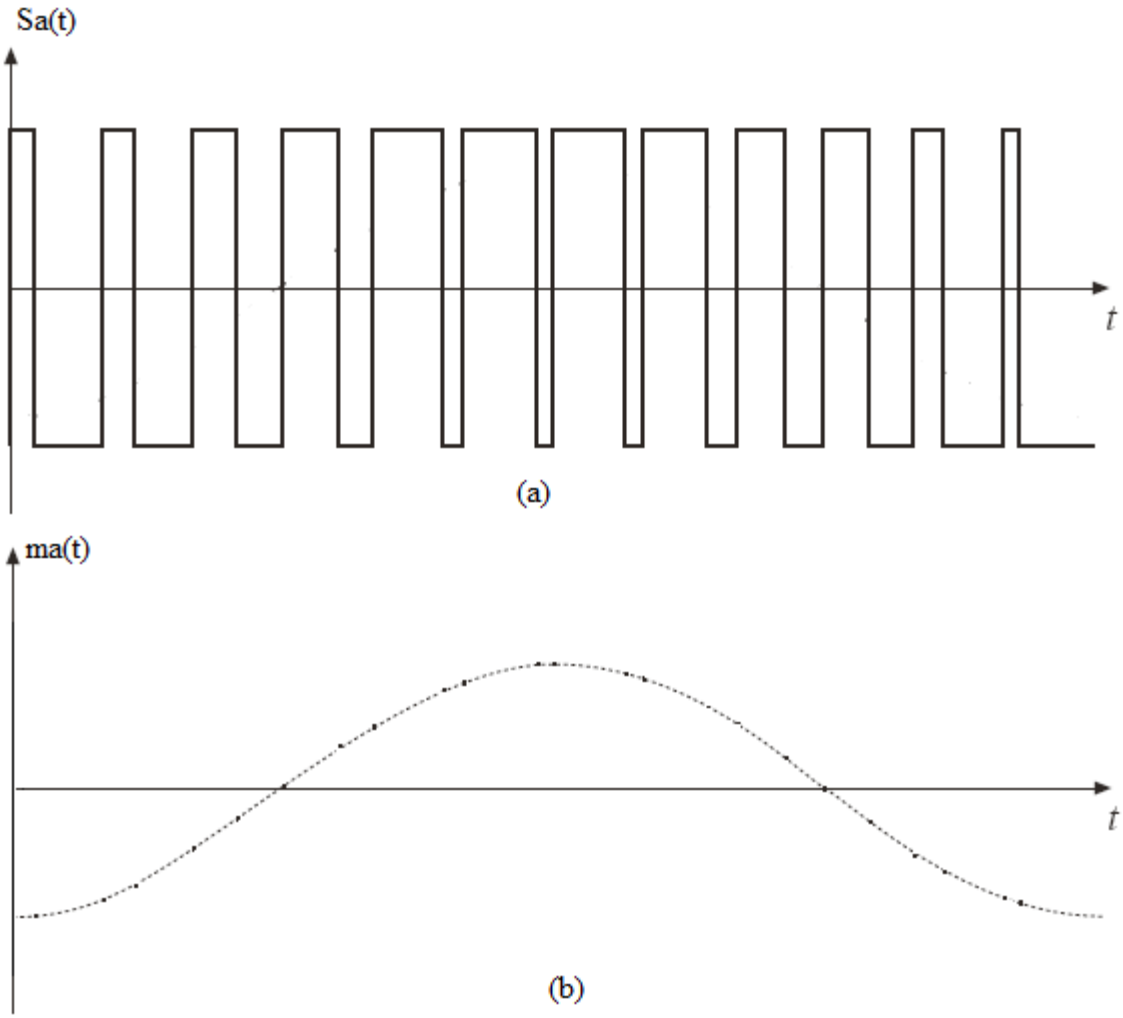

Figure 2.4(a) Typical switch function, $S_a(t)$ and (b) Input Signal, $m_a(t)$ [9]

2.3.3 VSC Voltage Control

By electronically generating the modulating signal to have the form:

$$m_a(t) = Msin(w_s t + \theta) \tag{2.4}$$

The a-phase voltage of the VSC is:

$$V_{sa}(t)=G\ Msin(w_s t + \theta) \tag{2.5}$$

Each phase voltage has electronic control over the magnitude M, the frequency w_s , and the phase angle θ .

Similarly, for the other phase, the modulating signals are generated.

$m_b(t) = Msin(w_s t + \theta - 120^0)$

$m_c(t) = Msin(w_s t + \theta - 240^0)$

The balanced 3-phase voltages $V_{sa}(t)$, $V_{sb}(t)$ and $V_{sc}(t)$ are produced by the VSC.

Figure 2.5 shows the three ideal voltage sources $V_{sa}(t)$, $V_{sb}(t)$ and $V_{sc}(t)$, which are the AC side equivalent voltages of the VSC of Figure 2.3. These voltages are the amplified form of the modulating signals $m_a(t)$, $m_b(t)$, and $m_c(t)$, the gain being $G=0.5K_1V_{dc}$.

2.3.4 *Injected DC Side Current*

When AC currents $i_a(t)$, $i_b(t)$ and $i_c(t)$ enter the VSC from the AC side, it can be shown from current continuity that the DC current flowing into the upper DC bus is,

$$I_{dc}=0.5[S_a(t)i_a(t)+ S_b(t)i_b(t)+ S_c(t)i_c(t)] \quad (2.6)$$

The ideal current source I_{dc} in Figure 2.5 is the equivalent circuit of the VSC on the DC side.

Multiplying V_{dc} in the R.H.S of Equation (2.6),

$$R.H.S=0.5[S_a(t)i_a(t)+ S_b(t)i_b(t)+ S_c(t)i_c(t)]\ V_{dc} \quad (2.7)$$

Substituting Equation (2.1) in Equation (2.7), it follows:

$$R.H.S= V_{sa}(t)i_a(t)+ V_{sb}(t)i_b(t)+ V_{sc}(t)i_c(t) =P_{ac} \quad (2.8)$$

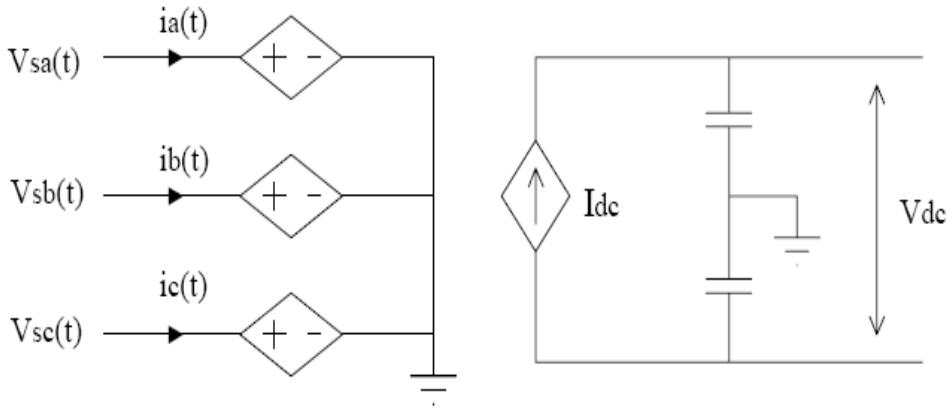

Figure 2.5 Equivalent circuit of VSC

Multiplying the L.H.S of Equation (2.6) by V_{dc}

$$L.H.S=V_{dc}I_{dc}=P_{dc} \quad (2.9)$$

Since L.H.S=R.H.S the power balance equation $P_{dc}=P_{ac}$ confirms the correctness of the formula of I_{dc} in (2.6).

As seen from the DC side, the VSC is an ideal current source. This property is important because it enables VSC stations in MVDC to be connected in parallel across a DC bus without any problem. In order to appreciate this advantage, one compares it with the thyristors based MVDC station in which the equivalent circuit on the DC side is an ideal voltage source. Paralleling thyristor based MVDC stations is problematic because communication channels are required to coordinate their DC voltage magnitudes to achieve balance.

2.4 Two Terminal VSC-MVDC

2.4.1 Main Circuits

Two VSC stations, connected back-to-back (on their DC sides) or through a long DC overhead line or cable, constitute point-to-point (two terminal) VSC-MVDC. As shown in the single line schematic in Figure 2.6, each VSC station consists of a VSC of Figure 2.3, a series filter (R_f, L_f—transformer leakage or reactor added between the VSC and the connected AC system), a DC capacitor C, and a carrier frequency filter (L_{HF}-C_{HF}). AC and DC circuit breakers, required for protection, are not shown.

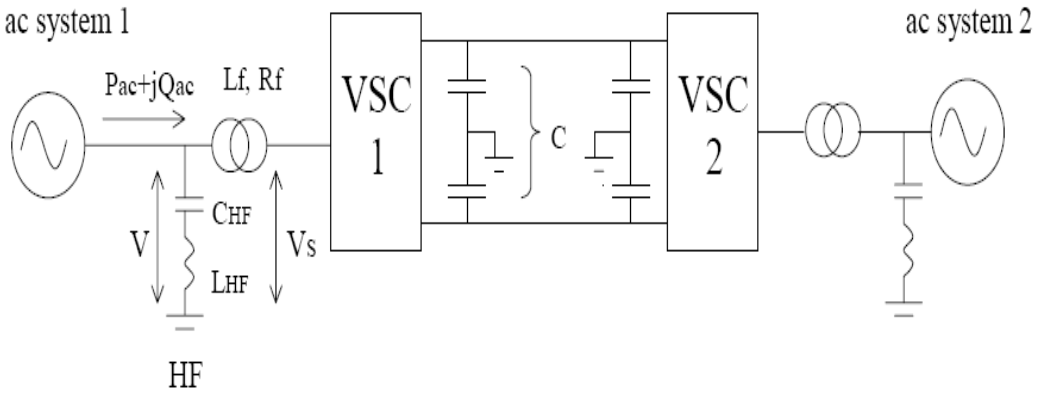

Figure 2.6 Two Terminal VSC-MVDC [7]

A. Voltage-Source Converter (VSC)

The basic building block of the VSC-MVDC is the IGBT (or GTO) bridge shown in Figure 2.3. PWM control, with a carrier frequency of 2 kHz, is considered acceptable from switching loss viewpoint. As the control requires fast response, the carrier frequency of 2 kHz assures a bandwidth of 2000/3 Hz for the signal channels.

B. Transformer

In the simulation models of the VSC station, the VSC is connected with the AC system via a wye-delta transformer. The functions of the transformer are:

1. To transform the voltage of the AC system to match the voltage level at the AC terminal of the VSC.
2. To prevent the zero-sequence current from entering the VSC during AC side faults. The AC system side of the transformer is wye connected with grounded neutral. The VSC side is delta connected and floats. Grounding on the VSC side is provided by the ground at the DC capacitor midpoint. The zero-sequence current of an unsymmetrical AC system fault has a path through the transformer wye-grounded neutral. On the VSC side, the zero-sequence current will circulate around without leaving the delta connected windings. AC faults on the VSC side are considered to be statistically rare.
3. To prevent "triplen switching harmonics" from entering the AC system since their associated currents cannot flow because of the transformer delta-connection.
4. To contribute their leakage inductances from the primary and secondary windings to the series filter inductances between the VSC and the connected AC system so that L_f is sufficiently large for the $L_f\ di_\phi/dt$ voltage (ϕ=a, b, c) to transfer energy from the lower AC voltage to the higher DC voltage during rectifier operation.

C. DC Capacitor

The DC capacitor C is designed to maintain a smooth voltage on the DC side. From the cost and fast transient response viewpoints, C should be small. The size of C has

to be kept large to meet the maximum ripple tolerance in the DC voltage. The DC capacitor also provides a diversionary path during abrupt interruptions of I_{dc} so that the large l dI_{dc}/dt voltages in the distributed DC line inductance l will be lowered. Its stored energy, $\frac{1}{2}CV_{dc}^2$, helps in smoothing the DC power flow transients.

D. Tuned L-C Carrier Frequency Filter

The series filter inductance functions as a low-pass filter for the current. However, because of the large switching voltage harmonics at carrier frequency, the Total Harmonic Distortion (THD) in voltage exceeds the standard limits. THD compliance is achieved by placing a tuned L_{HF}-C_{HF} carrier frequency in shunt at the interconnection of the AC system with the transformer as shown in Figure 2.6 [37]. The filter consists of a series L_{HF}-C_{HF} circuit tuned to the carrier frequency, which "short-circuits" the carrier frequency voltage, so that it will not propagate beyond this point.

E. DC line

VSC-MVDC is vulnerable to DC faults and research work has been carried out to investigate economical ways of protecting VSC-MVDC against DC faults by IGBT circuit breakers or AC circuit breakers on the AC side has been discussed in [18]. VSC-MVDC is not intended for very long distance DC transmission as is the case for thyristor based MVDC because of the exposure of overhead lines to lightning, which commonly is the origin of many DC faults. For the time being, VSC-MVDC, is envisioned for back-to-back asynchronous links (where both the VSC stations can be housed under a shielded roof which is grounded), for underground and underwater transmission using cables where the DC lines are not exposed to lightning.

It is interesting to note that parallel to the advancement in the VSC technology is the development of the extruded DC cable [17], which is cheaper and lighter than the commonly used self-contained oil-filled cable or mass-impregnated DC cable. The extruded DC cable is sensitive to the voltage reversal and, thus, not usable in the thyristors based MVDC, where the DC current is unidirectional but power reversals require the reversal of V_{dc}. However, the extruded DC cable is very appropriate for VSC-MVDC because the DC voltage, V_{dc}, is unidirectional and power reversals require the reversal of the direction of I_{dc}.

2.4.2 Control of VSC-MVDC

Neglecting the distributed capacitance and inductance of the DC line but retaining R_{dc} to represent the DC line resistance and using the equivalent circuit of Figure 2.5 to represent each VSC station, Figure 2.6 is modeled by Figure 2.7.

The following assumptions are made: the DC voltage of VSC1 is V_{dc1} and I_{dc} flows from VSC1 to VSC2. Then, from Kirchhoff's voltage law,

$$V_{dc2}=V_{dc1}-R_{dc}I_{dc} \tag{2.10}$$

For the DC capacitor C of VSC1, by applying Kirchhoff's current law, the dynamic equation is

$$C\frac{dV_{dc1}}{dt} = I_{dc1} - I_{dc} \tag{2.11}$$

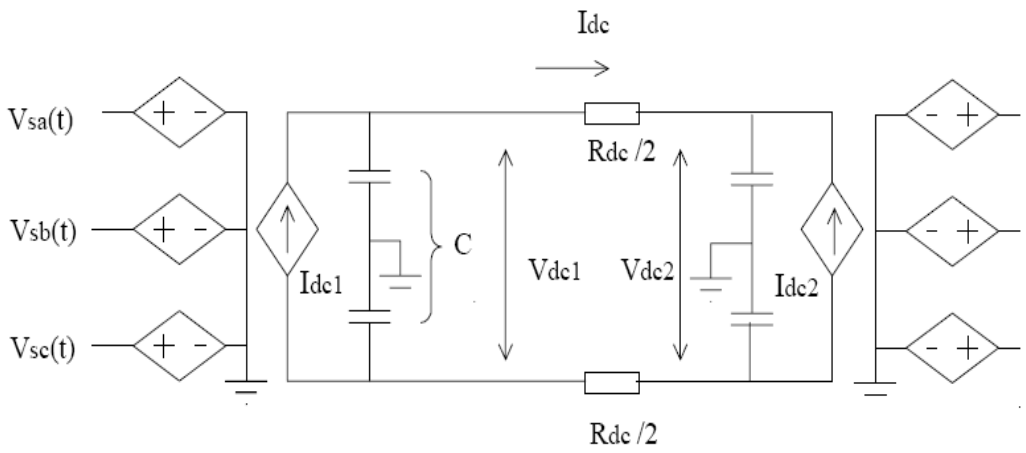

Figure 2.7 Equivalent circuit of two-terminal VSC-MVDC

where,

$I_{dc1}=P_{ac1}/V_{dc1}$ (2.12)

P_{ac1} is the AC side power of VSC1.

For the DC capacitor of VSC2, the dynamic equation is:

$$C\frac{dV_{dc2}}{dt} = I_{dc2} + I_{dc} \quad (2.13)$$

where,

$I_{dc2}=P_{ac2}/V_{dc2}$ (2.14)

P_{ac2} is the AC side power of VSC2.

2.4.3 *Coordination of Real Power through VSC-MVDC*

On the AC side of a VSC station in Figure 2.7, any demand of reactive power Q_{ac} is not apparent on the DC side. Only the real powers P_{ac1} and P_{ac2} make their appearances as I_{dc1} and I_{dc2} through Equations (2.12) and (2.14). The coordinated control of the VSC-MVDC system must be able to use local feedback control to satisfy the power balance equation:

$$P_{ac1} + P_{ac2} - R_{dc} I_{dc}^2 = 0 \quad (2.15)$$

The power balance can be maintained by making one VSC as a Power Dispatcher and the other as a DC Voltage Regulator.

A. Power Dispatcher

For example, VSC2 of Figure 2.6 is assigned the role of the Power Dispatcher, which is charged with the duty of delivering a reference power P_{ref2}. In this thesis, positive and negative signs for VSC power denote rectifier and inverter operation, respectively. The power error, $\varepsilon_p = P_{ref2} - P_{ac2}$ is then used in negative feedback through the modulation control signals to null the error.

B. DC Voltage Regulator

For example, VSC1 of Figure 2.6 is assigned the role of regulating the DC voltage. It is assigned a DC voltage reference V_{dcref} and the voltage error is used in negative feedback through the modulation control signals to null the error by injecting sufficient real power P_{ac1}. The injected DC current is I_{dc1}, obtained through Equation 2.12. When $\varepsilon_{Vdc} = 0$, $V_{dc1}=V_{dcref}$ and from Equation 2.11 $I_{dc}=I_{dc1}$. Under steady state, $-I_{dc1}=I_{dc2}$. Multiplying Equation 2.10 by I_{dc}, the power balance in Equation 2.15 is obtained.

The DC Voltage Regulator serves the functions of [38]:

(1) Providing a DC voltage reference in the DC network from which the DC voltage V_{dc2} of VSC2, for example, takes its value $V_{dc2}=V_{dcref}-I_{dc}R_{dc}$.

(2) To satisfy the power balance equation in the system, it acts as a power slack.

2.5 Advantages of VSC

Some of the advantages of employing the Voltage Source Converter (VSC) are as follows:

1. Pulse-width modulation (PWM) switching technique permits rapid, independent control of active and reactive power
2. The power flow can be reversed only by changing the direction of the DC current, without changing the polarity of DC voltage.
3. Communications are not needed for the converters and it is helpful to build shunt multi-terminal DC systems with convenient power flow control and high reliability [58].
4. Control of both active and reactive power is bi-directional and continuous across the entire operating range [59, 60].
5. Reactive power control capability allows each converter to act as a Static Synchronous Compensator (STATCOM) to regulate the AC voltage at either terminal independently [58].
6. Converters can be located at points in the network with relatively low short circuit levels minimizing the need for network reinforcements or remedial measures.
7. DC capacitor can supply reactive power [58].
8. Faster responses are attained due to the increased switching frequency of the PWM control.
9. Low-order harmonics are practically non-existent and, hence, the sizes of the harmonic filters are small.

2.6 Multi-Terminal MVDC (MTDC)

The equivalent circuit of the VSC is an ideal current source, I_{dc}, on the DC side (Figure 2.5). This feature makes it easy to integrate a number of VSCs in parallel on their DC sides to a DC grid.

2.6.1 Characteristics of MTDC

The MTDC system is, in effect, a natural extension of the two-terminal VSC-MVDC. They share the common characteristics and operating principles, which are summarized as follows:

1) The converter in a MTDC system can be either an inverter or a rectifier, depending on its power direction. In order to maintain power balance in the DC grid, at least one VSC must be assigned to operate as a DC Voltage Regulator, regulates the DC voltage across the network and automatically functions as a power slack and ensures that the power balance requirement of the DC grid is satisfied. The other VSCs operate as Power Dispatchers or inverters to passive loads.
2) Each VSC is governed by its local control and operated independently. As a result, dedicated telecommunication channels are not needed to provide fast centralized multi-converter control of the MTDC system. For the Power Dispatchers, their real power reference settings are planned in DC Load Flow studies for the entire MTDC system. Their reactive power settings can be set at any values within the MVA rating limit of the individual VSC. In the DC load flow studies, the power slack of the DC Voltage Regulator must be adequate for a sudden demand for inverter or rectifier

power to make up for the power unbalance following an accidental loss of any one VSC station.

3) If any one VSC is taken out of (or restored in) service, it is simple matter of disconnecting (or connecting) it with the DC grid. The power difference incurred by this change in connection will be made up by the DC Voltage Regulator, with care taken to ensure that the DC Voltage Regulator has the capacity to provide sufficient slack, or rescheduling power reference settings of the remaining Power Dispatchers. Therefore, the MTDC system is valued for this "plug-and-operate" capability. Within limits, the DC grid can keep on expanding by adding more VSCs. This is a valued feature since future expansion is difficult to predict.
4) The DC grid allows variable frequency generation systems (such as microturbines, wind turbines, and photovoltaic DC in a micro grid applications) to be integrated. Mass storage systems often involve a storage stage via inverter-motor and recovery through generator-rectifier. Their inverter/rectifiers can be served by the VSC stations of MTDC, with the same AC machines acting as motors/generators.

2.7 Summary

This chapter has provided the background information of the architectures proposed by the U.S. Navy, and general overview of the Voltage Source Converters (VSCs). It introduces the main circuits present in the two-terminal VSC, including its advantages, and then discusses the characteristics of the MTDC system.

CHAPTER III

PROBLEM DESCRIPTION AND TEST CASE

This chapter presents the motivation behind the work. A simplified MVDC shipboard power system test case, used in this work, will be discussed. The methodology and the proposed algorithms for the optimal control of voltage and power, developed in this work will also be discussed in this chapter.

3.1 Introduction

The VSC based MVDC SPSs are tightly-coupled, power-limited systems and their performance needs to be evaluated for security, reliability, and survivability. A Multi-Zonal MVDC SPS will employ several VSCs exchanging power through a DC network. The current flow pattern in the DC grid and the DC voltages across the VSCs will change under a system fault, accidental loss of a VSC, or the system reconfiguration. The DC over-voltage may lead to failure of the solid-state switches and DC under-voltage may cause waveform distortion. Hence, DC grid voltage should be maintained within a narrow range (usually 5% around its nominal value) under the pre-fault as well as the post-fault conditions. This requires the determination of optimal settings of DC voltage reference and power reference of the VSCs.

3.2 Problem Statement

The need for the optimal control of voltage and power at the voltage source converters has been stated in the previous sections. There is the need for calculating the DC voltage reference and power reference setting values in advance before sudden loss of any VSC, so that the DC voltage across all the VSCs will continue to lie within their desirable limits.

The purpose of this research work is to develop a control algorithm to maintain the DC voltage across all the VSCs within its desirable limits in steady state and under any contingency. This has been formulated as an optimization problem. The proposed algorithms have been coded in MATLAB.

3.3 Test Case

This section gives an outline of the test case considered in this work.

3.3.1 Simplified MVDC Multi Zonal Shipboard System

Figure 3.1 shows a simplified model of the MVDC shipboard power system, derived from the notional MVDC shipboard power system, discussed in chapter II, and shown in Figure 2.2. In Figure 3.1, VSC5 is assumed to act as DC Voltage Regulator and bus 5 is, therefore, the slack bus and all other converters are considered to operate as Power Dispatchers. The VSC3 and VSC5 are assumed to act as rectifiers, connected to the main generators on the AC side. VSC1 and VSC2 are also assumed to act as rectifiers, connected to the auxiliary generators on the AC side. All the loads are assumed to be fed from VSC4, operating as an inverter. Assumptions of all the load at one VSC can be easily extended for several VSC's with loads for more practical case studies.

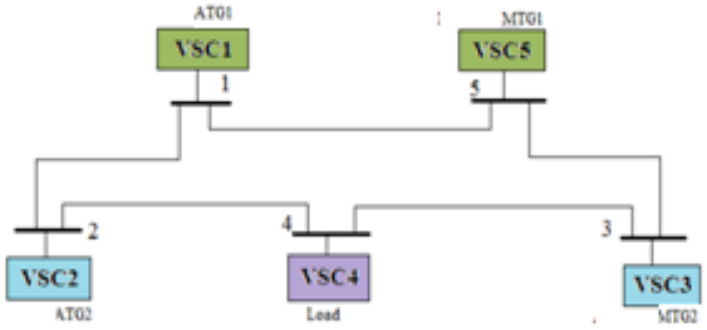

Figure 3.1 Simplified MVDC Shipboard Power System

The converter real power reference settings are given in Table 3.1 and the DC line parameters are given in Table 3.2. The DC line resistance will be a very small value as the cable length between the converters will be few meters and the value has been calculated as given in [19] for MVDC system of 5 kV voltage rating, and considering the DC resistance at 25^{o}C as 0.011 ohms per 1000 feet .

Table 3.1 Converter Power Reference Settings

VSC	**Real Power (p.u)**
#1	0.01
#2	0.02
#3	0.25
#4	-0.45
#5	Slack bus

Table 3.2 DC Line Resistance of MVDC Network

Line ID	From Bus	To Bus	DC Line Resistance (p.u)
L15	1	5	0.001
L12	1	2	0.01
L24	2	4	0.001
L43	4	3	0.001
L53	5	3	0.01

3.4 Methodology & Proposed Algorithms

The methodology followed in the thesis for the optimal control of power and voltage in a multi-zonal shipboard power system is discussed below.

For the optimal control of DC voltages, V_{dci}, across every Voltage Source Converter, a sensitivity based method was employed for tuning the DC voltage reference, V_{dcref}, of the voltage regulator. This ensures that the DC voltage at every power dispatcher is within desirable limits under steady state conditions. To achieve initial operating conditions Newton-Raphson method was used for solving the power flow equations. Then a small perturbation was introduced in the DC voltage reference and a voltage sensitivity index was used for estimating the desired voltage reference, V_{dcref}. This numerical formulation and methodology will be discussed in chapter IV. MATLAB codes have been developed to solve the Newton-Raphson and Voltage Sensitivity methods.

In most of the cases, by tuning the V_{dcref} of the DC voltage regulator, the DC voltages at every converter can be kept within desirable limits using the method described above. However, under some circumstances, such as heavily-loaded long lines in the DC network, the method does not provide a feasible solution. In such cases, the power reference settings of the power dispatchers have to be revised. For the optimal control of power and voltage at every converter, the tuning of DC voltage reference of DC voltage regulator and adjusting power reference settings of power dispatchers have to be done simultaneously. There are two sets of constraints, which have to be met. An optimization problem has been formulated and discussed in detail in Chapters V. For solving the optimization problem, three different formulations of the objective function have been used. The optimization problem has been solved using three different methods, based on a conventional and two evolutionary optimization base methods. Chapters V, VI and VII will discuss the three different algorithms in detail.

A brief overview of the three algorithms used to solve the optimization problem is presented below.

3.4.1 Conventional Method

Chapter V discusses the conventional (Lagrange Multiplier) based optimization method for optimal control of power and voltage. MATLAB code has been developed to numerically solve the Newton-Raphson method and Lagrange multiplier method.

3.4.2 Genetic Algorithms

Chapter VI discusses, in detail, the genetic algorithm approach for solving the optimization problem. A genetic algorithm was selected for solving the optimization problem because of the fact that this can be applied irrespective of the nature of the objective function and making it useful for functions that are highly nonlinear, noncontinuous. The genetic algorithm has the advantage that it does not get stuck on a local optimum, which may be the case with other algorithms. A MATLAB code for GA, available in [20], has been used. The optimization problem was defined in the separate .m file. Chapter VI presents the genetic algorithm terminologies, flowchart of the genetic algorithm operations. The chapter also discusses why evolutionary algorithm has been used to solve the optimization problem.

3.4.3 Biogeography Based Optimization

Chapter VII discusses, in detail, a Biogeography Based Optimization (BBO) method including its basic concepts, techniques (operators), and approach for solving the optimization problems. MATLAB code for BBO, available in [20], has been used. The optimization problem is defined in the separate .m file. Chapter VII presents the BBO terminologies, and a flowchart describing the BBO procedure. The BBO approach present in this work is one of the early attempts for solving the power system optimization problem. The chapter also demonstrates the performance of the BBO algorithm.

3.5 Summary

This chapter provides an overview of the problem description, the need for optimal control, and the description of the simplified MVDC shipboard test case. A brief summary about the methodology followed to solve the optimization problem and the proposed algorithms used to find the optimal values of the power and voltage reference setting at power dispatcher and voltage regulator, respectively, are also given in this chapter.

CHAPTER IV

A SENSITIVITY BASED METHOD FOR OPTIMAL VOLTAGE REGULATION

This chapter explains, in detail, the tuning of DC voltage reference of the Voltage Regulator such that the DC voltages at all other VSCs are within desired limits. It also presents the concept of Newton-Raphson power flow, in brief, followed by the voltage sensitivity index calculation. The method is applied on the simplified MVDC power system and the results are presented in this chapter.

4.1. Introduction

In a multi-zonal Voltage Source Converter (VSC) based Medium Voltage DC (MVDC) Shipboard Power System (SPS), one key issue is to ensure that the DC voltages, $\mathbf{V}_{dci}$, across every Voltage-Source Converter (say i^{th} VSC) lie within the desirable limits, $\mathbf{V}_{min} \leq \mathbf{V}_{dci} \leq \mathbf{V}_{max}$. This chapter presents, the formulation of a method in which the voltage reference, $\mathbf{V}_{dcref}$, of the DC Voltage Regulator is adjusted until $\mathbf{V}_{min} \leq \mathbf{V}_{dci} \leq \mathbf{V}_{max}$ are met, for given power reference settings of the Power Dispatchers [7, 21]. The lower limit, $\mathbf{V}_{min}$, ensures that the VSCs do not become over-modulated, where low frequency harmonics appear on the AC side. The magnitudes of the output AC voltages of the VSCs decrease with the decrease in the DC voltage. The upper limit, $\mathbf{V}_{max}$, ensures that the maximum safe voltage allowed across the solid-state switches, such as Insulated Gate

Bipolar Transistors (IGBTs), is not exceeded. It is always possible to increase $\mathbf{V}_{max}$ by increasing the number of IGBTs, connected in series in the upper and lower switches in the VSC. Thus, increasing $\mathbf{V}_{max}$ results in an increase in the cost.

The proper operation of MVDC SPS requires that, at all times, the DC voltage constraints, $\mathbf{V}_{min} \leq \mathbf{V}_{dci} \leq \mathbf{V}_{max,}$ are satisfied. For a given power reference setting to the Power Dispatchers, $[\mathbf{P}_{ref1}, \mathbf{P}_{ref2,} \ldots \mathbf{P}_{refN}]^T$, the voltage reference, $\mathbf{V}_{dcref}$, of the DC Voltage Regulator can be adjusted until $\mathbf{V}_{min} \leq \mathbf{V}_{dci} \leq \mathbf{V}_{max}$ constraints are met. When the voltage reference, $\mathbf{V}_{dcref}$, can not be found to satisfy the voltage limits, the power reference settings have to be revised, usually by lessening the loads or redispatching other generators.

The voltage limits $\mathbf{V}_{min} \leq \mathbf{V}_{dci} \leq \mathbf{V}_{max}$ have to be satisfied in steady-state and under contingencies. Following the loss of a VSC unit, the current flow pattern of the DC grid changes and DC bus voltages assume new values. As the surviving VSCs can be destroyed by over-voltages within a fraction of a second, there is no time to reset the VSC settings (i.e., the voltage reference, $\mathbf{V}_{dcref}$, of the DC Voltage Regulator and the converter's power references, $[\mathbf{P}_{ref1}, \mathbf{P}_{ref2,} \ldots, \mathbf{P}_{refN}]^T$). For this reason, $\mathbf{V}_{dcref}$, or $[\mathbf{P}_{ref1}, \mathbf{P}_{ref2,} \ldots \mathbf{P}_{refN}]^T$, which can meet the voltage constraints before and after the loss of any VSC, should be determined in the very beginning before the loss of any converter. However, one does not know, which VSC will be lost. Hence, every possible case of a VSC being lost has been included except the loss of the DC Voltage Regulator.

In a multi-zonal MVDC SPS, it is the responsibility of the DC Voltage Regulator (VR) to regulate the DC voltage across its DC bus to $\mathbf{V}_{dcref}$. In fulfilling this

responsibility, the VR automatically serves as a slack bus to balance the power in the DC network.

4.2 Methodology

4.2.1. System Under Study

Consider the multi-terminal MVDC system, as shown in Figure 4.1, which consists of N+1 VSC stations. The $(N+1)^{th}$ VSC station, VSC(N+1), is assumed to be operating as Voltage Regulator (VR) and serves as the slack bus to balance power in the DC network. The other converters are assumed to be operating as Power Dispatchers, that is, they regulate their real power outputs. The DC lines are represented by pure resistances.

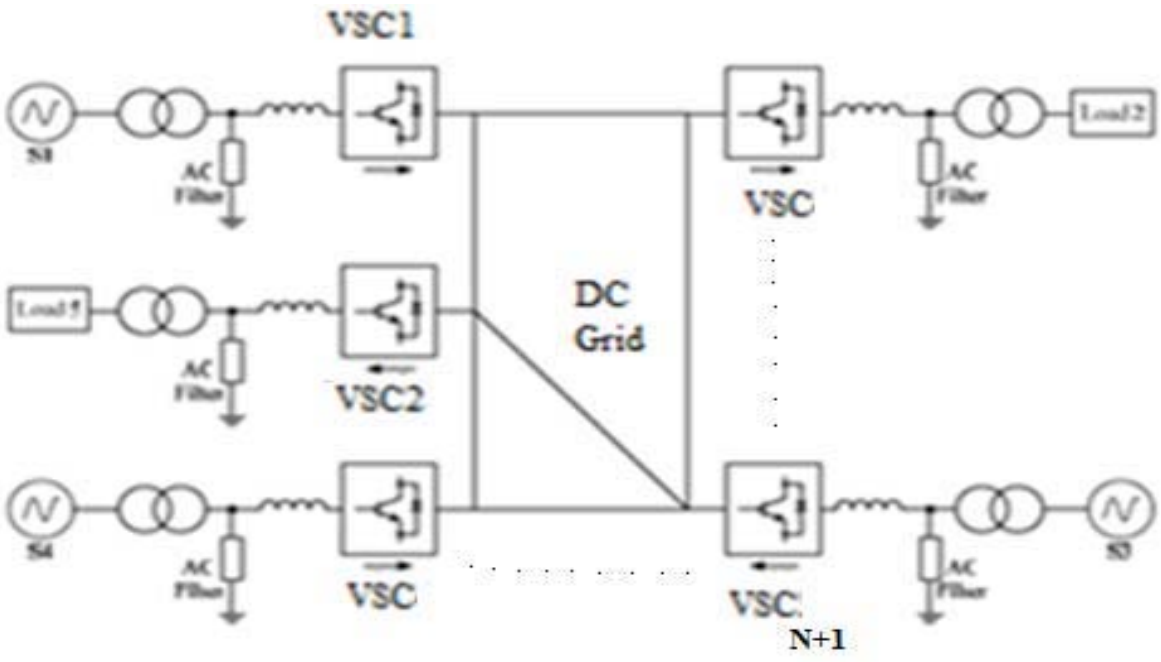

Figure 4.1 Typical (N+1) terminal VSC based MVDC system [6]

4.2.2. Network Equations

For the multi-terminal MVDC system in Figure 4.1, the relationships between the DC bus voltages and currents can be written as follows:

$$\begin{bmatrix} \mathbf{I}_{dc1} \\ \mathbf{I}_{dc2} \\ \vdots \\ \mathbf{I}_{dc(N+1)} \end{bmatrix} = \begin{bmatrix} y_{11} & y_{12} & \cdots & y_{1(N+1)} \\ y_{21} & y_{22} & \cdots & y_{2(N+1)} \\ \vdots & \vdots & \cdots & \vdots \\ y_{(N+1)1} & y_{(N+1)2} & \ddots & y_{(N+1)(N+1)} \end{bmatrix} \begin{bmatrix} \mathbf{V}_{dc1} \\ \mathbf{V}_{dc2} \\ \vdots \\ \mathbf{V}_{dc(N+1)} \end{bmatrix} \tag{4.1}$$

where,

$\mathbf{I}_{dci}$ is the dc current injected into the dc network at bus i

$\mathbf{V}_{dci}$ is the dc voltage at bus i

y_{ii} is the self admittance of bus i

y_{ij} is the mutual admittance between bus i and j

i,j = 1,2,….. (N+1)

The steady state DC power injected at bus i, $\mathbf{P}_i$, is expressed as

$$\mathbf{P}_i = \mathbf{V}_{dci}\mathbf{I}_{dci}$$

Expressing the above relation in the matrix form, one obtains

$$\begin{bmatrix} \boldsymbol{P}_1 \\ \boldsymbol{P}_2 \\ \vdots \\ \boldsymbol{P}_{N+1} \end{bmatrix} = \begin{bmatrix} \boldsymbol{V}_{dc1} & & & \\ & \boldsymbol{V}_{dc2} & & \\ & & \ddots & \\ & & & \boldsymbol{V}_{dc(N+1)} \end{bmatrix} \begin{bmatrix} \boldsymbol{I}_{dc1} \\ \boldsymbol{I}_{dc2} \\ \vdots \\ \boldsymbol{I}_{dc(N+1)} \end{bmatrix} \tag{4.2}$$

Using Equation (4.1) to replace the vector of current injections in Equation (4.2), it follows that

$$\begin{bmatrix} \mathbf{P}_1 \\ \mathbf{P}_2 \\ \vdots \\ \mathbf{P}_{N+1} \end{bmatrix} = \begin{bmatrix} \mathbf{V}_{dc1} & & & \\ & \mathbf{V}_{dc2} & & \\ & & \ddots & \\ & & & \mathbf{V}_{dc(N+1)} \end{bmatrix} \begin{bmatrix} y_{11} & y_{12} & \cdots & y_{1(N+1)} \\ y_{21} & y_{22} & \cdots & y_{2(N+1)} \\ \vdots & \vdots & \cdots & \vdots \\ y_{(N+1)1} & y_{(N+1)2} & \ddots & y_{(N+1)(N+1)} \end{bmatrix} \begin{bmatrix} \mathbf{V}_{dc1} \\ \mathbf{V}_{dc2} \\ \vdots \\ \mathbf{V}_{dc(N+1)} \end{bmatrix} \tag{4.3}$$

Equation (4.3) can also be expressed as

$$\begin{bmatrix} \boldsymbol{P} \\ P_{N+1} \end{bmatrix} = \begin{bmatrix} [\boldsymbol{Diag}(\boldsymbol{V_{dc}})] & 0 \\ 0 & V_{dc(N+1)} \end{bmatrix} \begin{bmatrix} [\boldsymbol{Y}] & \boldsymbol{y_N} \\ \boldsymbol{y_N^T} & y_{(N+1)(N+1)} \end{bmatrix} \begin{bmatrix} \boldsymbol{V_{dc}} \\ V_{dc(N+1)} \end{bmatrix} \tag{4.4}$$

where,

$\mathbf{P} = [\mathbf{P}_1, \mathbf{P}_2, \ldots\ldots \mathbf{P}_N]^T$,

$\mathbf{V}_{dc} = [\mathbf{V}_{dc1}, \mathbf{V}_{dc2}, \ldots\ldots, \mathbf{V}_{dcN}]^T$

$\mathbf{y}_N = [y_{1(N+1)}, y_{2(N+1)}, \ldots\ldots\ldots y_{N(N+1)}]^T$

$$[\boldsymbol{Diag}(\boldsymbol{V_{dc}})] = \begin{bmatrix} \boldsymbol{V}_{dc1} & & & \\ & \boldsymbol{V}_{dc2} & & \\ & & \ddots & \\ & & & \boldsymbol{V}_{dc(N+1)} \end{bmatrix}$$

$$[\boldsymbol{Y}] = \begin{bmatrix} y_{11} & y_{12} & \cdots & y_{1N} \\ y_{21} & y_{22} & & y_{2N} \\ \vdots & \vdots & \cdots & \vdots \\ y_{N1} & y_{N2} & \ddots & y_{NN} \end{bmatrix}$$

Rewriting Equation (4.4) as

$$\mathbf{P} = [\boldsymbol{Diag}(\boldsymbol{V_{dc}})]\,[\mathbf{Y}]\,\mathbf{V_{dc}} + \mathbf{V}_{dc(N+1)}[\boldsymbol{Diag}(\boldsymbol{V_{dc}})]\,\mathbf{y_N} \tag{4.5}$$

$$P_{N+1} = \mathbf{V}_{dc(N+1)}\,\boldsymbol{y_N^T}\mathbf{V_{dc}} + \mathbf{V}^2_{dc(N+1)}\,y_{(N+1)(N+1)} \tag{4.6}$$

Since the $(N+1)^{th}$ converter, VSC(N+1), is the DC Voltage Regulator, $\mathbf{V}_{dc(N+1)} = \mathbf{V}_{dcref}$. Furthermore, since VSC (N+1) is a power slack,

$$\boldsymbol{P_{N+1}} = -(\boldsymbol{P_1} + \boldsymbol{P_1} + \cdots + \boldsymbol{P_N} + \boldsymbol{P_{Loss}})$$

Therefore, Equations (4.5) and (4.6) become

$$\mathbf{P} = [\boldsymbol{Diag}(\boldsymbol{V_{dc}})]\,[\mathbf{Y}]\,\mathbf{V_{dc}} + \mathbf{V}_{dcref}\,[\boldsymbol{Diag}(\boldsymbol{V_{dc}})]\,\mathbf{y_N} \tag{4.7}$$

$$P_{N+1} = \mathbf{V}_{dc(N+1)}\,\boldsymbol{y_N^T}\mathbf{V_{dc}} + \mathbf{V}^2_{dcref}\,y_{(N+1)(N+1)} \tag{4.8}$$

The $(N+1)^{th}$ order Equations (4.1) to (4.3) are reduced to a problem of N unknowns in the N tuple voltage vector $\mathbf{V}_{dc}$ of Equation (4.7). To solve the voltages, $\boldsymbol{V}_{dc} = [\boldsymbol{V}_{dc1}, \boldsymbol{V}_{dc2}, \dots\dots\dots V_{dcN}]^T$ in the nonlinear algebraic Equation (4.7), for a given N tuple power reference setting vector $\boldsymbol{P} = \left[\boldsymbol{P}_{ref1}, \boldsymbol{P}_{ref2}, \dots\dots, \boldsymbol{P}_{refN}\right]^T$, one needs to use iterative techniques, such as the Gauss-Seidel or Newton-Raphson method. In general, the Newton-Raphson method is more preferred because of its quadratic convergence and numerical robustness.

4.2.3. Power Flow Solution by Newton-Raphson Method

As the Newton-Raphson method is well known, only an outline is presented here, with reference to solving the power flow of the DC network.

The main steps are as follows:

1) Start with $V_{dc}^{(j)} = \left[V_{dc1}^{(j)}, V_{dc2}^{(j)}, \dots\dots\dots, V_{dcN}^{(j)}\right]^T$ at the j^{th} iteration (j=1,2,..), and compute the power mismatch $\Delta P(j)$ between the vector of specified power setting $\boldsymbol{P} = \left[\boldsymbol{P}_{ref1}, \boldsymbol{P}_{ref2}, \dots\dots, \boldsymbol{P}_{refN}\right]^T$ and the calculated power at the j^{th} iteration

$$\boldsymbol{P} = \left[\boldsymbol{P}_1\left(V_{dc}^{(j)}\right), \boldsymbol{P}_2\left(V_{dc}^{(j)}\right), \dots\dots, \boldsymbol{P}_N(V_{dc}^{(j)})\right]^T$$

$$\Delta \boldsymbol{P}^{(j)} = \begin{bmatrix} \boldsymbol{P}_{ref1} - \boldsymbol{P}_1\left[V_{dc}^{(j)}\right] \\ \boldsymbol{P}_{ref2} - \boldsymbol{P}_2\left[V_{dc}^{(j)}\right] \\ \vdots \\ \boldsymbol{P}_{refN} - \boldsymbol{P}_N\left[V_{dc}^{(j)}\right] \end{bmatrix}$$

2) Calculate the N x N Jacobian matrix in the j[th] iteration, $[\mathbf{J}^{(j)}]$

$$[\boldsymbol{J}^{(j)}] = \begin{bmatrix} \frac{\partial \boldsymbol{P}_1\left[V_{dc}^{(j)}\right]}{\partial \boldsymbol{V}_{dc1}} & \frac{\partial \boldsymbol{P}_1\left[V_{dc}^{(j)}\right]}{\partial \boldsymbol{V}_{dc2}} & \cdots & \frac{\partial \boldsymbol{P}_1\left[V_{dc}^{(j)}\right]}{\partial \boldsymbol{V}_{dcN}} \\ \frac{\partial \boldsymbol{P}_2\left[V_{dc}^{(j)}\right]}{\partial \boldsymbol{V}_{dc1}} & \frac{\partial \boldsymbol{P}_2\left[V_{dc}^{(j)}\right]}{\partial \boldsymbol{V}_{dc2}} & \cdots & \frac{\partial \boldsymbol{P}_2\left[V_{dc}^{(j)}\right]}{\partial V_{dcN}} \\ \vdots & \vdots & \vdots & \vdots \\ \frac{\partial \boldsymbol{P}_N\left[V_{dc}^{(j)}\right]}{\partial \boldsymbol{V}_{dc1}} & \frac{\partial \boldsymbol{P}_N\left[V_{dc}^{(j)}\right]}{\partial \boldsymbol{V}_{dc2}} & \cdots & \frac{\partial \boldsymbol{P}_N\left[V_{dc}^{(j)}\right]}{\partial \boldsymbol{V}_{dcN}} \end{bmatrix}$$

3) Solve the following equation for voltage correction $\Delta \mathbf{V}_{dc}(j)$

$$[\boldsymbol{J}^{(j)}]\Delta V_{dc}^{(j)} = \Delta \boldsymbol{P}^{(j)}$$

4) Update the voltages

$$V_{dc}^{(j+1)} = V_{dc}^{(j)} + \Delta V_{dc}^{(j)}$$

The above process is repeated until $||\Delta \boldsymbol{P}^{(j)}|| \leq \boldsymbol{\varepsilon}$ (where $\boldsymbol{\varepsilon}$ is the error tolerance) or until the number of iterations exceeds a specified maximum. In this work, error tolerance is taken as 10e-3 p.u. on 100 MVA power base.

4.2.4. Voltage Sensitivity Indices

For an initial setting of the DC voltage reference, $\boldsymbol{V}_{dcref} = \boldsymbol{V}_{dcref}^{0}$ and for a given specification of the power reference setting vector, $\boldsymbol{P} = \left[\boldsymbol{P}_{ref1}, \boldsymbol{P}_{ref2}, \ldots\ldots, \boldsymbol{P}_{refN}\right]^T$, let the solution of Equation (4.7), obtained by the Newton-Raphson method, be $\boldsymbol{V}_{dc,0} = \left[\boldsymbol{V}_{dc1,0}, \boldsymbol{V}_{dc2,0}, \ldots\ldots\ldots, \boldsymbol{V}_{dcN,0}\right]^T$. When $\mathbf{V}_{dcref}$

has a small perturbation change from $\boldsymbol{V}_{dcref}^{0}$ to $\boldsymbol{V}_{dcref}^{0} + \Delta\boldsymbol{V}_{dcref}$, one expects that the solution to Equation (4.7) will be of the form $\boldsymbol{V}_{dc} = [\boldsymbol{V}_{dc1,0} + \Delta\boldsymbol{V}_{dc1}, \boldsymbol{V}_{dc2,0} + \Delta\boldsymbol{V}_{dc2}, \ldots\ldots\ldots, \boldsymbol{V}_{dcN,0} + \Delta\boldsymbol{V}_{dcN}]^{T}$. This selection derives the voltage sensitivities $\frac{\partial \boldsymbol{V}_{dci}}{\partial \boldsymbol{V}_{dcref}}$, i=1,2,….N, from analytic continuity, so that the perturbation DC voltage $\Delta\boldsymbol{V}_{dci}$ at the i[th] VSC station, due to the perturbation $\Delta\boldsymbol{V}_{dcref}$ can be estimated from

$$\Delta\boldsymbol{V}_{dci} = \frac{\partial V_{dci}}{\partial \boldsymbol{V}_{dcref}} \Delta\boldsymbol{V}_{dcref}.$$

Perturbing Equation (4.7) around $\boldsymbol{V}_{dc,0} = [\boldsymbol{V}_{dc1,0}, \boldsymbol{V}_{dc2,0}, \ldots\ldots\ldots, \boldsymbol{V}_{dcN,0}]^{T}$

$$\begin{bmatrix} \Delta\boldsymbol{P}_1 \\ \Delta\boldsymbol{P}_2 \\ \vdots \\ \Delta\boldsymbol{P}_N \end{bmatrix} = \begin{bmatrix} \frac{\partial \boldsymbol{P}_1}{\partial \boldsymbol{V}_{dc1}} & \frac{\partial \boldsymbol{P}_1}{\partial \boldsymbol{V}_{dc2}} & \cdots & \frac{\partial \boldsymbol{P}_1}{\partial \boldsymbol{V}_{dcN}} \\ \frac{\partial \boldsymbol{P}_2}{\partial \boldsymbol{V}_{dc1}} & \frac{\partial \boldsymbol{P}_2}{\partial \boldsymbol{V}_{dc2}} & \cdots & \frac{\partial \boldsymbol{P}_2}{\partial \boldsymbol{V}_{dcN}} \\ \vdots & \vdots & \vdots & \vdots \\ \frac{\partial \boldsymbol{P}_N}{\partial \boldsymbol{V}_{dc1}} & \frac{\partial \boldsymbol{P}_N}{\partial \boldsymbol{V}_{dc2}} & \cdots & \frac{\partial \boldsymbol{P}_N}{\partial \boldsymbol{V}_{dcN}} \end{bmatrix}_{(\boldsymbol{V}_{dc}=\boldsymbol{V}_{dc0})} \begin{bmatrix} \Delta\boldsymbol{V}_{dc1} \\ \Delta\boldsymbol{V}_{dc2} \\ \vdots \\ \Delta\boldsymbol{V}_{dcN} \end{bmatrix} + (\Delta\boldsymbol{V}_{dcref}) \begin{bmatrix} \frac{\partial \boldsymbol{P}_1}{\partial \boldsymbol{V}_{dcref}} \\ \frac{\partial \boldsymbol{P}_2}{\partial \boldsymbol{V}_{dcref}} \\ \vdots \\ \frac{\partial \boldsymbol{P}_N}{\partial \boldsymbol{V}_{dcref}} \end{bmatrix}$$

$$\begin{bmatrix} \Delta\boldsymbol{P}_1 \\ \Delta\boldsymbol{P}_2 \\ \vdots \\ \Delta\boldsymbol{P}_N \end{bmatrix} = [\boldsymbol{J}^{0}] \begin{bmatrix} \Delta\boldsymbol{V}_{dc1} \\ \Delta\boldsymbol{V}_{dc2} \\ \vdots \\ \Delta\boldsymbol{V}_{dcN} \end{bmatrix} + (\Delta\boldsymbol{V}_{dcref}) \begin{bmatrix} \frac{\partial \boldsymbol{P}_1}{\partial \boldsymbol{V}_{dcref}} \\ \frac{\partial \boldsymbol{P}_2}{\partial \boldsymbol{V}_{dcref}} \\ \vdots \\ \frac{\partial \boldsymbol{P}_N}{\partial \boldsymbol{V}_{dcref}} \end{bmatrix} \tag{4.8}$$

where,

$\Delta\boldsymbol{V}_{dcref}$ is the perturbation of the voltage reference of the DC voltage regulator

$[\boldsymbol{J}^{0}]$ is the Jacobian matrix evaluated at $\boldsymbol{V}_{dc0}$

As all the VSCs, except the VSC(N+1), are Power Dispatchers, their real power perturbations are maintained through feedback control to be:

$$\Delta \boldsymbol{P}_1 = \Delta \boldsymbol{P}_2 = \cdots = \Delta \boldsymbol{P}_N = 0.$$

Therefore, equation (4.8) becomes

$$0 = [\boldsymbol{J}^0] \begin{bmatrix} \Delta \boldsymbol{V}_{dc1} \\ \Delta \boldsymbol{V}_{dc2} \\ \vdots \\ \Delta \boldsymbol{V}_{dcN} \end{bmatrix} + \left(\Delta \boldsymbol{V}_{dcref}\right) \begin{bmatrix} \frac{\partial \boldsymbol{P}_1}{\partial \boldsymbol{V}_{dcref}} \\ \frac{\partial \boldsymbol{P}_2}{\partial \boldsymbol{V}_{dcref}} \\ \vdots \\ \frac{\partial \boldsymbol{P}_N}{\partial \boldsymbol{V}_{dcref}} \end{bmatrix} \tag{4.9}$$

Premultiplying Equation (4.9) by $[\boldsymbol{J}^0]^{-1}$ and rearranging the equation, one obtains

$$\begin{bmatrix} \Delta \boldsymbol{V}_{dc1} \\ \Delta \boldsymbol{V}_{dc2} \\ \vdots \\ \Delta \boldsymbol{V}_{dcN} \end{bmatrix} = -[\boldsymbol{J}^0]^{-1} \left(\Delta \boldsymbol{V}_{dcref}\right) \begin{bmatrix} \frac{\partial \boldsymbol{P}_1}{\partial \boldsymbol{V}_{dcref}} \\ \frac{\partial \boldsymbol{P}_2}{\partial \boldsymbol{V}_{dcref}} \\ \vdots \\ \frac{\partial \boldsymbol{P}_N}{\partial \boldsymbol{V}_{dcref}} \end{bmatrix} = \left(\Delta \boldsymbol{V}_{dcref}\right) \begin{bmatrix} \frac{\partial \boldsymbol{V}_1}{\partial \boldsymbol{V}_{dcref}} \\ \frac{\partial \boldsymbol{V}_2}{\partial \boldsymbol{V}_{dcref}} \\ \vdots \\ \frac{\partial \boldsymbol{V}_N}{\partial \boldsymbol{V}_{dcref}} \end{bmatrix} \tag{4.10}$$

Since, by definition

$$\begin{bmatrix} \Delta \boldsymbol{V}_{dc1} \\ \Delta \boldsymbol{V}_{dc2} \\ \vdots \\ \Delta \boldsymbol{V}_{dcN} \end{bmatrix} = \left(\Delta \boldsymbol{V}_{dcref}\right) \begin{bmatrix} \frac{\partial \boldsymbol{V}_1}{\partial \boldsymbol{V}_{dcref}} \\ \frac{\partial \boldsymbol{V}_2}{\partial \boldsymbol{V}_{dcref}} \\ \vdots \\ \frac{\partial \boldsymbol{V}_N}{\partial \boldsymbol{V}_{dcref}} \end{bmatrix}$$

It follows that

$$\begin{bmatrix} \frac{\partial \boldsymbol{V}_1}{\partial \boldsymbol{V}_{dcref}} \\ \frac{\partial \boldsymbol{V}_2}{\partial \boldsymbol{V}_{dcref}} \\ \vdots \\ \frac{\partial \boldsymbol{V}_N}{\partial \boldsymbol{V}_{dcref}} \end{bmatrix} = -[\boldsymbol{J}^0]^{-1} \left(\Delta \boldsymbol{V}_{dcref}\right) \begin{bmatrix} \frac{\partial \boldsymbol{P}_1}{\partial \boldsymbol{V}_{dcref}} \\ \frac{\partial \boldsymbol{P}_2}{\partial \boldsymbol{V}_{dcref}} \\ \vdots \\ \frac{\partial \boldsymbol{P}_N}{\partial \boldsymbol{V}_{dcref}} \end{bmatrix} \tag{4.11}$$

Equation (4.11) gives the sensitivity of the voltage $\mathbf{V}_{dci}$ (i=1,2,…N) to the voltage reference $\Delta \mathbf{V}_{dcref}$. This type of sensitivity information is very useful for estimating the expected voltage changes which result from the variation of the voltage reference.

Theoretically, Equation (4.11) is accurate only in the vicinity of $\mathbf{V}_{dc0}$, the steady-state operation point. When this operating point varies, the sensitivities should be re-calculated.

4.2.5. Estimating the Desired Voltage Reference

Having derived the voltage sensitivities, the perturbation voltages $\Delta \boldsymbol{V}_{dci} = \frac{\partial \boldsymbol{V}_{dci}}{\partial \boldsymbol{V}_{dcref}} \Delta \boldsymbol{V}_{dcref}$, i=1,2,…N, are readily estimated to form the voltage vector $\boldsymbol{V}_{dc} = \left[\boldsymbol{V}_{dc1,0} + \Delta \boldsymbol{V}_{dc1}, \boldsymbol{V}_{dc2,0} + \Delta \boldsymbol{V}_{dc2}, \ldots\ldots, \boldsymbol{V}_{dcN,0} + \Delta \boldsymbol{V}_{dcN}\right]^T$. It is a matter of adjusting $\Delta \boldsymbol{V}_{dcref}$ in $\boldsymbol{V}_{dcref} = \boldsymbol{V}^0_{dcref} + \Delta \boldsymbol{V}_{dcref}$ until $\mathbf{V}_{dci}$ satisfies the constraints $\boldsymbol{V}_{min} \leq \boldsymbol{V}_{dci} \leq \boldsymbol{V}_{max}$, i=1,2,…N. Before proceeding to show how $\Delta \boldsymbol{V}_{dcref}$ will be adjusted, it is necessary to introduce a superscript k to identify the operating conditions which have to be treated simultaneously. As has already been alluded to, all the reference settings, $\mathbf{V}_{dcref}$ and $\mathbf{P}_{refi}$, i=1,2,….N must be determined so that the constraints $\boldsymbol{V}_{min} \leq \boldsymbol{V}_{dci} \leq \boldsymbol{V}_{max}$, i=1,2,…N are always* satisfied. This is because there is no time to reset the references under transients before the over-voltages would destroy the IGBTs.

Note: Always* means, before the loss of a VSC station and after the loss of VSC_k, k=1,2,….N.

A. Pre- and Post-fault conditions

The superscript k is used to identify the post-fault condition when the k^{th} converter (VSC_k) is lost. When the k^{th} converter (VSC_k) is permanently lost then the vector of

power reference setting of the k[th] VSC station is $\mathbf{P}_{\text{ref k}}$=0. The power reference setting vector is $\boldsymbol{P}^k = \left[\boldsymbol{P}_{ref1}, \boldsymbol{P}_{ref2}, \ldots\ldots, \boldsymbol{P}_{ref(k-1)}, \boldsymbol{P}_{refk} = 0, \boldsymbol{P}_{ref(k+1)}, \ldots. \boldsymbol{P}_{refN}\right]^T$. The solution to Equation (4.7) is $\boldsymbol{V}_{dc}^k = \left[\boldsymbol{V}_{dc1}^k, \boldsymbol{V}_{dc2}^k, \ldots\ldots, \boldsymbol{V}_{dcN}^k\right]^T$. The pre-fault condition is identified by the superscript k=0. Thus, the vector of pre-fault power reference setting is $\boldsymbol{P}^0 = \left[\boldsymbol{P}_{ref1}, \boldsymbol{P}_{ref2}, \ldots\ldots, \boldsymbol{P}_{refN}\right]^T$. The solution to Equation (4.7) is the voltage vector $\boldsymbol{V}_{dc}^0 = [\boldsymbol{V}_{dc1}^0, \boldsymbol{V}_{dc2}^0, \ldots\ldots, \boldsymbol{V}_{dcN}^0]^T$, where the superscript 0 in $\boldsymbol{V}_{dci}^0$ $(for\ k = 0)$ identifies it as pre-fault solution.

B. Limits on $\Delta\mathbf{V}_{\text{dcref}}$, $\Delta\mathbf{V}_{\text{dci,refmin}}^{\text{k}}$ and $\Delta\mathbf{V}_{\text{dci,refmax}}^{\text{k}}$

The unknown voltages $\boldsymbol{V}_{dc}^0$ and $\boldsymbol{V}_{dc}^k$ are solved using an initial guess of the DC voltage reference setting $\boldsymbol{V}_{dcref}^0$. The bus voltage solutions $\boldsymbol{V}_{dci}^k$ (i=1,2,…N, and k=0,1,2,…N), in general, do not satisfy all $\boldsymbol{V}_{min} \leq \boldsymbol{V}_{dci}^k \leq \boldsymbol{V}_{max}$ constraints. To bring the voltages back within their limits, one needs to find a new value of the DC voltage reference setting from the initial guess $\boldsymbol{V}_{dcref}^0$. Let $\Delta\boldsymbol{V}_{dcref}$ represent a small change in $\boldsymbol{V}_{dcref}^0$. Then $\boldsymbol{V}_{dcref} = \boldsymbol{V}_{dcref}^0 + \Delta\boldsymbol{V}_{dcref}$ and the new value of $\boldsymbol{V}_{dci}^k$ is approximately given by $\boldsymbol{V}_{dci}^k + \frac{\partial \boldsymbol{V}_{dci}^k}{\partial \boldsymbol{V}_{dcref}} \Delta\boldsymbol{V}_{dcref}$. From Equation (4.11), $\frac{\partial \boldsymbol{V}_{dci}^k}{\partial \boldsymbol{V}_{dcref}}$ is obtained by solving the N-voltage sensitivity vector $\left[\frac{\partial \boldsymbol{V}_{dc1}^k}{\partial \boldsymbol{V}_{dcref}}, \frac{\partial \boldsymbol{V}_{dc2}^k}{\partial \boldsymbol{V}_{dcref}}, \ldots\ldots\ldots, \frac{\partial \boldsymbol{V}_{dcN}^k}{\partial \boldsymbol{V}_{dcref}}\right]^T$.

From the initial guess $\boldsymbol{V}_{dcref}^0$, one can infer what $\Delta\boldsymbol{V}_{dcref}$ should be from the inequality:

$$\boldsymbol{V}_{min} \leq \boldsymbol{V}_{dci}^k + \frac{\partial \boldsymbol{V}_{dci}^k}{\partial \boldsymbol{V}_{dcref}} \Delta\boldsymbol{V}_{dcref} \leq \boldsymbol{V}_{max} \tag{4.12}$$

Subtracting $\boldsymbol{V}_{dci}^k$ throughout equation (4.12) yields,

$$\boldsymbol{V}_{min} - \boldsymbol{V}_{dci}^{k} \leq \frac{\partial \boldsymbol{V}_{dci}^{k}}{\partial \boldsymbol{V}_{dcref}} \Delta \boldsymbol{V}_{dcref} \leq \boldsymbol{V}_{max} - \boldsymbol{V}_{dci}^{k} \tag{4.13}$$

where, i=1,2,3…N and k=0,1,2,…N.

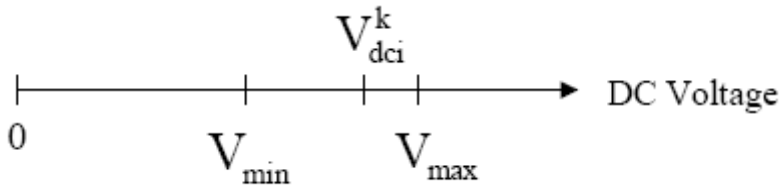

Figure 4.2(a) The solution range for $\boldsymbol{V}_{dci}^{k}$ [5]

Figure 4.2 (a) illustrates the solution $\boldsymbol{V}_{dci}^{k}$, of an ith VSC (VSC$_i$) for the kth case, which lies between the voltage limits $\mathbf{V}_{min}$ and $\mathbf{V}_{max}$. In this illustration, the amount $(\boldsymbol{V}_{max} - \boldsymbol{V}_{dci}^{k})$, before the upper limit $\mathbf{V}_{max}$ is reached, means that there is room to increase $\Delta\mathbf{V}_{ref}$. Using the computed voltage sensitivity index, the upper limit, placed on $\Delta\mathbf{V}_{dcref}$ is,

$$\Delta \boldsymbol{V}_{dci,refmax}^{k} = (\boldsymbol{V}_{max} - \boldsymbol{V}_{dci}^{k}) \Big/ \frac{\partial \boldsymbol{V}_{dci}^{k}}{\partial \boldsymbol{V}_{dcref}} \tag{4.14}$$

The amount $\left(\boldsymbol{V}_{min} - \boldsymbol{V}_{dci}^{k}\right)$, before the lower limit $\mathbf{V}_{min}$ is reached, means that the lower limit, placed on $\Delta\mathbf{V}_{dcref}$ is,

$$\Delta \boldsymbol{V}_{dci,refmin}^{k} = (\boldsymbol{V}_{min} - \boldsymbol{V}_{dci}^{k}) \Big/ \frac{\partial \boldsymbol{V}_{dci}^{k}}{\partial \boldsymbol{V}_{dcref}} \tag{4.15}$$

Dividing Equation (4.13) by $\frac{\partial \boldsymbol{V}_{dci}^{k}}{\partial \boldsymbol{V}_{dcref}}$ and using the definition of Equation (4.14) and Equation (4.15), the constraints placed on $\boldsymbol{V}_{dci}^{k}$ are now placed on $\Delta \boldsymbol{V}_{dcref}$ as,

$$\Delta \boldsymbol{V}_{dci,refmin}^{k} \leq \Delta \boldsymbol{V}_{dcref} \leq \Delta \boldsymbol{V}_{dci,refmax}^{k}$$

These are illustrated in Figure 4.2 (b).

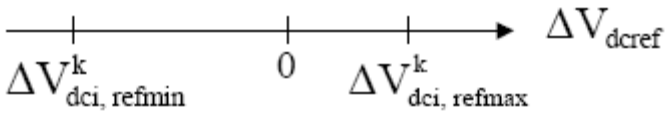

Figure 4.2(b) Allowed $\Delta \boldsymbol{V}_{dcref}$ due to $\boldsymbol{V}_{dci}^{k}$limits [5]

C. Common Range of $\Delta \mathbf{V}_{\text{dcref}}$

Figure 4.3 illustrates some lower limits $\Delta \boldsymbol{V}_{dci,refmin}^{k}$ and upper limits $\Delta \boldsymbol{V}_{dci,refmax}^{k}$, taken from cases similar to Figure 4.2(b). The problem of finding the $\boldsymbol{V}_{dcref} = \boldsymbol{V}_{dcref}^{0} + \Delta \boldsymbol{V}_{dcref}$, for which $\boldsymbol{V}_{min} \leq \boldsymbol{V}_{dci}^{k} \leq \boldsymbol{V}_{max}$, i=1,2,…N and k=0,1,2….N, is reduced to finding the upper and lower bounds for $\Delta \mathbf{V}_{\text{dcref}}$. These are, the upper bound, $\Delta \mathbf{V}_{\text{dcrefmax}}$

$$\Delta \boldsymbol{V}_{dcfrefmax} = min\{\Delta \boldsymbol{V}_{dci,refmax}^{k}, i = 1,2, \ldots . N, k = 0,1,2, \ldots N\} \quad (4.16)$$

and, the lower bound, $\Delta \mathbf{V}_{\text{dcrefmin}}$

$$\Delta \boldsymbol{V}_{dcfrefmin} = max\{\Delta \boldsymbol{V}_{dci,refmin}^{k}, i = 1,2, \ldots . N, k = 0,1,2, \ldots N\} \quad (4.17)$$

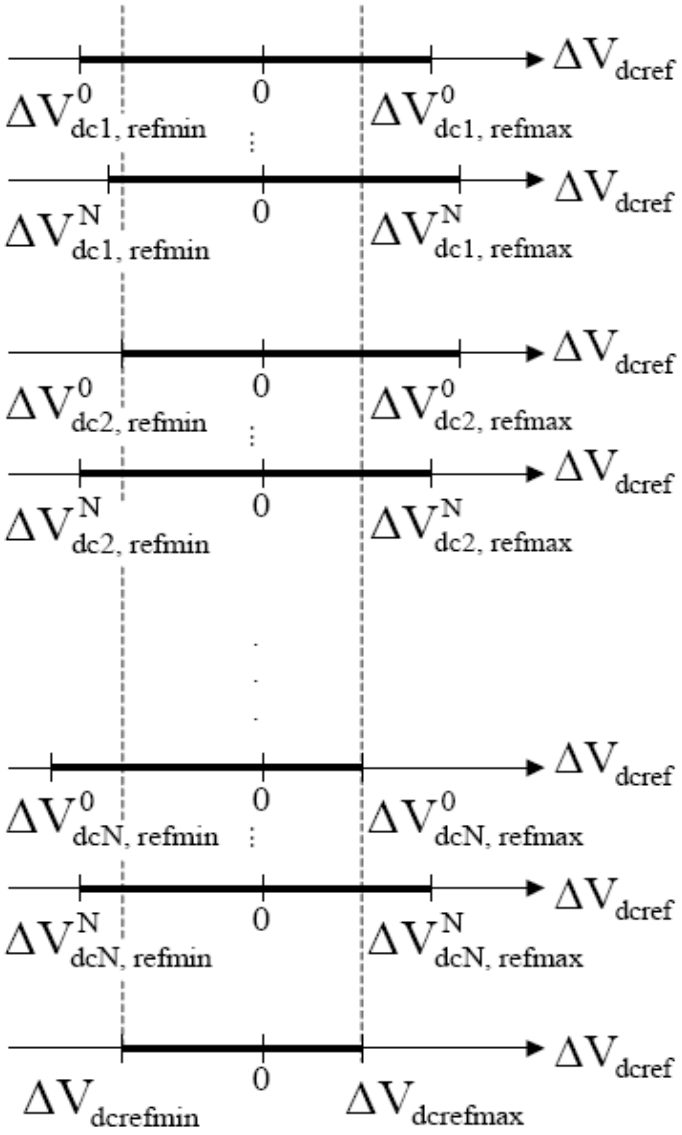

Figure 4.3 The common range of $\Delta \boldsymbol{V}_{dcref}$ subject to voltage limits on all $\boldsymbol{V}_{dci}^{k}$ [5]

Therefore, the suitable setting for $\mathbf{V}_{\text{dcref}}$ would be

$$\boldsymbol{V}_{dcref}^{0} + \Delta \boldsymbol{V}_{dcrefmin} \leq \boldsymbol{V}_{dcref} \leq \boldsymbol{V}_{dcref}^{0} + \Delta \boldsymbol{V}_{dcrefmax} \tag{4.18}$$

Note that Equation (4.18) is obtained via the sensitivity $\frac{\partial \boldsymbol{V}_{dci}^{k}}{\partial \boldsymbol{V}_{dcref}}$ (i=1,2,…N and k=0,1,2….N), i.e., using the linear term of the Taylor series, which expands $\Delta \boldsymbol{V}_{dci}^{k}$ in terms of $\Delta \mathbf{V}_{\text{dcref}}$. Normally, it has sufficient accuracy to make $\boldsymbol{V}_{dci}^{k}$ to comply with $\boldsymbol{V}_{min} \leq \boldsymbol{V}_{dci}^{k} \leq \boldsymbol{V}_{max}$. However, it is recommended to recalculate power flows with the selected $\boldsymbol{V}_{dcref}^{*}$ from Equation (4.18). If $\boldsymbol{V}_{dcref}^{*}$ is not able to derive the dc voltages to stay in the specified margin, it can be a new guess for $\mathbf{V}_{\text{dcref}}$, then repeat the voltage sensitivity calculation and update Equation (4.18).

4.3 Test Results

The voltage sensitivity based approach was applied to a simplified model of the MVDC shipboard power system, shown in Figure 3.1, in chapter III. VSC5 is taken to operate in voltage regulator mode and other VSCs in power dispatcher mode. The acceptable range of reference settings of the voltage regulator $\boldsymbol{V}_{dcref}^{*}$ has been determined for all the conditions, including all VSCs in service and loss of any one of VSCs except for VSC operating as Voltage Regulator (i.e. VSC5). The maximum of all V_{dcrefmin} and the minimum of all V_{dcrefmax} determined for all conditions are taken as the minimum and maximum values of the V_{dcref}. Table 4.1 lists the range of allowable $\mathbf{V}_{\text{dcref}}$ for k=0,1,2,3,4.

From Table 4.1, it can be observed that the acceptable range for voltage reference setting of the VSC5 (voltage regulator) is 0.9516 p.u. to1.0485p.u. In order to verify the effectiveness of the common bound of $\mathbf{V}_{\text{dcref}}$, Tables 4.2 and 4.3 list the corresponding

bus voltages when the voltage reference $\mathbf{V}_{dcref}$ is set to 0.9527p.u. and 1.0485p.u., respectively.

Table 4.1 Allowable $\mathbf{V}_{ref}$ for different conditions and common accepted bound for the reference setting of VSC5.

No.	Conditions	Allowable Voltage Reference (p.u)	
		$\mathbf{V}_{dcrefmin}$	$\mathbf{V}_{dcrefmax}$
1	All VSCs in service	0.9513	1.05
2	Loss of VSC1	**0.9516**	1.0489
3	Loss of VSC2	0.9513	1.0487
4	Loss of VSC3	0.9473	1.05
5	Loss of VSC4	0.9490	**1.0485**
Accepted Common range for all conditions		**0.9516**	**1.0485**

Tables 4.2 and 4.3, show that all the DC bus voltages are within the specified limits, i.e., between V_{min} (0.95 p.u.) and V_{max} (1.05 p.u). This indicates that the calculated voltage reference bound satisfies voltage constraints in all the conditions in the given system.

Table 4.2 DC bus voltages with $\mathbf{V}_{dcref}$=0.9527p.u.

No.	Conditions	DC Voltage (p.u.)				
		$\mathbf{V}_{dc1}$	$\mathbf{V}_{dc2}$	$\mathbf{V}_{dc3}$	$\mathbf{V}_{dc4}$	$\mathbf{V}_{dc5}$
1	All VSCs in service	0.9527	0.9526	0.9518	0.9515	0.9527
2	Loss of VSC1	0.9527	0.95 26	0.9518	0.9516	0.9527
3	Loss of VSC2	0.9526	0.9525	0.9518	0.9515	0.9527
4	Loss of VSC3	0.9525	0.9523	0.9540	0.9501	0.9527
5	Loss of VSC4	0.9529	0.9530	0.9530	0.95 41	0.9527

Table 4.3 DC bus voltages with $\mathbf{V}_{dcref}$=1.0485p.u.

No.	Conditions	DC Voltage (p.u.)				
		$\mathbf{V}_{dc1}$	$\mathbf{V}_{dc2}$	$\mathbf{V}_{dc3}$	$\mathbf{V}_{dc4}$	$\mathbf{V}_{dc5}$
1	All VSCs in service	1.0485	1.0484	1.0477	1.0473	1.0485
2	Loss of VSC1	1.0485	1.0484	1.0477	1.0473	1.0485
3	Loss of VSC2	1.0485	1.0484	1.0477	1.0473	1.0485
4	Loss of VSC3	1.0484	1.0482	1.0426	1.0460	1.0485
5	Loss of VSC4	1.0487	1.0489	1.0485	1.05	1.0485

4.4. Summary

The proper operation of MVDC SPS requires that, all the times, the DC voltage constraints, $\mathbf{V}_{min} \leq \mathbf{V}_{dci} \leq \mathbf{V}_{max,}$ are satisfied, even under the condition that any VSC station can be lost through an accidental fault. For a given power reference setting to the Power Dispatchers, $[\mathbf{P}_{ref1}, \mathbf{P}_{ref2,} \ldots \mathbf{P}_{refN}]^T$, the voltage reference, $\mathbf{V}_{dcref}$, of the DC Voltage Regulator can be adjusted until $\mathbf{V}_{min} \leq \mathbf{V}_{dci} \leq \mathbf{V}_{max}$ are met. This chapter presented a voltage sensitivity method [5] for ensuring that all the DC voltages meet their voltage constraints by adjusting the DC voltage reference setting of the VSC acting as Voltage Regulator. This method has been applied to a simplified model of the Shipboard MVDC power system and the results are presented in this chapter.

CHAPTER V

A CONVENTIONAL OPTIMIZATION BASED METHOD FOR OPTIMAL POWER AND VOLTAGE CONTROL

This chapter gives a brief introduction to the conventional optimization based method, explains in detail the mathematical formulation of the optimization based method using conventional Lagrange multiplier approach, and the major solution steps for calculating the VSCs' reference power settings. The three alternative formulations, with different objective functions, are considered in this work and are included in this chapter. At the end of this chapter, the results are presented with the three different objective functions.

5.1 Introduction

In most of the cases, by adjusting $\mathbf{V}_{dcref}$ of the DC Voltage Regulator (VR), the DC voltages can be kept within desirable margins, using the method described in the chapter IV. However, under certain circumstances, such as in heavily-loaded long lines in the DC network, the method does not provide a feasible solution.

In such cases, the power reference settings of the Power Dispatchers have to be simultaneously revised. In this chapter, it is assumed that the Voltage Regulator (VR) has enough MVA rating to supply mismatch power and maintain power balance in the DC

network. In revising the power reference settings of the converter stations, it is necessary to consider that the power reference setting of each VSC is kept within its operational lower and upper limits, $\mathbf{P}_{mini}$ and $\mathbf{P}_{maxi}$, respectively. Thus, there are, now, two sets of constraints, which have to be met:

1. The DC voltage constraints, $\boldsymbol{V}_{min} \leq \boldsymbol{V}_{dci}^{k} \leq \boldsymbol{V}_{max}$, i=1,2,…N and k=0,1,2….N

The voltage vector $\boldsymbol{V}_{dc}^{k} = \left[\boldsymbol{V}_{dc1}^{k}, \boldsymbol{V}_{dc2}^{k}, \ldots\ldots, \boldsymbol{V}_{dcN}^{k}\right]^{T}$ is the solution of equation (4.7) in chapter IV, for the power reference setting vector

$$\boldsymbol{P}^{k} = \left[\boldsymbol{P}_{ref1}, \boldsymbol{P}_{ref2}, \ldots\ldots, \boldsymbol{P}_{ref(k-1)}, \boldsymbol{P}_{refk} = 0, \boldsymbol{P}_{ref(k+1)}, \ldots\ldots, \boldsymbol{P}_{refN}\right]^{T}$$

As discussed in chapter IV, the superscript k identifies the case when the k^{th} VSC is lost. The case k=0, is for the pre-faulted case.

2. The operational power limits of the VSCs, $\mathbf{P}_{mini} < \mathbf{P}_{refi} < \mathbf{P}_{maxi}$, i=1,2,….N.

In the first place, there is a physical power constraint imposed on each VSC, which is dictated by the MVA rating. However, the constraints $\mathbf{P}_{mini} < \mathbf{P}_{refi} < \mathbf{P}_{maxi}$, i=1,2,….N, may also be applied to determine the operation of the multi-zonal MVDC. For example, Power Dispatchers may have to follow power schedules determined by the contracts and the limit set the envelope, $\mathbf{P}_{mini} < \mathbf{P}_{refi} < \mathbf{P}_{maxi}$, i=1,2,….N of the power schedules. Power Dispatchers, which serve sensitive loads (i.e. near-zero tolerance in power deviations), are given narrow power limits ($\mathbf{P}_{mini}$,$\mathbf{P}_{maxi}$).

5.2 Proposed Optimization Based Problem Formulation

In finding the power reference settings, which can satisfy both the voltage and the power constraints, the problem is formulated as an optimization problem, which is then

solved by the conventional Lagrange Multiplier method [12] in this chapter. In order to illustrate the basic concepts, a scalar example is first presented before proceeding to the vectorial formulation.

A. An Example of Scalar Formulation

Consider a Three-terminal VSC-MVDC with three VSC stations, VSC1, VSC2 and VSC3, as shown in Figure 5.1. VSC3 is assumed to have enough MVA rating and operate as a DC Voltage Regulator, whose DC voltage is regulated at V_{dcref}. The DC voltage of VSC1 and VSC2, $\mathbf{V}_{dci}$, i=1,2, has to be kept within limits, i.e., $\mathbf{V}_{min} \leq \mathbf{V}_{dci} \leq \mathbf{V}_{max}$. The quadratic voltage function $\boldsymbol{C_V = W_{VN}(V_{min} - V_{dci})^2 + W_{VX}(V_{dci} - V_{max})^2}$, with $\mathbf{W_{VN}}$ and $\mathbf{W_{VX}}$ being voltage penalty factors, has a minimum at $\boldsymbol{V_{dci} = (V_{min} + V_{max})/2}$ if (W_{VN}=W_{VX}), which is an acceptable solution since $\mathbf{V}_{dci}$ lies between the upper and lower limits.

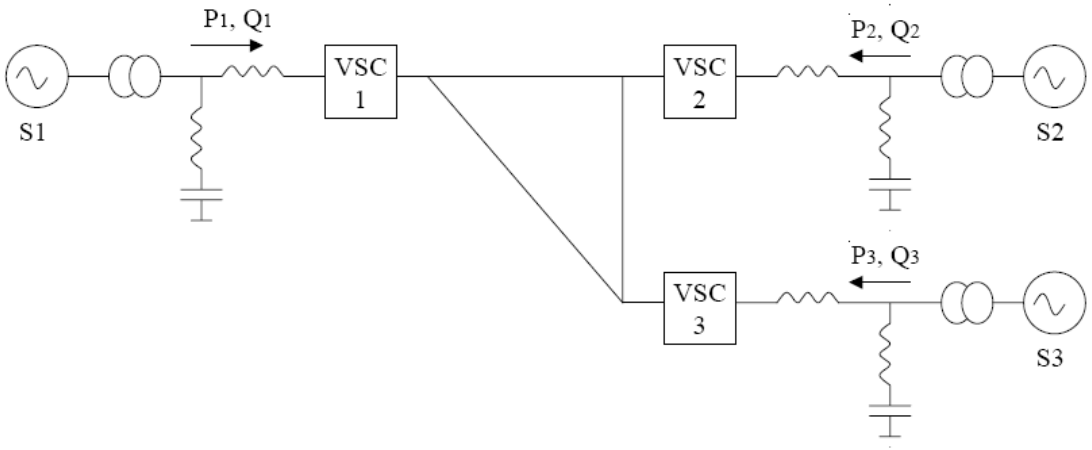

Figure 5.1 A Sample Three-Terminal VSC-MVDC system [7]

The power reference setting of VSC1, $\mathbf{P}_{refi}$, i=1,2, has to be kept within power limits, $\mathbf{P}_{mini}<\mathbf{P}_{refi}<\mathbf{P}_{maxi}$. The quadratic power function $\boldsymbol{C_P = W_{PN}(P_{mini} - P_{refi})^2 + W_{PX}(P_{refi} - P_{maxi})^2}$, with $\mathbf{W_{PN}}$ and $\mathbf{W_{PX}}$ being power penalty factors, has a minimum at $\boldsymbol{P_{refi} = (P_{mini} + P_{maxi})/2}$ if (W_{PN}=W_{PX}), because it lies between the power limits is an acceptable solution.

Therefore, the overall objective function to be minimized [5] is:

$$\boldsymbol{C = C_V + C_P}$$

$$\boldsymbol{C = W_{VN}(V_{min} - V_{dci})^2 + W_{VX}(V_{dci} - V_{max})^2 + W_{PN}(P_{mini} - P_{refi})^2 + W_{PX}(P_{refi} - P_{maxi})^2}$$

However, $\mathbf{V}_{dci}$ is not an independent variable, being a solution in the nonlinear power equation $\mathbf{F}(\mathbf{V}_{dci},\mathbf{P}_{refi})=0$, with $\mathbf{P}_{refi}$ being the truly independent variable. Treatment of this problem is well known and consists of transforming it into an optimization problem i.e.,

Minimize

$$\boldsymbol{C}(\mathbf{V_i}, \mathbf{P_{refi}}) = \boldsymbol{W_{VN}(V_{min} - V_{dci})^2 + W_{VX}(V_{dci} - V_{max})^2 + W_{PN}(P_{mini} - P_{refi})^2 + W_{PX}(P_{refi} - P_{maxi})^2} \quad (5.1)$$

subject to

$$\mathbf{F}(\mathbf{V}_{dci},\mathbf{P}_{refi})=0$$

Combining the function $\boldsymbol{C}(\mathbf{V_i}, \mathbf{P_{refi}})$ and the constraint $\mathbf{F}(\mathbf{V}_{dci},\mathbf{P}_{refi})=0$, the standard techniques is to minimize the following unconstrained function.

$$\boldsymbol{L = C(V_i, P_{refi}) + \lambda F(V_i, P_{refi})} \quad (5.2)$$

where $\boldsymbol{\lambda}$ is the Lagrange multiplier.

B. Vectorial Formulation

i) Pre-fault case: All VSCs in Service

Recalling that the multi-terminal DC system of Figure. 4.1 consists of N+1 converter stations and VSC(N+1) is assigned to operate as the DC Voltage Regulator (VR), the objective is to ensure

1. The DC voltage at each VSC station satisfies the voltage constraints $\mathbf{V}_{min} \leq \mathbf{V}_{dci} \leq \mathbf{V}_{max}$, i=1,2,…N.
2. The power at each VSC station satisfies the operational power limits $\mathbf{P}_{mini} < \mathbf{P}_{refi} < \mathbf{P}_{maxi}$, i=1,2,….N.

Since the DC voltage of VR is regulated at $\mathbf{V}_{dcref}$, the DC voltages of the other N converters, expressed by the N-tuple dc voltage vector $\boldsymbol{V_{dc}} = [\boldsymbol{V_{dc1}}, \boldsymbol{V_{dc2}}, \dots\dots\dots, \boldsymbol{V_{dcN}}]^T$, are solutions to (4.7) for a power reference setting vector $\boldsymbol{P} = [\boldsymbol{P_{ref1}}, \boldsymbol{P_{ref2}}, \dots\dots, \boldsymbol{P_{refN}}]^T$. Equation (4.7) is expressed as $\mathbf{F}(\mathbf{P},\mathbf{V}_{dc})=0$.

Defining the vectors of voltage limits as,

$$\boldsymbol{V_{min}} = [\boldsymbol{V_{min}}, \boldsymbol{V_{min}}, \dots\dots, V_{min}]^T, \boldsymbol{V_{max}} = [\boldsymbol{V_{max}}, \boldsymbol{V_{max}}, \dots\dots, \boldsymbol{V_{max}}]^T$$

the voltage constraint expressed in vectorial form is,

$$\boldsymbol{V_{min} \leq V_{dc} \leq V_{max}}$$

Defining the vectors of operational power limits to be,

$$\boldsymbol{P}_{min} = [\boldsymbol{P}_{min1}, \boldsymbol{P}_{min2}, \dots\dots, \boldsymbol{P}_{minN}]^T, \boldsymbol{P}_{max} = [\boldsymbol{P}_{max1}, \boldsymbol{P}_{max2}, \dots\dots, \boldsymbol{P}_{maxN}]^T$$

the operational power constraint expressed in vectorial form is,

$$\boldsymbol{P}_{min} \leq \boldsymbol{P} \leq \boldsymbol{P}_{max}$$

The objective function to be minimized is,

Minimize

$$\boldsymbol{C}(\boldsymbol{P}, \boldsymbol{V}_{dc}) = \{(\boldsymbol{P}_{min} - \boldsymbol{P})^T[\boldsymbol{W}_{PN}](\boldsymbol{P}_{min} - \boldsymbol{P}) + (\boldsymbol{P} - \boldsymbol{P}_{max})^T[\boldsymbol{W}_{PX}](\boldsymbol{P} - \boldsymbol{P}_{max})\} +$$

$$\{(\boldsymbol{V}_{min} - \boldsymbol{V}_{dc})^T[\boldsymbol{W}_{VN}](\boldsymbol{V}_{min} - \boldsymbol{V}_{dc}) + (\boldsymbol{V}_{dc} - \boldsymbol{V}_{max})^T[\boldsymbol{W}_{VX}](\boldsymbol{V}_{dc} - \boldsymbol{V}_{max})\} \quad (5.3)$$

subject to

$$\boldsymbol{F}(\boldsymbol{P}, \boldsymbol{V}_{dc}) = 0$$

where,

$[\boldsymbol{W}_{VN}]$ and $[\boldsymbol{W}_{VX}]$ are diagonal penalty factor matrices for the voltages. $[\boldsymbol{W}_{PN}]$ and $[\boldsymbol{W}_{PX}]$ are diagonal penalty factor matrices for the converter powers. If a voltage or converter power constraint is violated, the corresponding penalty factor is given a large positive value. For converters that supply power to sensitive loads, their corresponding penalty factors are always assigned to be a large value and their upper and lower power limits are set to the same values, which force the converter power to be fixed at the specified targets.

ii) Pre-fault and Post Fault cases k=0,1,2….N

The voltage margins must be met not only when all the VSCs are in service but also when any one of the VSCs (except for the VR) is lost. The superscript k=0 in $\boldsymbol{V}_{dc}^0$ is again

applied to denote the solution when all the VSCs are in operation. The superscript k in $\boldsymbol{V}_{dc}^{k}$ is the solution when VSC_k is lost.

The power reference setting of the Power Dispatchers, $\boldsymbol{P} = \left[\boldsymbol{P}_{ref1}, \boldsymbol{P}_{ref2}, \ldots\ldots, \boldsymbol{P}_{refN}\right]^{T}$, must be determined from the very beginning before a VSC is lost. As each of the surviving VSCs continues to deliver the power assigned to it after the loss of VSC_k for example, the power reference setting vector is

$$\boldsymbol{P}^{k} = \left[\boldsymbol{P}_{ref1}, \boldsymbol{P}_{ref2}, \ldots\ldots, \boldsymbol{P}_{ref(k-1)}, \boldsymbol{P}_{refk} = 0, \boldsymbol{P}_{ref(k+1)}, \ldots\ldots, \boldsymbol{P}_{refN}\right]^{T}$$

The solution to Equation (4.7) is $\boldsymbol{V}_{dc}^{k} = \left[\boldsymbol{V}_{dc1}^{k}, \boldsymbol{V}_{dc2}^{k}, \ldots\ldots, \boldsymbol{V}_{dcN}^{k}\right]^{T}$. The pre-fault conditions are identified by the superscript k=0.

For all the cases, k=0,1,2,….N, (4.7) is expressed as

$$\boldsymbol{F}\left(\boldsymbol{P}^{k}, \boldsymbol{V}_{dc}^{k}\right) = 0 \quad (k = 0,1,2 \ldots . N)$$

where,

$\boldsymbol{V}_{dc}^{k} = \left[\boldsymbol{V}_{dc1}^{k}, \boldsymbol{V}_{dc2}^{k}, \ldots\ldots, \boldsymbol{V}_{dcN}^{k}\right]^{T}$ (k=0,1,2…N) denotes the DC voltages;

$\boldsymbol{F}(\boldsymbol{P}^{0}, \boldsymbol{V}_{dc}^{0}) = 0$ is the power flow equation when all the converter are in service;

$\boldsymbol{F}\left(\boldsymbol{P}^{k}, \boldsymbol{V}_{dc}^{k}\right) = 0$ is the power flow equation when the k^{th} converter (VSC_k) is lost;

The requirements of the voltage constraints are,

$\boldsymbol{V}_{min} \leq \boldsymbol{V}_{dc}^{k} \leq \boldsymbol{V}_{max}$ (k=0,1,2….N)

The requirements of the operational power limits are,

$$\boldsymbol{P}_{min} \leq \boldsymbol{P} \leq \boldsymbol{P}_{max}$$

With the above discussed formulation, three optimization formulations with different objective function were considered which are discussed below.

1. Optimization Formulation [5]

This formulation, as presented in [5], minimizes the deviation of power from its maximum and minimum limiting values ($\mathbf{V}_{min}$, $\mathbf{V}_{max}$) and the deviation of power from its maximum and minimum limiting values ($\mathbf{P}_{min}$, $\mathbf{P}_{max}$).

The objective function to be minimized consists of the summation of all the (N+1) cases

$$\boldsymbol{C}\left(\boldsymbol{P}, \boldsymbol{V}_{\boldsymbol{dc}}^{\boldsymbol{0}}, \boldsymbol{V}_{\boldsymbol{dc}}^{\boldsymbol{1}}, \ldots\ldots, \boldsymbol{V}_{\boldsymbol{dc}}^{\boldsymbol{N}}\right)$$

$$= \{(\boldsymbol{P} - \boldsymbol{P}_{\boldsymbol{min}})^{\boldsymbol{T}}[\boldsymbol{W}_{\boldsymbol{PN}}](\boldsymbol{P} - \boldsymbol{P}_{\boldsymbol{min}}) + (\boldsymbol{P} - \boldsymbol{P}_{\boldsymbol{max}})^{\boldsymbol{T}}[\boldsymbol{W}_{\boldsymbol{Px}}](\boldsymbol{P} - \boldsymbol{P}_{\boldsymbol{max}})\}$$

$$+ \sum_{\boldsymbol{k=0}}^{\boldsymbol{N}} \left\{\left(\boldsymbol{V}^{\boldsymbol{k}} - \boldsymbol{V}_{\boldsymbol{min}}\right)^{\boldsymbol{T}}\left[\boldsymbol{W}_{\boldsymbol{VN}}^{\boldsymbol{k}}\right]\left(\boldsymbol{V}^{\boldsymbol{k}} - \boldsymbol{V}_{\boldsymbol{min}}\right)\right.$$

$$\left. + \left(\boldsymbol{V}^{\boldsymbol{k}} - \boldsymbol{V}_{\boldsymbol{max}}\right)^{\boldsymbol{T}}\left[\boldsymbol{W}_{\boldsymbol{VX}}^{\boldsymbol{k}}\right]\left(\boldsymbol{V}^{\boldsymbol{k}} - \boldsymbol{V}_{\boldsymbol{max}}\right)\right\} \tag{5.4}$$

subject to

$$\boldsymbol{F}\left(\boldsymbol{P}^{k}, \boldsymbol{V}_{dc}^{k}\right) = 0 \quad (k = 0,1,2 \ldots . N)$$

where $\left[\boldsymbol{W}_{\boldsymbol{VN}}^{\boldsymbol{k}}\right]$ and $\left[\boldsymbol{W}_{\boldsymbol{VX}}^{\boldsymbol{k}}\right]$ are diagonal penalty factor matrices for the voltages V_{dc}^{k}, k=0,1,2….N.

2. Alternative-1 Formulation

This formulation tries to minimize the deviation of power from its target value (P_{tar}) and deviation of DC voltage from its target value (V_{tar}). The target value of the power can be the base case desired values of reference settings of dispatchers and the target value of DC bus voltages can be taken as the nominal value (1.0 p.u.).

Minimize

$$\boldsymbol{C}\left(\boldsymbol{P}, \boldsymbol{V}_{\boldsymbol{dc}}^{\boldsymbol{0}}, \boldsymbol{V}_{\boldsymbol{dc}}^{\boldsymbol{1}}, \ldots., \boldsymbol{V}_{\boldsymbol{dc}}^{\boldsymbol{N}}\right) =$$

$$(\boldsymbol{P}-\boldsymbol{P}_{\boldsymbol{tar}})^{\boldsymbol{T}}[\boldsymbol{W}_{\boldsymbol{p}}](\boldsymbol{P}-\boldsymbol{P}_{\boldsymbol{tar}}) + \sum_{\boldsymbol{k}=\boldsymbol{0}}^{\boldsymbol{N}}\left\{\left(\boldsymbol{V}^{\boldsymbol{k}}-\boldsymbol{V}_{\boldsymbol{tar}}\right)^{\boldsymbol{T}}[\boldsymbol{W}_{\boldsymbol{v}}]\left(\boldsymbol{V}^{\boldsymbol{k}}-\boldsymbol{V}_{\boldsymbol{tar}}\right)\right\} \quad (5.5)$$

subject to

$$\boldsymbol{F}\left(\boldsymbol{P}^{k}, \boldsymbol{V}_{dc}^{k}\right) = 0 \quad (k = 0,1,2 \ldots. N)$$

3. Alternative-2 Formulation

This formulation minimizes the deviation of power from its maximum and minimum limiting values but the deviation of the DC voltage from its target value.

Minimize

$$\boldsymbol{C}\left(\boldsymbol{P}, \boldsymbol{V}_{\boldsymbol{dc}}^{\boldsymbol{0}}, \boldsymbol{V}_{\boldsymbol{dc}}^{\boldsymbol{1}}, \ldots., \boldsymbol{V}_{\boldsymbol{dc}}^{\boldsymbol{N}}\right) = \{(\boldsymbol{P}-\boldsymbol{P}_{\boldsymbol{min}})^{\boldsymbol{T}}[\boldsymbol{W}_{\boldsymbol{pN}}](\boldsymbol{P}-\boldsymbol{P}_{\boldsymbol{min}}) + (\boldsymbol{P}-\boldsymbol{P}_{\boldsymbol{max}})^{\boldsymbol{T}}[\boldsymbol{W}_{\boldsymbol{px}}](\boldsymbol{P}-$$

$$\boldsymbol{P}_{\boldsymbol{max}})\} + \sum_{\boldsymbol{k}=\boldsymbol{0}}^{\boldsymbol{N}}\left\{\left(\boldsymbol{V}^{\boldsymbol{k}}-\boldsymbol{V}_{\boldsymbol{tar}}\right)^{\boldsymbol{T}}[\boldsymbol{W}_{\boldsymbol{v}}]\left(\boldsymbol{V}^{\boldsymbol{k}}-\boldsymbol{V}_{\boldsymbol{tar}}\right)\right\} \quad (5.6)$$

subject to

$$\boldsymbol{F}\left(\boldsymbol{P}^{k}, \boldsymbol{V}_{dc}^{k}\right) = 0 \quad (k = 0,1,2 \ldots. N)$$

In this thesis, all the weight factors have been considered to be unity for the sake of testing the proposed algorithms.

5.3 Optimal Solution Using Lagrange Multiplier Method

The above optimization formulation can be solved by applying the Lagrange Multiplier method [22]. Adding an additional term to include the equality constraints yields an unconstrained function

$$\boldsymbol{L} = \boldsymbol{C}\left(\boldsymbol{P}, \boldsymbol{V}_{\boldsymbol{dc}}^{\boldsymbol{0}}, \boldsymbol{V}_{\boldsymbol{dc}}^{\boldsymbol{1}}, \ldots., \boldsymbol{V}_{\boldsymbol{dc}}^{\boldsymbol{N}}\right) + \sum_{\boldsymbol{k}=\boldsymbol{0}}^{\boldsymbol{N}} \boldsymbol{\lambda}_{\boldsymbol{k}}^{\boldsymbol{T}} \boldsymbol{F}\left(\boldsymbol{P}^{\boldsymbol{k}}, \boldsymbol{V}_{\boldsymbol{dc}}^{\boldsymbol{k}}\right) \quad (5.7)$$

where, $\boldsymbol{\lambda_k^T}$, (k=0,1,….N) are unknown quantities, called Lagrange Multipliers.

The necessary condition to minimize the unconstrained function is obtained by setting the partial derivatives of the function L, with respect to its variables, equal to zero i.e.,

$$\frac{\partial \boldsymbol{L}}{\partial \boldsymbol{P}} = \frac{\partial \boldsymbol{C}}{\partial \boldsymbol{P}} + \sum_{k=0}^{N} \frac{\partial \boldsymbol{F}^T\left(\boldsymbol{P}^k, \boldsymbol{V}_{dc}^k\right)}{\partial \boldsymbol{P}} \lambda_k = 0 \tag{5.8}$$

$$\frac{\partial \boldsymbol{L}}{\partial \boldsymbol{V}_{dc}^k} = \frac{\partial \boldsymbol{C}}{\partial \boldsymbol{V}_{dc}^k} + \sum_{k=0}^{N} \frac{\partial \boldsymbol{F}^T\left(\boldsymbol{P}^k, \boldsymbol{V}_{dc}^k\right)}{\partial \boldsymbol{V}_{dc}^k} \lambda_k = 0 \qquad (k = 0,1,2, \ldots . N) \tag{5.9}$$

$$\frac{\partial \boldsymbol{L}}{\partial \lambda_k} = \boldsymbol{F}\left(\boldsymbol{P}^k, \boldsymbol{V}_{dc}^k\right) = 0 \qquad (k = 0,1,2, \ldots N) \tag{5.10}$$

Eliminating λ_k (k=0,1,2…N) in the above equations result in

$$\frac{\partial \boldsymbol{C}}{\partial \boldsymbol{P}} - \left\{ \sum_{k=0}^{N} \frac{\partial \boldsymbol{F}^T\left(\boldsymbol{P}^k, \boldsymbol{V}_{dc}^k\right)}{\partial \boldsymbol{V}_{dc}^k} \left[\frac{\partial \boldsymbol{F}^T\left(\boldsymbol{P}^k, \boldsymbol{V}_{dc}^k\right)}{\partial \boldsymbol{V}_{dc}^k} \right]^{-1} \frac{\partial \boldsymbol{C}}{\partial \boldsymbol{V}_{dc}^k} \right\} = 0 \tag{5.11}$$

$$\boldsymbol{F}\left(\boldsymbol{P}^k, \boldsymbol{V}_{dc}^k\right) = 0 \qquad (k = 0,1,2, \ldots N) \tag{5.12}$$

Note that Equation (5.12) is the original power flow equation of Equation (4.7). These are nonlinear algebraic equations and can be solved by the Newton-Raphson method. Equation (5.11) actually shows the sensitivity relationship between the function $\boldsymbol{C}(\boldsymbol{P}, \boldsymbol{V}_{dc}^0, \boldsymbol{V}_{dc}^1, \ldots . , \boldsymbol{V}_{dc}^N)$ and the control variables **P**, which can be defined as the gradient of $\boldsymbol{C}(\boldsymbol{P}, \boldsymbol{V}_{dc}^0, \boldsymbol{V}_{dc}^1, \ldots . , \boldsymbol{V}_{dc}^N)$ with respect to **P**, i.e.,

$$\nabla \boldsymbol{C}_P = \frac{\partial \boldsymbol{C}}{\partial \boldsymbol{P}} - \left\{ \sum_{k=0}^{N} \frac{\partial \boldsymbol{F}^T\left(\boldsymbol{P}^k, \boldsymbol{V}_{dc}^k\right)}{\partial \boldsymbol{V}_{dc}^k} \left[\frac{\partial \boldsymbol{F}^T\left(\boldsymbol{P}^k, \boldsymbol{V}_{dc}^k\right)}{\partial \boldsymbol{V}_{dc}^k} \right]^{-1} \frac{\partial \boldsymbol{C}}{\partial \boldsymbol{V}_{dc}^k} \right\}$$

To minimize the function $\boldsymbol{C}(\boldsymbol{P}, \boldsymbol{V}_{dc}^{0}, \boldsymbol{V}_{dc}^{1}, \ldots, \boldsymbol{V}_{dc}^{N})$, one can start with an estimated value of $\mathbf{P}^{(j)}$ and compute the gradient $\nabla \mathbf{C}_{\mathrm{P}}^{(j)}$. Then, using steepest decent approach, a new value, $\mathbf{P}^{(j+1)}$, is found in the direction of negative gradient, i.e.,

$$\boldsymbol{P}^{(j+1)}=\boldsymbol{P}^{(j)}\text{-}\alpha\nabla \mathrm{C}_{\mathrm{P}}^{(j)}$$

where, α is a system dependent factor for modifying the step size.

The process is repeated in the direction of negative gradient until the gradient $\nabla \mathbf{C}_{\mathrm{P}}^{(j)}$ is less than a pre-specified accuracy, i.e.

$$\left|\nabla \mathbf{C}_{\mathrm{P}}^{(j)}\right| \leq \boldsymbol{\varepsilon}_{\mathrm{P}}$$

This algorithm is also known as the first order gradient method.

5.4 Major Solution Steps

The above three alternative formulations with different objective functions, along with the equality constraints, have been solved using Lagrange multiplier approach, based on first order gradient approach.

The main steps for calculating the VSC power reference setting adjustment is summarized as follows:

1. Start with an initial value $\mathbf{P}^{(j)}$, j=1;
2. Solve the power flow equation, $\boldsymbol{F}\left(\boldsymbol{P}^{k}(j), \boldsymbol{V}_{dc}^{k}(j)\right) = 0 \qquad (k = 0,1,2, \ldots N)$

   for $\mathbf{V}_{\mathrm{dc}}^{\mathrm{k}}(\mathrm{j}) = \left[\mathbf{V}_{\mathrm{dc1}}^{\mathrm{k}}(\mathrm{j}), \mathbf{V}_{\mathrm{dc2}}^{\mathrm{k}}(\mathrm{j}), \ldots \ldots, \mathbf{V}_{\mathrm{dcN}}^{\mathrm{k}}(\mathrm{j})\right]^{\mathrm{T}}$ (k=0,1,2…N);

3. Examine if the voltage or converter power constraints are violated, an determine the penalty factors in $\left[\boldsymbol{W}_{\boldsymbol{VN}}^{\boldsymbol{k}}\right]$, $\left[\boldsymbol{W}_{\boldsymbol{VX}}^{\boldsymbol{k}}\right]$, $[\boldsymbol{W}_{\boldsymbol{PN}}]$ and $[\boldsymbol{W}_{\boldsymbol{PX}}]$;
4. Compute the gradient $\nabla \boldsymbol{C}_P^{(j)}$

$$\nabla \boldsymbol{C}_P = \frac{\partial \boldsymbol{C}}{\partial \boldsymbol{P}} - \left\{ \sum_{k=0}^{N} \frac{\partial \boldsymbol{F}^T\left(\boldsymbol{P}^k, \boldsymbol{V}_{dc}^k\right)}{\partial \boldsymbol{V}_{dc}^k} \left[\frac{\partial \boldsymbol{F}^T\left(\boldsymbol{P}^k, \boldsymbol{V}_{dc}^k\right)}{\partial \boldsymbol{V}_{dc}^k} \right]^{-1} \frac{\partial \boldsymbol{C}}{\partial \boldsymbol{V}_{dc}^k} \right\}$$

5. Update VSC power reference setting using

   $\mathbf{P}^{(j+1)}=\mathbf{P}^{(j)}-\alpha \nabla C_P^{(j)}$,

   and advance iteration count, j=j+1.
6. Repeat 2-5 steps until $\left|\nabla \boldsymbol{C}_P^{(j)}\right|$ is less than a set tolerance. In this work, tolerance has been taken as 10e-3 p.u. on 100MVA power base.

Note that, adjusting converter power reference setting always involves redistribution of power among converters. This may not be desirable in system operation. Therefore, it is applied only when no feasible voltage reference can be found to take care of the voltages.

5.5 Results on MVDC System

In order to simulate a situation, where voltage sensitivity based method is not able to provide optimal setting of voltage regulator to satisfy the DC voltage constraints at other buses, the DC line resistances of the test case, discussed in chapter III, were increased to 10 times their base values. In this work, for simplicity, the penalty weights are taken as 1.0 p.u. and the P^{tar} as 0.5 p.u. and V^{tar} as 1.0 p.u. The converter power

reference settings are the same as in Table 3.1 in chapter III. In addition, VSC4 is assumed to supply sensitive loads so that $\boldsymbol{P}_{ref4}$ must be maintained at their set point. Table 5.1 presents the results with the voltage sensitivity method, described in chapter IV. As can be seen from this table, there is no feasible common range for $\mathbf{V}_{dcref}$ of the voltage regulator. To solve the problem, code was developed in MATLAB environment.

Table 5.1 Allowed V_{ref} for different cases

No.	Conditions	Allowable Voltage Reference (p.u)	
		$\mathbf{V}_{dcrefmin}$	$\mathbf{V}_{dcrefmax}$
1	All VSCs in service	0.9704	1.0056
2	Loss of VSC1	0.9567	**0.9658**
3	Loss of VSC2	**0.9952**	1.0801
4	Loss of VSC3	0.9801	1.0234
5	Loss of VSC4	0.9362	0.9856
Accepted Common range for all conditions		No Feasible Range Available	

Table 5.2 DC voltages subject to VSC power setting adjustment with Existing formulation [5]

No.	Conditions	DC Voltage (p.u.)				
		$\mathbf{V}_{dc1}$	$\mathbf{V}_{dc2}$	$\mathbf{V}_{dc3}$	$\mathbf{V}_{dc4}$	$\mathbf{V}_{dc5}$
1	All VSCs in service	0.9825	0.96	0.9790	0.9546	1.0
2	Loss of VSC1	0.9821	0.9659	0.9716	0.9643	1.0
3	Loss of VSC2	0.9819	0.9586	0.9782	0.9632	1.0
4	Loss of VSC3	0.9791	0.9532	0.9573	0.9576	1.0
5	Loss of VSC4	1.0045	1.0095	1.0154	1.0188	1.0
Adjusted Converter Power(p.u) $\mathbf{P}_{ref1}$=0.0041, $\mathbf{P}_{ref2}$ =0.0088, $\mathbf{P}_{ref3}$ =0.1222, $\mathbf{P}_{ref4}$ =-0.4600, $\mathbf{P}_{ref5}$ =0.3248						

Table 5.3 DC voltages subject to VSC power setting adjustment with New Alternative-1 formulation

No.	Conditions	DC Voltage (p.u.)				
		$\mathbf{V}_{dc1}$	$\mathbf{V}_{dc2}$	$\mathbf{V}_{dc3}$	$\mathbf{V}_{dc4}$	$\mathbf{V}_{dc5}$
1	All VSCs in service	1	0.9874	0.9954	0.9639	1.0
2	Loss of VSC1	0.9918	0.9814	0.993	0.96	1.0
3	Loss of VSC2	0.9935	0.9728	0.989	0.9542	1.0
4	Loss of VSC3	0.9928	0.9712	0.964	0.9896	1.0
5	Loss of VSC4	1.022	1.0369	1.034	1.0381	1.0
Adjusted Converter Power(p.u) $\mathbf{P}_{ref1}$=0.0836, $\mathbf{P}_{ref2}$ =0.0905, $\mathbf{P}_{ref3}$ =0.2567, $\mathbf{P}_{ref4}$ =-0.4600, $\mathbf{P}_{ref5}$ =0.0293						

Tables 5.2, 5.3 and 5.4 present the results with the adjusted converter power settings, obtained by the proposed optimization based method, with the three different objective functions. The voltages are within desired limits in the pre-fault and all the post-fault cases. More importantly, power reference setting of VSC4 is still maintained at their original value, which ensures that the VSC4 will supply uninterrupted power to the sensitive load. From these tables, it can be observed that the Alternative-1 formulation gives the most optimal results as the DC voltages of the VSCs for both the pre- and post-fault cases are closer to their nominal value 1p.u.

Table 5.4 DC voltages subject to VSC power setting adjustment for New Alternative-2 formulation

No.	Conditions	DC Voltage (p.u.)				
		$\mathbf{V}_{dc1}$	$\mathbf{V}_{dc2}$	$\mathbf{V}_{dc3}$	$\mathbf{V}_{dc4}$	$\mathbf{V}_{dc5}$
1	All VSCs in service	0.9826	0.9600	0.9790	0.9546	1.0
2	Loss of VSC1	0.9821	0.9595	0.9716	0.9643	1.0
3	Loss of VSC2	0.9819	0.9586	0.9782	0.9632	1.0
4	Loss of VSC3	0.9791	0.9532	0.9573	0.9576	1.0
5	Loss of VSC4	1.0045	1.0095	1.0154	1.0188	1.0
Adjusted Converter Power(p.u) $\mathbf{P}_{ref1}$=0.0044, $\mathbf{P}_{ref2}$ =0.0091, $\mathbf{P}_{ref3}$ =0.1225, $\mathbf{P}_{ref4}$ =-0.4600, $\mathbf{P}_{ref5}$ =0.3240						

5.6 Summary

This chapter has explained, in detail, the formulation of an Optimization based method using conventional Lagrange Multiplier approach for optimal control of power and voltage in the MVDC system. Three alternative formulations, with different objective functions, are discussed. The chapter summarized the steps for calculating the optimal reference power settings of VSCs. To demonstrate the successful implementation of the algorithm, the method has been applied to the simplified of a MVDC shipboard power system and the test results were presented with three different alternative objective functions.

CHAPTER VI

A GENETIC ALGORITHM BASED OPTIMAL CONTROL OF POWER AND VOLTAGE

This chapter discusses some basic concepts of Genetic Algorithms (GAs), including the terminology and its operators. The mathematical problem formulation and the application of a genetic algorithm to solve the optimal power and voltage control of the MVDC system are also dealt in this chapter.

6.1 Introduction

Genetic Algorithms (GAs) are part of the evolutionary algorithms family, which are meta-heuristic computational methods [27]. The genetic algorithms are powerful stochastic search algorithms based on the Darwin's concept of natural selection and natural genetics, designed to find a global optimum solution for a wide range of problems. The genetic algorithms were invented by John Holland [28] in the early 1970s and applied to several practical optimization problems since late 1980s [29].

The mathematical model of a large power system network is nonlinear and nonconvex. One of the classical approaches to solve such problems has been the gradient method using Lagrange multipliers. The solution of a practical optimization problem may require solving very large systems expressed in terms of nonlinear equations. It is not

unusual to have 5,000 buses in a large practical power system with 10,000s unknown variables that must be constrained by as many equations. In addition there can be 10,000 inequality constraints on these variables. Inverting the large matrices and solving the large matrix equations is very formidable task. The matrices are extremely sparse, and special numerical techniques may be employed to ensure accuracy and stability. The inequality constraints contribute an additional layer of difficulty to the problem [64]. Evolutionary algorithms avoid most of the above mathematical difficulties and consequently, these are being employed increasingly to the solution of large, intractable power system problems.

In this work, the optimization problem is solved in two stages. First, numerical techniques, such as Newton-Raphson method, are used to solve the power flow problem. This part of the solution guarantees that the equality constraints, satisfying Kirchhoff's laws, are met. Then the solution to this power flow problem is used as the starting point (initial guess) for the various numerical techniques used to solve the optimization problem.

The genetic algorithm can be used to solve problems that are difficult to solve with the classical (conventional) algorithms. Independent of the objective function complexity, such as functions which are highly nonlinear, discontinuous, or has unreliable or undefined derivative, the algorithm can be applied and the more accurate optimal solution can be obtained. The genetic algorithms are more flexible than most of the conventional algorithms because they use only the objective function values (solution set) produced in the previous iteration as input to the present iteration, while most of the traditional optimization methods uses, the derivative information of the objective

function [26]. The main differences between genetic algorithms and other optimization methods are summarized in Table 6.1 [26].

Table 6.1 Differences between GAs and Traditional Algorithms [26]

No.	Traditional Algorithms	Genetic Algorithm
1.	Generates a single point at each iteration.	Generates a population of points at each iteration.
2.	The sequence of points (adaptive search) approaches an optimal solution.	Searches the optimal solution through parallel computation. The best point in the population approaches an optimal solution.
3.	Selects the next point in the sequence by a deterministic computation	Selects the next population by computation which uses random number generation.
4.	Inflexible method, because of lot of approximations in model representation	More flexible and robust
5.	Generally requires objective functions to be continuous, smooth and differentiable.	Applied to solve complex functions that are nonsmooth, noncontinuous and nondifferentialble.
6.	End search at local optimum.	Search for global optimum point.

6.2 Terminology

Some of the genetic algorithm terminologies are [26] as following:

1) Chromosome: Each possible solution point in a set of solution points is referred as chromosome.

2) Gene: Each position in the chromosome is referred as a gene and its particular value represents a value for some variable of the problem.

3) Population size: It consists of chromosomes, which represent the solution set for the problem. The population size depends on the nature of the problem. Usually, it lies in the range of 30-100.
4) Fitness: The fitness function is used as measure to evaluate the solution set.
5) Initialization: The initial population (individual solutions) is randomly generated from the wide range of possible solutions.
6) Selection: Based on the fitness value of the individual solutions, a proportion of the existing population is selected to breed a new generation.
7) Crossover Operator: It is the main genetic operator. It operates on two individuals and recombines their genetic material to generate new individuals in the next population. Usually lies in the range of 0.5 to 1.0.
8) Mutation: It is the background operator, which produces new population (individual solution) set by altering the value of few genes. Usually lies in the range of 0.001-0.05.
9) Reproduction: Offspring are created for the next generation population of solutions through genetic operators, such as crossover and mutation.
10) Stopping rule: The generation of populations (individual solutions) is repeated until a stopping condition, such as the maximum number of generations (iterations) is reached and a solution satisfying the minimum criteria is found.
11) Elitism Strategy: It is usually used to make sure that the best-fitted individual in a generation appears in the population of the next generation.

The terminology is depicted in Figures 6.1.

Chromosome:

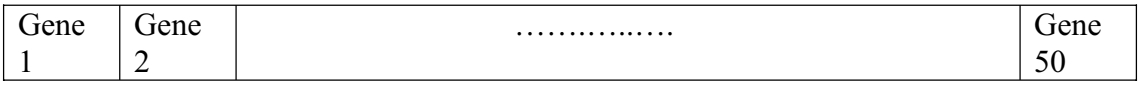

Gene:

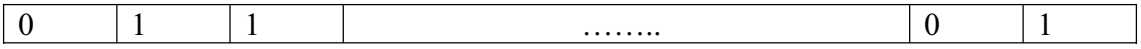

Single Point Crossover Type:

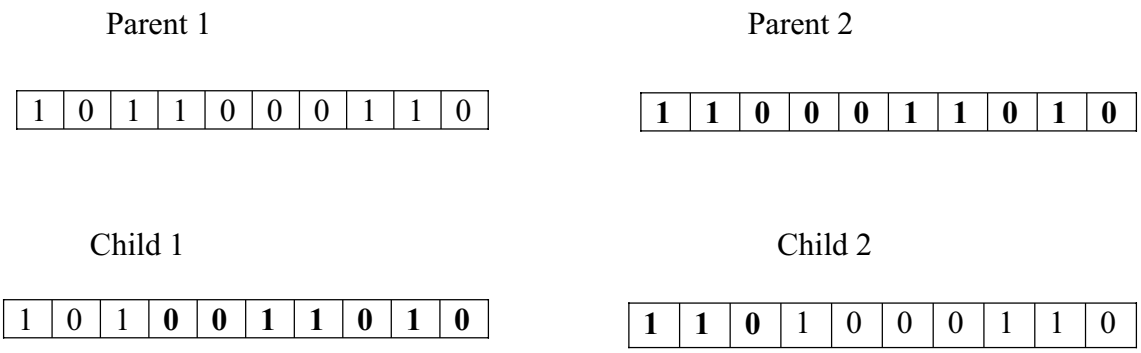

Bit Mutation:

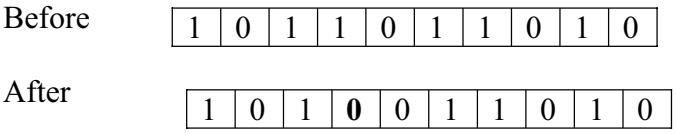

Figure 6.1 Genetic Algorithm Terminologies

6.3 Solution Steps with Genetic Algorithm

A flowchart for solution of an optimization problem using the Genetic Algorithm is given in Figure 6.2. The outline of the algorithm is as follows:

1) Randomly generate a set of initial population within the search space.
2) Calculate the fitness for each chromosome in the population.
3) The algorithm creates a new population in each iteration. At each step, to create the new population, the algorithm performs the following steps:
    (a) Compute the fitness values for each chromosome.
    (b) Based on fitness value of each individual, select them.
    (c) The individuals (chromosomes) with low fitness value are chosen from the current population and are passed to the next population.
    (d) Through crossover and mutation process, generate the new population.
    (e) Replace the current population with the new population to form the next generation.
4) Check for feasibility of the solution, i.e. each chromosome should satisfy both the equality and inequality constraints.
5) Go to step 3.
6) Terminate, if the stopping criteria has been reached, and return the solution.

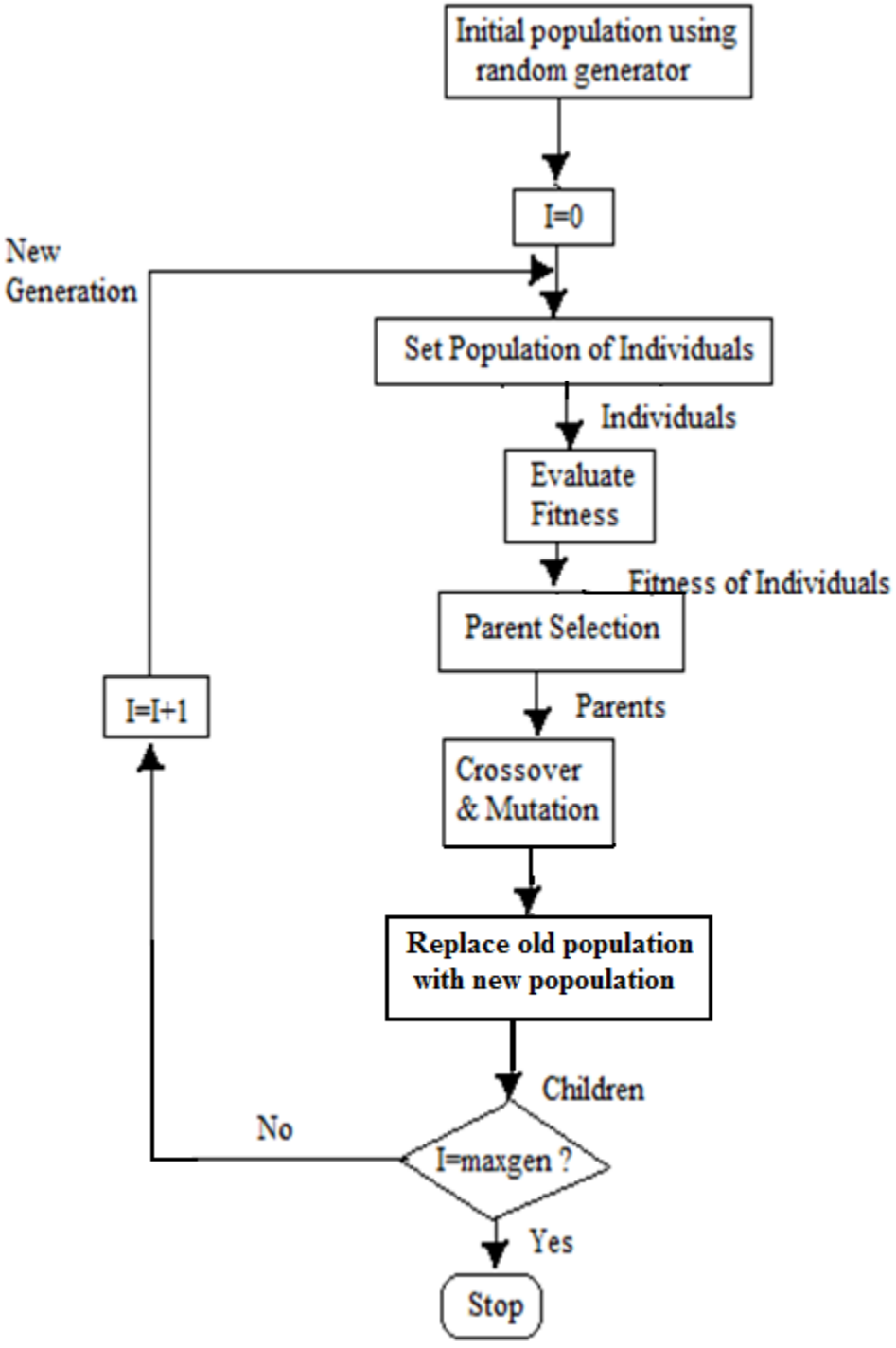

Figure 6.2 Flowchart showing the Genetic Algorithm [26]

6.4 Genetic Algorithm Applied to Optimal Voltage and Power Control

6.4.1 Tunable Parameters

As with most of the evolutionary algorithms, the operation of the genetic algorithm depends mostly on the tuning of multiple parameters. The parameter values must be such that the algorithm should provide an optimal solution while working quickly. In this work, the genetic algorithm parameters values considered are as follows,

Number of genes=10

Population size=50

Selection Method=Elistim search

Elitism parameter=2

Crossover type=single point

Mutation parameter=0.01

Stopping criteria=maximum number of generations=50.

6.4.2 The Optimization Problem Formulation

The three optimization formulations, with different objective function, discussed in chapter V, are being summarized below for ready reference.

1. An Existing Optimization Formulation [5]

The objective function to be minimized is:

Minimize

$$\boldsymbol{C}\left(\boldsymbol{P}, \boldsymbol{V}_{\boldsymbol{dc}}^{\boldsymbol{0}}, \boldsymbol{V}_{\boldsymbol{dc}}^{\boldsymbol{1}}, \ldots\ldots, \boldsymbol{V}_{\boldsymbol{dc}}^{\boldsymbol{N}}\right)$$

$$= \{(\boldsymbol{P} - \boldsymbol{P}_{\boldsymbol{min}})^{\boldsymbol{T}}[\boldsymbol{W}_{\boldsymbol{PN}}](\boldsymbol{P} - \boldsymbol{P}_{\boldsymbol{min}}) + (\boldsymbol{P} - \boldsymbol{P}_{\boldsymbol{max}})^{\boldsymbol{T}}[\boldsymbol{W}_{\boldsymbol{Px}}](\boldsymbol{P} - \boldsymbol{P}_{\boldsymbol{max}})\}$$

$$+ \sum_{\boldsymbol{k=0}}^{\boldsymbol{N}} \left\{\left(\boldsymbol{V}^{\boldsymbol{k}} - \boldsymbol{V}_{\boldsymbol{min}}\right)^{\boldsymbol{T}}\left[\boldsymbol{W}_{\boldsymbol{VN}}^{\boldsymbol{k}}\right]\left(\boldsymbol{V}^{\boldsymbol{k}} - \boldsymbol{V}_{\boldsymbol{min}}\right)\right.$$

$$\left. + \left(\boldsymbol{V}^{\boldsymbol{k}} - \boldsymbol{V}_{\boldsymbol{max}}\right)^{\boldsymbol{T}}\left[\boldsymbol{W}_{\boldsymbol{VX}}^{\boldsymbol{k}}\right]\left(\boldsymbol{V}^{\boldsymbol{k}} - \boldsymbol{V}_{\boldsymbol{max}}\right)\right\}$$

subject to

$$\boldsymbol{F}\left(\boldsymbol{P}^{k}, \boldsymbol{V}_{\boldsymbol{dc}}^{k}\right) = 0 \quad (k = 0,1,2 \ldots . N)$$

2. Alternative-1 Formulation:

The objective function to be minimized is:

Minimize

$$\boldsymbol{C}\left(\boldsymbol{P}, \boldsymbol{V}_{\boldsymbol{dc}}^{\boldsymbol{0}}, \boldsymbol{V}_{\boldsymbol{dc}}^{\boldsymbol{1}}, \ldots\ldots, \boldsymbol{V}_{\boldsymbol{dc}}^{\boldsymbol{N}}\right)$$

$$= (\boldsymbol{P} - \boldsymbol{P}_{\boldsymbol{tar}})^{\boldsymbol{T}}\left[\boldsymbol{W}_{\boldsymbol{p}}\right](\boldsymbol{P} - \boldsymbol{P}_{\boldsymbol{tar}}) + \sum_{\boldsymbol{k=0}}^{\boldsymbol{N}} \left\{\left(\boldsymbol{V}^{\boldsymbol{k}} - \boldsymbol{V}_{\boldsymbol{tar}}\right)^{\boldsymbol{T}}[\boldsymbol{W}_{\boldsymbol{v}}]\left(\boldsymbol{V}^{\boldsymbol{k}} - \boldsymbol{V}_{\boldsymbol{tar}}\right)\right\}$$

subject to

$$\boldsymbol{F}\left(\boldsymbol{P}^{k}, \boldsymbol{V}_{\boldsymbol{dc}}^{k}\right) = 0 \quad (k = 0,1,2 \ldots . N)$$

3. Alternative-2 Formulation:

The objective function to be minimized is:

Minimize

$$\boldsymbol{C}\left(\boldsymbol{P}, \boldsymbol{V}_{\boldsymbol{dc}}^{\boldsymbol{0}}, \boldsymbol{V}_{\boldsymbol{dc}}^{\boldsymbol{1}}, \ldots, \boldsymbol{V}_{\boldsymbol{dc}}^{\boldsymbol{N}}\right)$$

$$= \left\{(\boldsymbol{P} - \boldsymbol{P}_{\boldsymbol{min}})^{\boldsymbol{T}}\left[\boldsymbol{W}_{\boldsymbol{pN}}\right](\boldsymbol{P} - \boldsymbol{P}_{\boldsymbol{min}}) + (\boldsymbol{P} - \boldsymbol{P}_{\boldsymbol{max}})^{\boldsymbol{T}}\left[\boldsymbol{W}_{\boldsymbol{px}}\right](\boldsymbol{P} - \boldsymbol{P}_{\boldsymbol{max}})\right\}$$

$$+ \sum_{\boldsymbol{k=0}}^{\boldsymbol{N}} \left\{\left(\boldsymbol{V}^{\boldsymbol{k}} - \boldsymbol{V}_{\boldsymbol{tar}}\right)^{\boldsymbol{T}}[\boldsymbol{W}_{\boldsymbol{v}}]\left(\boldsymbol{V}^{\boldsymbol{k}} - \boldsymbol{V}_{\boldsymbol{tar}}\right)\right\}$$

subject to

$$\boldsymbol{F}\left(\boldsymbol{P}^{k}, \boldsymbol{V}_{\boldsymbol{dc}}^{\boldsymbol{k}}\right) = 0 \quad (k = 0,1,2 \ldots . N)$$

6.4.3 Results on MVDC System

The above genetic algorithm based approach was applied to the simplified model of MVDC shipboard power system, shown in Figure 3.1 in chapter III, with DC line resistance values taken as in chapter V. MATLAB code for the GA used to generate results, available in [20], has been used. The optimization problem was defined in the separate .m file.

Tables 6.2, 6.3 and 6.4 present the results with the adjusted converter power settings, obtained by the proposed optimization based method, with the three different objective functions. The voltages are within desired limits during pre-fault and all the post-fault cases. More importantly, power reference setting of VSC4 is still maintained at their original value, which ensures that the VSC4 will supply uninterrupted power to the sensitive load.

Table 6.2 DC voltages subject to GA based VSC power setting adjustment with Existing formulation [5]

No.	Conditions	DC Voltage (p.u.)				
		V_{dc1}	V_{dc2}	V_{dc3}	V_{dc4}	V_{dc5}
1	All VSCs in service	0.983	0.9833	0.9742	0.9664	1.0
2	Loss of VSC1	0.985	0.97	0.9532	0.9544	1.0
3	Loss of VSC2	0.9737	0.9501	0.9811	0.968	1.0
4	Loss of VSC3	0.9711	0.9590	0.9637	0.9721	1.0
5	Loss of VSC4	0.9981	1.002	1.019	1.018	1.0
Adjusted Converter Power (p.u) P_{ref1}=0.0039, P_{ref2}=0.0081, P_{ref3}=0.13, P_{ref4}= - 0.46, P_{ref5}=0.35						

Table 6.3 DC voltages subject to GA based VSC power setting adjustment with New Alternative-1 formulation

No.	Conditions	DC Voltage (p.u.)				
		V_{dc1}	V_{dc2}	V_{dc3}	V_{dc4}	V_{dc5}
1	All VSCs in service	1.0199	0.9912	0.9817	0.976	1.0
2	Loss of VSC1	0.9928	0.99	0.996	1.004	1.0
3	Loss of VSC2	0.9866	0.9748	0.98	0.979	1.0
4	Loss of VSC3	1.0008	0.985	0.9659	0.9853	1.0
5	Loss of VSC4	0.9981	1.02	1.003	1.0095	1.0
Adjusted Converter Power (p.u) P_{ref1}=0.09, P_{ref2}=0.087, P_{ref3}=0.174, P_{ref4}= -0.46, P_{ref5}= 0.109						

Table 6.4 DC voltages subject to GA based VSC power setting adjustment for New Alternative-2 formulation

No.	Conditions	DC Voltage (p.u.)				
		V_{dc1}	V_{dc2}	V_{dc3}	V_{dc4}	V_{dc5}
1	All VSCs in service	0.967	0.97	0.9799	0.953	1.0
2	Loss of VSC1	0.9855	0.999	0.9643	0.9721	1.0
3	Loss of VSC2	0.982	0.9511	0.9844	0.9601	1.0
4	Loss of VSC3	0.973	0.9709	0.9599	0.981	1.0
5	Loss of VSC4	1.01	0.9989	1.009	1.019	1.0
Adjusted Converter Power (p.u) P_{ref1}=0.005, P_{ref2}=0.0089, P_{ref3}=0.178, P_{ref4}= -0.46, P_{ref5}= 0.268						

6.5 Summary

This chapter has provided an overview of genetic algorithm, the terminology used, and the major steps used in the algorithm. The algorithm was applied to the optimal power and voltage control problem with three different objective functions and the results on the MVDC shipboard power system has been presented in this chapter.

CHAPTER VII

OPTIMAL VOLTAGE AND POWER CONTROL USING A BIOGEOGRAPHY BASED OPTIMIZATION METHOD

This chapter describes, in detail, a Biogeography Based Optimization (BBO) technique and its application to optimal power and voltage control problem. BBO concept is mainly based on migration and mutation. The concept and mathematical formulation of migration and mutation steps will be defined in this chapter. At the end of the chapter, the results on MVDC power system will be presented.

7.1 Introduction

The main differences between the evolutionary algorithms and classical algorithms, along with the problems that arise in solving a complex optimization problem, using the classical approach, were presented in chapter VI. A GA based method was used to solve the optimal voltage and power control problem, which has been presented in chapter VI. Literature survey shows that a relatively new evolutionary method [23], known as Biogeography Based Optimization (BBO) method, provides better results as compared to the other evolutionary algorithms. This algorithm has not been attempted to solve the given power system optimization problem. An attempt has been made, in this chapter, to apply the Biogeography Based Optimization (BBO)

method to solve optimal power and voltage control problem. A MATLAB code, which is already developed in [20], has been used in this work.

Biogeography Based Optimization (BBO) is a part of the evolutionary algorithms family. Biogeography is the study of the geographical distribution of biological organisms [23]. Similar to the other evolutionary algorithms, such as Genetic Algorithms (GAs), and Artificial Neural Networks (ANNs), which are based on the mathematics of biological genetics and the biological neurons, the mathematics of biogeography has inspired the development of a new approach called as the Biogeography Based Optimization (BBO) [23].

Classical algorithms for solving the optimization problems rely strongly on initial values and convexity for their success in determining global optima. The algorithms frequently get trapped in local optima or diverge. Modern heuristic techniques, such as GA and, more generally, evolutionary algorithms, have proven to be effective in solving such problems [26]. These techniques are based on science and mathematics of biological genetics, which seek to understand and model the way populations in nature, such as insects, animals, and humans, "solve" evolutionary problems. In the BBO model, problem solutions are represented as islands, and the sharing of features between solutions is represented as immigration and emigration between the islands.

The science of biogeography was first discovered and developed by Alfred Wallace [24] and Charles Darwin [25]. Until the 19th century, biogeography was mainly descriptive and historical. Eugene Munroe was the first to introduce mathematical models of biogeography in 1948 [27] and later in 1967s, Robert MacArthur and Edward Wilson were the first to introduce, to develop and to publish it [28]. The biogeography-based

optimization [23] is based on the observation that the migration of species among a group of neighboring islands, combined with mutation of the individual species, will tend over many generations to produce islands that attract and keep large numbers of species through immigration. Other islands will lose species through extinction or emigration and will sometimes become desolate. The Biogeography Based Optimization algorithm seeks to model this behavior in a way that causes an "optimal" island to emerge from the original population of islands.

BBO has certain features in common with other population-based algorithms. Like Genetic Algorithm (GA) and Particle Swarm Optimization (PSO), BBO also shares information amongst the solutions but BBO does not involve in reproduction like GA. While GA solutions are lost at the end of the each iteration, BBO maintains its set of solutions from one iteration to the next like PSO. PSO solutions do not change directly; first their velocities are changed and then positions (solutions) are changed. However, BBO solutions are changed directly via migration from other solutions [23].

7.2 Biogeography Based Optimization Concepts

Biogeography Based Optimization (BBO) [23] is founded on the observation that the migration of species among a group of neighboring islands, combined with mutation of the individual species, will tend over many generations to produce islands that attract and keep large numbers of species through immigration. Other islands will lose species through extinction or emigration and will sometimes become desolate. The BBO algorithm seeks to model this behavior in a way that causes an "optimal" island to emerge from the original population of islands.

In a group of neighboring islands, species of plants and animals will migrate over time between the islands by various means, being carried along by driftwood, fish, birds, and the wind. Over evolutionary periods of time, some islands may tend to accumulate more species than others, because they possess certain environmental features that are more suitable to sustaining those species than islands with fewer species. This ability to sustain larger number of species can be associated with a fitness measure that one can quantify by assigning a Habitant suitability index (*HSI*) to each island. The value of the *H*SI depends on many features of the island. If a value is assigned to each feature, then the HSI is a function of these values. Each of these values is represented by a suitability index variable (SIV). These mappings are summarized as follows:

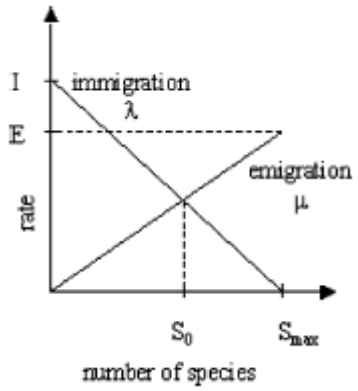

Figure 7.1 Island Migration Rates vs. Species [23]

An island, with a large number of species (a large HSI), has an abundance of species, which can emigrate to other islands, so its rate of emigration denoted by μ, is correspondingly large. The island is also less likely to be able to sustain further immigration of species because of the growing demand on its finite environmental resources, so its immigration rate, denoted by λ, is small. For many applications, it

suffices to assume a linear relationship between an island's HSI and its immigration and emigration rates and that these rates are the same for all islands under consideration (the population). Figure 7.1 shows the relation between the migration rate and the number of species.

BBO concept is mainly based on Migration and Mutation. The concept and mathematical formulation of Migration and Mutation steps are discussed in next section.

7.3 Biogeography Based Optimization Technique

7.3.1 Migration

The BBO algorithm [23] is similar to other population based optimization techniques, where population of candidate solutions is represented as vector of real numbers. Each real number in the array is considered as one SIV. Fitness of each set of candidate solution is evaluated using SIV. In BBO, a term HIS is used, which is analogous to fitness function in other population based techniques, such as GAs, to represent the quality of each candidate solution set. The solution (habitant), with more number of species, has high HSI value.

Figure 7.2 shows a candidate solution to a sample problem. For simplicity it is assumed that each solution (habitat) has an identical species curve (i.e. E=I). From the Figure 7.2, it can be observed that S_1 solution has low number of species, that means it has low HSI value compared to S_2, which has a high HSI solution, i.e. it contains more number of species. From the Figure 7.2, it can be summarized that the S_1 has higher

immigration rate λ_1 and lower emigration rate μ_1 as compared to the immigration rate λ_2 and the emigration rate μ_2 for S_2.

The emigration and immigration rates of each solution are used to modify the solutions (habitats). Using Habitat Modification Probability, each solution is modified based on the other solutions. Immigration rate λ, of each solution is used to probabilistically decide whether or not to modify each SIV in that solution. After selecting the SIV for modification, emigration rate μ, of other solutions is used to probabilistically select which solutions among the population set will migrate [23].

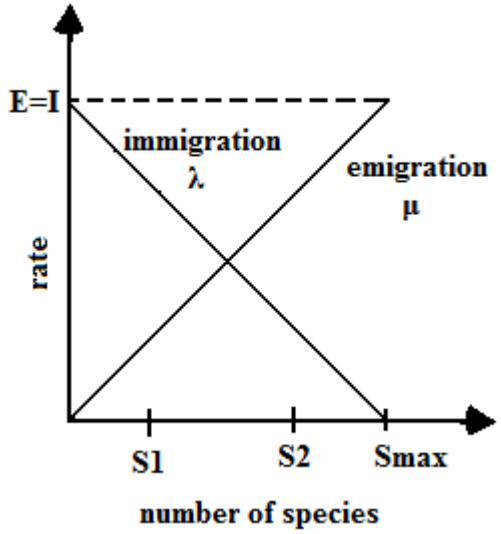

Figure 7.2 A candidate solution [23]

The main difference between recombination approach of evolutionary strategies (ES) and migration process of BBO is that, in ES, global recombination process is used to create a completely new solution, while in BBO, migration is used to bring changes within the existing solutions. In the immigration process, some of the solutions may get corrupted. To prevent this, few elite solutions are kept in BBO algorithm.

7.3.2 *Mutation*

Due to some natural calamities or other events, HSI of a natural habitat can change suddenly and it may deviate from its equilibrium value. In BBO, this event is represented by the mutation of SIV and species count probabilities are used to determine mutation rates. The probability of each species count can be calculated using the differential equation (7.1) [23] given below:

$$P_s' = \begin{cases} -(\lambda_s + \mu_s)P_s + \mu_{s+1}P_{s+1} & S = 0 \\ -(\lambda_s + \mu_s)P_s + \lambda_{s-1}P_{s-1} + \mu_{s+1}P_{s+1} & 1 \le S \le S_{max} - 1 \\ -(\lambda_s + \mu_s)P_s + \lambda_{s-1}P_{s-1} & S = S_{max} \end{cases} \quad (7.1)$$

where,

P_s: the probability of habitat contains exactly S species,

P_{s+1}: the probability of habitat contains S+1 species,

P_{s-1}: the probability of habitat contains S-1 species,

λ_s,μ_s: the immigration and emigration rate for habitat contains S species,

λ_{s+1},μ_{s+1}: the immigration and emigration rate for habitat contains S+1 species,

λ_{s-1},μ_{s-1}: the immigration and emigration rate for habitat contains S -1species,

Immigration rate (λ_s) and emigration rate (μ_s) can be evaluated by the Equations (7.2) and (7.3) [23], given below:

$$\lambda_s = I\left(1 - \frac{s}{s_{max}}\right) \quad (7.2)$$

$$\mu_s = E\frac{s}{s_{max}} \quad (7.3)$$

Each population member has an associated probability, which indicates the likelihood that it exists as a solution for a given problem. If the probability of a given

solution is very low, then that solution is likely to mutate to some other solution. Similarly, if the probability of some other solution is high, then that solution has very little chance to mutate. Therefore, very high HSI solutions and very low HSI solutions are equally improbable for mutation, i.e. they have less chances to produce more improved SIVs in the later stage. But medium HSI solutions have better chances to create much better solutions after mutation operation. Mutation rate of each set of solution can be calculated in terms of species count probability using the Equation (7.4) [23]:

$$m(s) = m_{max}\left(1 - \frac{P_s}{P_{max}}\right) \tag{7.4}$$

where,

m(s) : the mutation rate for habitat contains S species,

m_{max} : maximum mutation rate,

P_{max} : maximum probability.

This mutation scheme tends to increase diversity among the populations. Without this modification, the highly probable solutions will tend to be more dominant in the population. This mutation approach makes both the low and the high HSI solutions in comparison to their earlier values. Few elite solutions are kept in mutation process, to save the features of a solution, so if a solution becomes inferior after the mutation process then the previous solution (solution of that set before mutation) can go back to that place again, if needed. So, mutation operation is a high risk process. It is normally applied to both, the poor and the better solutions. Since medium quality solutions are in improving state, it is better not to apply mutation on such solution.

Here, mutation of a selected solution is performed simply by replacing it with randomly generated new solution set.

7.4 Major Solution Steps of BBO

A flowchart for the Biogeography Based Optimization (BBO) is given in Figure 7.3. The main steps used in the BBO algorithm are as following [23]:

1) Initialize the BBO parameters.
2) The initial position of SIV of each habitat should be randomly selected, while satisfying different equality and inequality constraints of optimization problem. Several numbers of habitats, depending upon the population size, are being generated. Each habitat represents a solution to the given problem.
3) Calculate the HSI i.e. value of objective function for each habitat of the population set for given emigration rate μ, immigration rate λ and species S.

   In the Optimization problem HSI^i indicates the objective function due to *i-th* set of generation value (i.e. *i-th* habitat).
4) Based on the HSI value, elite habitant are identified.
5) Modify each non-elite habitat using immigration and emigration rates.
6) Update each habitant using Equation (7.2) and recalculate each HSI.
7) Feasibility of a problem solution is verified, i.e. each SIV should satisfy equality and inequality constraints.
8) Go to step-3 for the next iteration.
9) Terminate if stopping condition has been reached.

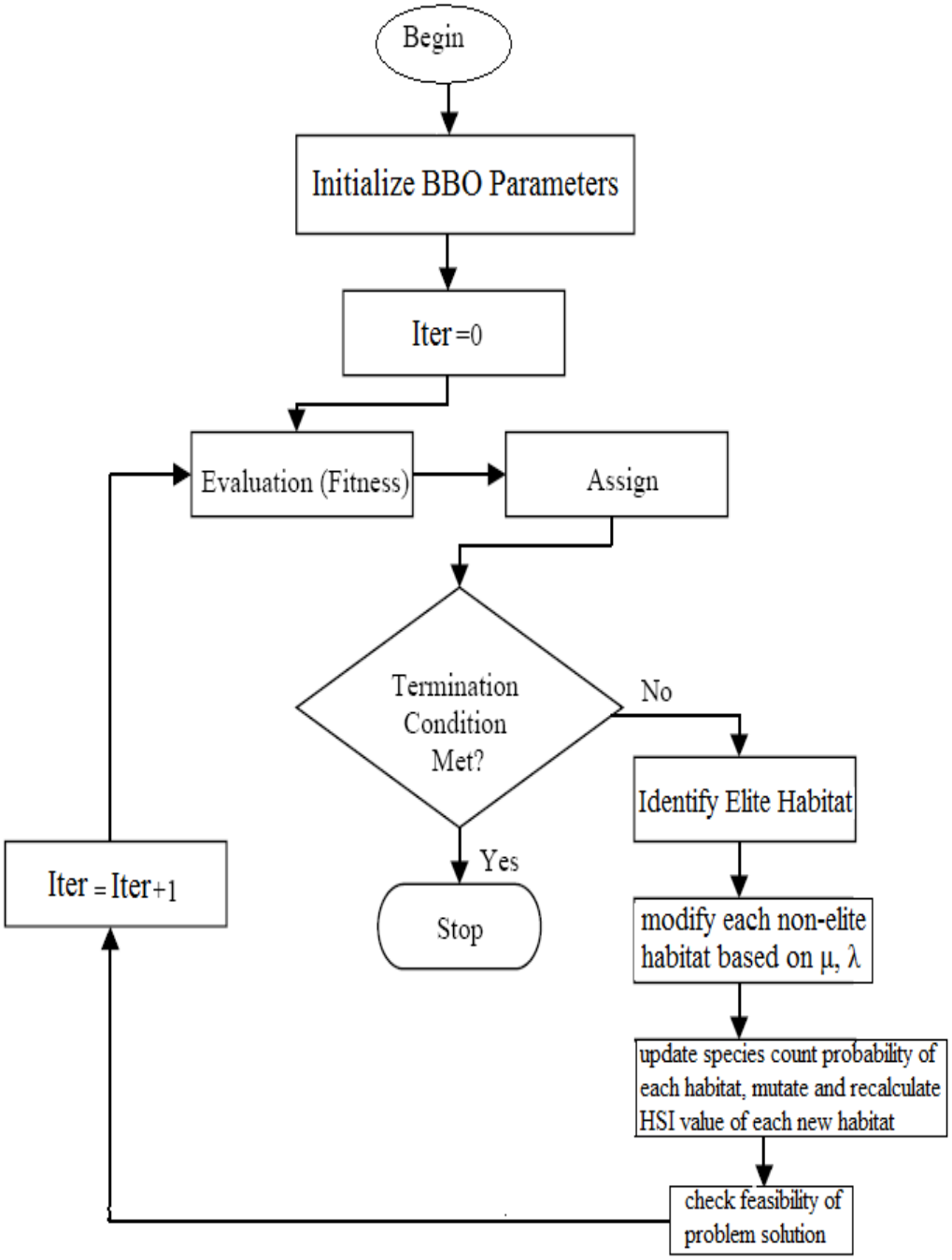

Figure 7.3 Flowchart of the BBO

7.5 Application of the BBO Algorithm to Optimal Power and Voltage Control Problem

7.5.1 Tunable Parameters

As already discussed in this and previous chapters, that the operation of the GA and BBO algorithm depends on their tunable parameters. The optimal values of the tuning parameters of the BBO, considered in this work, are as follows,

Habitat Modification Probability = 1;

Mutation Probability=0.05,

Maximum immigration rate, I=1,

Maximum emigration rate, E=1,

Step size for numerical integration, dt=1,

Number of iterations=50,

Maximum species count, S_{max}=10,

Elitism parameter=2,

Number of SIVs=number of Generations=10,

Number of habitats=10.

7.5.2 The Optimization Problem Formulation

The three optimization formulations, with different objective functions, discussed in chapter V, are summarized below for ready reference.

1. An Existing Optimization Formulation [5]

The objective function to be minimized is:

Minimize

$$\boldsymbol{C}\left(\boldsymbol{P}, \boldsymbol{V}_{\boldsymbol{dc}}^{\boldsymbol{0}}, \boldsymbol{V}_{\boldsymbol{dc}}^{\boldsymbol{1}}, \ldots\ldots, \boldsymbol{V}_{\boldsymbol{dc}}^{\boldsymbol{N}}\right)$$

$$= \{(\boldsymbol{P} - \boldsymbol{P}_{\boldsymbol{min}})^{\boldsymbol{T}}[\boldsymbol{W}_{\boldsymbol{PN}}](\boldsymbol{P} - \boldsymbol{P}_{\boldsymbol{min}}) + (\boldsymbol{P} - \boldsymbol{P}_{\boldsymbol{max}})^{\boldsymbol{T}}[\boldsymbol{W}_{\boldsymbol{Px}}](\boldsymbol{P} - \boldsymbol{P}_{\boldsymbol{max}})\}$$

$$+ \sum_{\boldsymbol{k=0}}^{\boldsymbol{N}} \left\{\left(\boldsymbol{V}^{\boldsymbol{k}} - \boldsymbol{V}_{\boldsymbol{min}}\right)^{\boldsymbol{T}}\left[\boldsymbol{W}_{\boldsymbol{VN}}^{\boldsymbol{k}}\right]\left(\boldsymbol{V}^{\boldsymbol{k}} - \boldsymbol{V}_{\boldsymbol{min}}\right)\right.$$

$$\left. + \left(\boldsymbol{V}^{\boldsymbol{k}} - \boldsymbol{V}_{\boldsymbol{max}}\right)^{\boldsymbol{T}}\left[\boldsymbol{W}_{\boldsymbol{VX}}^{\boldsymbol{k}}\right]\left(\boldsymbol{V}^{\boldsymbol{k}} - \boldsymbol{V}_{\boldsymbol{max}}\right)\right\}$$

subject to

$$\boldsymbol{F}\left(\boldsymbol{P}^{k}, \boldsymbol{V}_{\boldsymbol{dc}}^{k}\right) = 0 \quad (k = 0,1,2 \ldots . N)$$

2. Alternative-1 Formulation:

The objective function to be minimized is:

Minimize

$$\boldsymbol{C}\left(\boldsymbol{P}, \boldsymbol{V}_{\boldsymbol{dc}}^{\boldsymbol{0}}, \boldsymbol{V}_{\boldsymbol{dc}}^{\boldsymbol{1}}, \ldots\ldots, \boldsymbol{V}_{\boldsymbol{dc}}^{\boldsymbol{N}}\right)$$

$$= (\boldsymbol{P} - \boldsymbol{P}_{\boldsymbol{tar}})^{\boldsymbol{T}}\left[\boldsymbol{W}_{\boldsymbol{p}}\right](\boldsymbol{P} - \boldsymbol{P}_{\boldsymbol{tar}}) + \sum_{\boldsymbol{k=0}}^{\boldsymbol{N}} \left\{\left(\boldsymbol{V}^{\boldsymbol{k}} - \boldsymbol{V}_{\boldsymbol{tar}}\right)^{\boldsymbol{T}}[\boldsymbol{W}_{\boldsymbol{v}}]\left(\boldsymbol{V}^{\boldsymbol{k}} - \boldsymbol{V}_{\boldsymbol{tar}}\right)\right\}$$

subject to

$$\boldsymbol{F}\left(\boldsymbol{P}^{k}, \boldsymbol{V}_{\boldsymbol{dc}}^{k}\right) = 0 \quad (k = 0,1,2 \ldots . N)$$

3. Alternative-2 Formulation:

The objective function to be minimized is:

Minimize

$$\boldsymbol{C}\left(\boldsymbol{P}, \boldsymbol{V}_{\boldsymbol{dc}}^{\boldsymbol{0}}, \boldsymbol{V}_{\boldsymbol{dc}}^{\boldsymbol{1}}, \ldots., \boldsymbol{V}_{\boldsymbol{dc}}^{\boldsymbol{N}}\right)$$

$$= \left\{(\boldsymbol{P}-\boldsymbol{P}_{\boldsymbol{min}})^{\boldsymbol{T}}\left[\boldsymbol{W}_{\boldsymbol{pN}}\right](\boldsymbol{P}-\boldsymbol{P}_{\boldsymbol{min}}) + (\boldsymbol{P}-\boldsymbol{P}_{\boldsymbol{max}})^{\boldsymbol{T}}\left[\boldsymbol{W}_{\boldsymbol{px}}\right](\boldsymbol{P}-\boldsymbol{P}_{\boldsymbol{max}})\right\}$$

$$+ \sum_{\boldsymbol{k=0}}^{\boldsymbol{N}} \left\{\left(\boldsymbol{V}^{\boldsymbol{k}}-\boldsymbol{V}_{\boldsymbol{tar}}\right)^{\boldsymbol{T}}[\boldsymbol{W}_{\boldsymbol{v}}]\left(\boldsymbol{V}^{\boldsymbol{k}}-\boldsymbol{V}_{\boldsymbol{tar}}\right)\right\}$$

subject to

$$\boldsymbol{F}\left(\boldsymbol{P}^{k}, \boldsymbol{V}_{dc}^{k}\right) = 0 \quad (k = 0,1,2 \ldots . N)$$

7.5.3 Results with BBO on the MVDC System

The above discussed BBO approach was applied to the simplified model of MVDC shipboard power system, shown in Figure 3.1 in chapter III, with DC line resistance taken as discussed in chapter V. MATLAB code used for the BBO, available in [20], has been used. The optimization problem is defined in the separate .m file.

Tables 7.1, 7.2 and 7.3 present the results with the adjusted converter power settings, obtained by the proposed BBO based method, with the three different objective functions. The voltages are within desired limits under the pre-fault and all the post-fault cases. More importantly, power reference setting of VSC4 is still maintained at their original value, which ensures that the VSC4 will supply uninterrupted power to the sensitive load.

Table 7.1 DC voltages subject to BBO based VSC power setting adjustment with Existing formulation [5]

No.	Conditions	DC Voltage (p.u.)				
		V_{dc1}	V_{dc2}	V_{dc3}	V_{dc4}	V_{dc5}
1	All VSCs in service	0.9856	0.9766	0.9742	0.9639	1.0
2	Loss of VSC1	0.9710	0.9596	0.9645	0.9634	1.0
3	Loss of VSC2	0.9564	0.9610	0.9781	0.9532	1.0
4	Loss of VSC3	0.9609	0.9799	0.983	0.9537	1.0
5	Loss of VSC4	0.9801	1.015	1.004	1.02	1.0
Adjusted Converter Power (p.u) P_{ref1}=0.0042, P_{ref2}=0.0072, P_{ref3}=0.0993, P_{ref4}= - 0.46, P_{ref5}=0.3483						

Table 7.2 DC voltages subject to BBO based VSC power setting adjustment with New Alternative-1 formulation

No.	Conditions	DC Voltage (p.u.)				
		V_{dc1}	V_{dc2}	V_{dc3}	V_{dc4}	V_{dc5}
1	All VSCs in service	0.991	0.9817	0.9976	0.9509	1.0
2	Loss of VSC1	0.9864	0.97	0.9953	0.9670	1.0
3	Loss of VSC2	0.9610	0.9584	0.9714	0.9817	1.0
4	Loss of VSC3	1.003	0.9639	0.9836	0.9853	1.0
5	Loss of VSC4	0.9976	1.0084	1.007	0.9959	1.0
Adjusted Converter Power (p.u) P_{ref1}=0.086, P_{ref2}=0.091, P_{ref3}=0.249, P_{ref4}= -0.46, P_{ref5}= 0.034						

Table 7.3 DC voltages subject to BBO based VSC power setting adjustment for New Alternative-2 formulation

No.	Conditions	DC Voltage (p.u.)				
		V_{dc1}	V_{dc2}	V_{dc3}	V_{dc4}	V_{dc5}
1	All VSCs in service	0.967	0.97	0.9799	0.953	1.0
2	Loss of VSC1	0.9855	0.999	0.9643	0.9721	1.0
3	Loss of VSC2	0.982	0.9511	0.9844	0.9601	1.0
4	Loss of VSC3	0.973	0.9709	0.9599	0.981	1.0
5	Loss of VSC4	1.01	0.9989	1.009	1.019	1.0
Adjusted Converter Power (p.u) P_{ref1}=0.005, P_{ref2}=0.0089, P_{ref3}=0.178, P_{ref4}= -0.46, P_{ref5}= 0.268						

7.6 Comparison of BBO Results with Conventional Lagrange and GA Methods

To demonstrate the performance of the BBO, the optimization results for three different objective functions, obtained by the BBO, are compared with the results obtained with a conventional method presented in chapter V and the genetic algorithm presented in chapter VI. The results are summarized in Table 7.4. The results have been compared in terms of the final objective function values, found with the three algorithms. Table 7.4 shows that the genetic algorithm provides the most optimal solution for the given optimization problem followed by the BBO. However, performance of the BBO can possibly be improved further by attempting different combination of its parameter values.

Table 7.4 Comparison of final objective function values with different algorithms

Objective Function	*With Conventional (Lagrange multiplier) Method (p.u)*	*With GA Method (p.u)*	*With BBO Method (p.u)*
Existing Optimization Formulation [5]	3.1981	2.1493	2.4977
New Alternative-1 Formulation	2.8467	2.0189	2.458
New Alternative-2 Formulation	2.998	2.09	2.399

7.7 Summary

This chapter has provided an overview of BBO algorithm, along with various terminologies used**,** its basic concepts and the major solution steps. The algorithm was applied to the optimal power and voltage control problem, with the three different objective functions and the results are presented on the MVDC shipboard power system. The performance of the BBO has also been compared with the GA based and Lagrange Multiplier based methods, presented in the previous two chapters.

CHAPTER VIII

CONCLUSIONS AND FUTURE WORK

8.1 Conclusions

This research work is focused on developing an algorithm for optimal voltage and power control in a multi-zonal shipboard MVDC power system. The conditions of operation in the multi-zonal MVDC system are set by: 1) the DC voltage reference of the DC Voltage Regulator; and 2) the real power reference settings of Power Dispatchers. From the knowledge of the resistances in the DC network and the DC voltage reference, the DC voltages across each Power Dispatcher are solved from the algebraic quadratic equations considering a fixed value of their real power reference settings. In general, the DC voltages migrate upwards or downwards with the DC voltage reference of the DC Voltage Regulator (VR). In most of the cases, by "tuning" the DC voltage reference, it is usually possible to bring all the DC bus voltages between the upper and lower bounds. A Voltage Sensitivity method has been successfully determine the optimal reference setting of the voltage regulators and demonstrated in chapter-IV.

In situations, where the "tuning" of voltage reference setting of the VR does not provide a feasible solution ensuring the DC bus voltage within limits, then it is necessary to adjust the real power reference settings of the Power Dispatchers until all the DC

voltages between the desired upper and lower bounds. The adjustment of the real power reference settings was formulated as an optimization problem and successfully solved on the MVDC system using a conventional approach in chapter-V and two evolutionary methods in chapters VI and VII.

As the destructive over-voltages will have appeared before 1) the DC voltage reference of the DC Voltage Regulator and 2) the real power reference settings of the Power Dispatchers can be reset, their settings must be chosen in the very beginning to satisfy both the pre-fault and the post-fault condition, any one of the Voltage Source Converters (VSCs). Thus, the Voltage Sensitivity method and the Optimization method have been formulated for the combined pre-fault as well as the post-fault situations.

In the first stage, a non-iterative voltage sensitivity based approach has been utilized to determine the optimal DC reference voltage setting of one of the VSCs, acting as Voltage Regulator, while keeping the other VSCs, in Power Dispatch mode, at their fixed power reference settings. Test results on a simplified representation of the multi-zonal notional MVDC architecture, presented in chapter-IV reveals that the sensitivity based method effectively determines the range of reference setting of voltage regulator that maintains the DC voltage at other VSC buses within acceptable limits under the pre-fault as well as the post fault conditions. However, in certain conditions, such as the one simulated by assuming higher values of the DC line resistances in chapter-V, the sensitivity based approach is not able to determine any feasible range/setting for the voltage regulator, that satisfies the voltage constraints in all the cases. In such situations, the second stage of simulation, employing an optimization based approach, is effectively used to readjust and determine the optimal power reference settings of the power

dispatchers. Three alternative formulations, with different objective functions, were tried out and it was found that the new alternative-1 formulation provides the most optimal solution. The optimization problem is solved using three different methods 1) Conventional (Lagrange multiplier) method in chapter-V 2) Genetic Algorithm (GA) based method in chapter-VI and 3) Biogeography Based Optimization(BBO) based method in chapter-VII. The test results, obtained through the application of the three algorithms, were also compared in terms of final objective function.

The major disadvantage of the heuristic method is the tuning of parameters. And also, their initial population can be randomly chosen.

The main contributions of this research work are summarized as follows:

1. The groundwork on multi-zonal MVDC shipboard power system architecture has been provided.
2. The main objective of developing an algorithm for the optimal control of voltage and power in MVDC multi-zonal shipboard power system has been discussed.
3. The two new alternative formulations of the optimization based approach to determine optimal reference power settings have been suggested.
4. An initial attempt of applying BBO method for solving the optimization problem had been discussed and the test results were compared with a conventional and the genetic algorithm based methods. All the three methods have successfully provided the optimal reference power setting values to ensure the DC bus voltages within acceptable range.

5. The voltage sensitivity method, conventional (Lagrange Multiplier) method, the genetic algorithm and the biogeography based optimization method were successfully implemented in MATLAB and tested on the simplified model of MVDC shipboard power system.

8.2 Future Work

The performance of the genetic algorithm and the BBO algorithms can be improved by investigating different ways of generating initial population and by tuning their parameters to achieve even better optimal solution.

In this thesis, a simplified model of the MVDC multi zonal shipboard power system model has been considered for the sake of proving the optimal voltage and power control concepts. A more practical and detailed representation of the MVDC model can be considered.

REFERENCES

[1] C. Petry and J. Rumburg, "Zonal electrical distribution systems: An affordable architecture for future," *Naval Engineers Journal,* Vol.105, May 1993. pp. 45-51.

[2] Norbert Doerry, "Next Generation Integrated Power System Technology Development Roadmap", November 2007.
https://www.neco.navy.mil/synopsis_file/N00024NGIPS_Technology_Dev_Roadmap_final_Distro_A.pdf

[3] RTDS Notional E-ship model Technical guide, Florida State University, Version 3.4, June 2008.

[4] Thomas L. Baldwin and Shani A. Lewis, "Distribution load flow methods for shipboard power systems", *IEEE Transactions on Industry Applications*, Vol. 40, No.5, Sep/Oct 2004, pp. 1183-1190.

[5] Weixing Lu and Boon Teck Ooi, "DC voltage limit compliance in voltage-Source converter based multi-terminal HVDC", *Proc of IEEE PES General Meeting*, 12-16 June 2005, Vol. 2, pp. 1322- 1327.

[6] Weixing Lu and Boon Teck Ooi, "Multiterminal DC transmission system for wind-farms", *Proc. of IEEE PES Winter Meeting,* Columbus, 2001, pp1091-1096.

[7] B. T. Ooi and X. Wang, "Boost type PWM-HVDC transmission system", *IEEE Transactions on Power Deliverty*, Vol. 6, No.4, October 1991. pp. 1557-1563.

[8] H. Saadat, "*Power System Analysis*", The McGraw-hill Companies, New York, 1999.

[9] N.Mohan, T.M.Undeland and W.P.Robbins, "*Power Electronics-Converters, Applications and Design*", John Wiley & Sons, Inc., 1989.

[10] Héctor F. Latorre S, "A Multichoice Control Strategy for a VSC-HVDC", PhD dissertation, Royal Institute of Technology, Sweden, 2008.

[11] Xiao-Ping Zhang, " Multi Terminal Voltage- Sourced Converter-Based HVDC models for Power Flow Analysis", *IEEE Trans.on Power Systems*, Vol 19, No.4, Nov 2004, pp. 1877-1883.

[12] C. Angeles-Camacho, O.L. Tortelli, E. Acha, and C.R. Fuerte-Esquivel, " Inclusion of a high voltage DC-voltage source converter model in a Newton–Raphson power flow algorithm", *IEE Proceedings - Generation, Transmission and Distribution*, November 2003, Vol. 150, Issue 6, pp. 691-696.

[13] X.F. Yuan, and S. J. Cheng, "Simulation Study for a Hybrid Multi-terminal HVDC System", *in Transmission and Distribution Conference and Exhibition, 2005/2006 IEEE Power Electronics Society*, August 2006.

[14] A.M. Cramer, R.R. Chan, S. D. Sudhoff, Y. Lee, M. R. Surprenant, N. S. Tyler, E. L. Zivi, and R. A. Youngs, "Modeling and simulation of an electric warship integrated engineering plant", *SAE Power System Conference*, Nov. 2006.

[15] A. Panosyan, B.R. Oswald, "Modified Newton-Raphson load flow analysis for integrated AC/DC power systems", *39th International Universities Power Engineering Conference*, 2004. Vol 3, pp. 1223- 1227.

[16] Edward Wilson Kimbark, "*Direct Current Transmission*", John Wiley & Sons, Inc., 1971.

[17] G. Asplund, "Application of HVDC Light to Power System Enhancement", *Proceeding of the IEEE Winter Power Meeting*, January 2000, Singapore.

[18] Lianxing Tang and Boon Teck Ooi, "Protection of VSC-multi-terminal HVDC against DC Faults", IEEE 33nd Annual Power Electronics Specialists Conference (PESC), Vol.2, 2002, pp. 719-724.

[19] "Gexol World Class Marine Cables" by Amercable Incorporated http://www.1st4cables.com/downloads/gexolcatalog.pdf

[20] http://academic.csuohio.edu/simond/bbo

[21] B. T. Ooi and X. Wang, "Voltage Angle Lock Loop Control of Boost Type Pwm Converter for HVDC Application", *IEEE Transactions on Power Electronics*, Vol 5, No. 2, April 1990, pp 229-235.

[22] K. Swain, and A. S. Morris, "A novel hybrid evolutionary programming method for function optimization", in *Proc. 2000 Congress on Evolutionary Computation*, Vol. 1, pp. 699-705, July 2000.

[23] Dan Simon, "Biogeography Based Opotimization", *IEEE Transactions on Evolutionary Computation*, Vol. 12, No. 6, December 2008.

[24] A. Wallace, "*The Geographical Distribution of Animals (Two Volumes)*", Adamant Media Corporation, Boston, MA 2005.

[25] C. Darwin, "The *Origin of Species*", New York: Gramercy, 1995.

[26] L. Lai and N. Sinha, " *Genetic Algorithms for solving optimal power flow problems*", Chapter 17, Modern Heuristic Optimization Techniques", pp. 471-500, IEEE Press, 2008.

[27] D. E. Goldberg, "*Genetic Algorithms in Search, optimization and Machine Learning*," Addison Wesly, Reading, 1989.

[28] J. H. Holland, "*Adaptation in natural and artificial systems*", Ann Arbor, MI: The University of Michingan Press, 1975.

[29] E. Munroe, "The geographical distribution of butterflied in the West Indies", PhD Dissertation, Cornell University, Thaca, New York, 1948.

[30] R. MacArthur and E. Wilson, "*The Theory of Biogeography*", Princeton University Press, 1967.

[31] J. H. Parl, S. O. Yang, H. S. Lee, and Y. M. Park, "Economic load dispatch using evolutionary algorithms", *in Proc. Int. Conf. on Intelligent Systems Applications to Power Systems*, pp. 441-445, 28th Jan – 2nd Feb, 1996.

[32] S. L. Ho, Shiyou Yang, Guangzheng Ni, E. W. C. Lo, and H. C. Wong, "A Particle swarm optimization-based method for multiobjective design optimizations", *IEEE Trans. Magnetics*, Vol. 41, No. 5, pp. 1756-1759, May 2005.

[33] T. Yalcionoz, H. Altun, and M. Uzam, "Economic dispatch solution using a genetic algorithm based on arithemetic crossover", *Proc. IEEE Proto Power Tech. Comference*, Proto, Protugal, Sep 2001.

[34] T. Wesche, G. Goertler, and W. Hubert, “Modified habitat suitability index model for brown trout in southeastern Wyoming”, *North Amer. J. Fisheries Manage.*, Vol. 7, pp. 232-237, 1987.

[35] T. Back, “*Evolutionary Algorithms in Theory and Practice*”, Oxford, U.K., Oxford University press, 1996.

[36] D. Simon, “*Optimal State Estimation*”, Wiley, New York, 2006.

[37] Yong Chang. "Improvement of power quality by VSC based multi-terminal HVDC", *Proceeding of the 2006 IEEE Power Engineering Society General Meeting*, 2006

[38] Wulue Pan, "Control Strategy Research of VSC Based Multiterminal HVDC System", *Proceeding of the 2006 IEEE PES Power Systems Conference and Exposition*, 2006

[39] Y. Zhu, Z. Yang, and J. Song, “A genetic algorithm with age and sexual features”, in *Proc. Int. Conf. Intell. Comput.*, 2006, pp. 634-640.

[40] S. Gustafson and E. Burke, “Speciating island model: An alternative parallel evolutionary algorithm”, *Parallel and Distributed Computing*, Vo1. 66, pp. 1025-1036, 2006.

[41] Z. Cai and Y. Wang, “ A multiobjective optimization-based evolutionary algorithm fo rconstrained optimiziation”, *IEEE Trans. Evol. Comput.*, Vol. 5, pp. 658-675, Dec. 2005.

[42] X. Yao, Y. Liu, and G. Lin, “Evolutionary programming made faster”, *IEEE Trans. Evol. Comput.*, Vol. 3, pp. 82-102, July 1999.

[43] W. Khatib and P. Fleming, “The stud GA: A mini revolution? in Parallel Problem Solving from Nature”, A. Eiben, T. Back, M. Schonauer, and H. Schwefel, Eds. New York, Springer, 1998.

[44] I. Parmee, “*Evolutionary and Adaptive Computing in Engineering Design*”, New York: Springer, 2001.

[45] H. Beyer, “*The Theory of Evolution Strategies*”, New York: Springer, 2001.

[46] E. Mezura-Montes and C. Coello, “A simple multimembered evolution strategy to solve constrained optimization problems,” *IEEE Trans. Evol. Comput.*, Vol. 9, pp. 1–17, Feb. 2005.

[47] G. Onwubolu and B. Babu, "*New Optimization Techniques in Engineering*", Berlin, Germany: Springer-Verlag, 2004.

[48] J. Reeve, "Multiterminal HVDC Power Systems", *IEEE Transactions on Apparatus and Systems*, Vol. PAS-99, No. 3, March/April 1980, pp 729-737.

[49] W. F. Long, J. Reeve, J. R. Mcnichol, R. E. Harrison and J. P. Bowled, " Considerations for Implementing Multiterminal DC Systems", *IEEE Transactions on Apparatus and Systems*, Vol. PAS-104, No. 9, September 1985, pp 2521-2530.

[50] Joachim Holtz, "Pulse Width Modulation – A Survey", *IEEE Transactions on Industrial Electronics*, Vol. 39, No. 5, December 1992, pp. 410-420.

[51] J. W. Dixon, A. B. Kulkarni, M. Nishimoto and B. T. Ooi, "Characteristics of a Controlled-Current PWM Rectifier-Inverter Link", *IEEE Transactions on Industry Applications*, Vol. 23, No. 6, November/December 1987, pp. 1027-1028.

[52] B. T. Ooi, "Pulse Width Modulation Power Transmission System", U.S. Patent 4,941,079, July 10, 1990.

[53] G. Asplund, K. Eriksson, K. Svensson, "DC Transmission based on Voltage Source Converters", CIGRE SC14 Colloquium in South Africa 1997.

[54] U. Axelsson, A.Holm, C. Liljegren, K. Eriksson and L. Weimers, "Gotland HVDC Light Transmission ---World's First Commercial Small Scale DC Transmission", *CIRED Conference*, Nice, France, May 1999.

[55] F. Schettler, H. Huang and N. Christl, "HVDC Transmission System using Voltage Sourced Converters-Design and Applications", *IEEE PES Summer Meeting*, July 2000.

[56] B. R. Andersen, L. Xu, P. J. Horton and P. Cartwright, "Topologies for VSC Transmission", *IEE Power Engineering Journal*, June 2002, pp142-150.

[57] Michael Bahrman, Abdel-Aty Edris, Rich Haley, "Asynchronous Back-to-Back HVDC Link with Voltage Source Converters", *Power System Conference*, Minnesota, USA, November 1999.

[58] Vijit Kinnares. "Harmonic Flow Analysis of HVDC Systems for Discrete Wavelet Transform ith Advanced of the Harmonic Impedances and Voltage Source Transients Model of AC-DCConverters", TENCON 2006 - 2006 IEEE Region 10 Conference.

[59] J. Holtz, "Pulse-width modulation for electronic power conversion," *Proc. IEEE*, vol. 82, pp. 1194–1214, Aug. 1994.

[60] H. Akagi, "The start-of-the-art of power electronics in Japan," *IEEE Trans. Power Electron.*, vol. 13, pp. 345–356, Mar. 1998.

[61] A. A. Edris *et al.*, "Emerging application of voltage source converter technology in back-to-back asynchronous tie," *Proc. of VII SEPOPE*,Curitiba, Brazil, May 21–26, 2000.

[62] T. Larsson *et al.*, "Eagle pass Back-to-Back tie: A dual purpose application of voltage source converter technology," *Proc. IEEE Power Eng. Soc.*, Vancouver, BC, Canada, July 15–19, 2001.

[63] G. Asplund, "HVDC using voltage source converters-a new way to build highly controllable and compact HVDC substations," *Proc. Cigré Conf.*, Paris, France, Aug.–Sept. 27–2, 2000.

[64] A. Wood and B. Wollenberg, *Power Generation Operation and Control*, Wiley-Interscience, NJ, 1996.